12-2015

# DEFINING THE MOLECULAR NETWORKS NECESSARY FOR THYMUS FATE AND ORGANOGENESIS

Kaitlin A. Reeh

**DEFINING THE MOLECULAR NETWORKS NECESSARY FOR THYMUS FATE AND ORGANOGENESIS**

**BY**

**Kaitlin Alyssa Gutierrez Reeh, Ph.D. Candidate**

**APPROVED:**

_____

Ellen R. Richie, Ph.D., Supervisory Professor

_____

Mark T. Bedford, Ph.D.

_____

Sharon Y. R. Dent, Ph.D.

_____

Steven A. Vokes, Ph.D.

_____

Richard D. Wood, Ph.D.

APPROVED:

_____

Dean, The University of Texas
Graduate School of Biomedical Sciences at Houston

# DEFINING THE MOLECULAR NETWORKS NECESSARY FOR THYMUS FATE AND ORGANOGENESIS

A

Dissertation

Presented to the Faculty of

The University of Texas Health Science Center at Houston

And

The University of Texas M.D. Anderson Cancer Center

Graduate School of Biomedical Sciences

in Partial Fulfillment

of the Requirements

for the degree of

DOCTOR OF PHILOSOPHY

By

Kaitlin Alyssa Gutierrez Reeh, Ph.D. Candidate

Houston, Texas

August 2015

## DEDICATION

This thesis is dedicated to the following individuals:

Dr. Thomas H. Welsh, Jr., Ph.D.
Mr. Jim Bob Hatley
Mr. Mike Carter
Dr. Craig King, D.V.M.

Thank you for investing the time to help an undergraduate realize and accomplish her dreams. If it were not for you, I would not be where I am today.

**ACKNOWLEDGEMENTS**

It takes a village to get through graduate school, and there are numerous people that have selflessly supported my journey through this process. I would first like to thank my mentor Dr. Ellen Richie for her endless (and tireless) efforts to ensure that I progressed as a scientist, writer and speaker. Both personally and professionally, I could not have asked for a better mentor. Thank you for your encouragement through the hard times, celebration during the good, and for teaching me to never take no for an answer. There are not enough words to convey how much I appreciate all that you have taught me. I would like to acknowledge my committee members, Dr. Mark Bedford, Dr. Sharon Dent, Dr. Brad McIntyre, Dr. Steven Vokes and last, but certainly not least, Dr. Richard Wood. Thank you all for your guidance (and patience) through every aspect of my project and through my growing pains as a scientist. Dr. Welsh, thank you for sharing your love of science. If it were not for you, I would never have found my love of research. Thank you for all of your support through the years. It is truly an honor to have worked for you.

Ms. Becky, thank you. You work tirelessly (and make it look effortless), to ensure that we are all taken care of. I appreciate all that you have done for me and I never would have made it through this process without you. I will miss you terribly and think of you always.

There is no way I would have made it through graduate school if it were not for my lab mates and friends. Carla, you are the most invaluable resource our lab has and our battleship would sink without you. Thank you for your wisdom and friendship. I admire you more than words can say. Michelle, your support and friendship through the years have been immense. Thank you from the bottom of my heart. Words truly cannot express how much I appreciate all that you have done. Ginny, The World's Best Postdoc. Your endless amounts of scientific and personal wisdom have made me both a better scientist and a better person. Nandini, thank you so much for your kind words, encouragement and unbelievable insight into culture, life and science. I deeply appreciate our friendship. Julia,

your hard work, courage and perseverance are inspiring. I hope one day you realize just how incredible you are. I am so proud to have had the opportunity to be your friend. Thank you for all that you have taught me. Matt, you have been the best brother I never asked for. Your kindness knows no limits and despite what you may say, you have the best heart. Thank you for all of the insulting notes on my lab bench. They made those hard times in lab bearable. I will never forget the friendship that you, Michelle and I have. If it were not for the two of you, I know my experience in graduate school would never have been the same. Dr. Keiichi Takata, thank you for your time you took guiding me through my rotation in Dr. Wood's lab. I learned a tremendous amount from you and appreciate all of your encouragement and guidance over the years. Thank you to Aimee, Andria, Sitaram, Vidya and Mandira, Pam and Jenn for your friendships. I have loved all of the laughs we have shared, the times spent in lab and adventures at retreats. I would also like to thank my dear friend Jen McKinney. I admire your strength and courage in every aspect of life. Thank you for your loyalty and friendship.

I would also like to thank the "Mouse House" staff for their endless patience with not only me, but also my copious amounts of mice. I would especially like to thank Meredith Spice for her vast amounts of knowledge and support over the years. I would also like to thank Ms. Margie, Ms. Tilda and Ms. Santa for their encouragement and support over the years. Ms. Margie, you have been a second mother to me and I will always appreciate our friendship. Thank you to Joe Rodriguez and Mary Henderson for your friendship and encouragement through my candidacy exam. I will treasure our friendship and the bellyaching laughs.

Through this all, my family has stood by my side. Thank you Bruce and Denise for your love and support from the day we moved to Fredericksburg. Kayla, thank you for your friendship and support throughout the years. Thank you for giving me the most beautiful niece and nephew. Lainey and Greyson, I love you to the moon and back. Aunt Patty and

Uncle Brent, thank you for your unconditional love and support. I love you all from the bottom of my heart.

Oma, thank you for teaching me that family is one's own definition. I love you. Emily, thank you for teaching me what true grace and strength are. Auntie M, thank you for your endless love and support.

Grandma, if it were not for you and the sacrifices you made for our family, this opportunity would never have been possible. You are the embodiment of unconditional love and acceptance and I live every day to honor you and that legacy.

Mama, thank you for teaching me to always do my best and have fun. You courage amazes me. Daddy, thank you for changing our stars. You make me special. Amy, my heaven is here with you. I would not be where I am or who I am without you and all of our adventures. Mark, you are the reason for this all and I love you. Lastly, thank you Grandma and Papa. There is not a day that goes by that I do not miss you. Thank you for teaching me that an education is second to none and that hard work and commitment can take you anywhere.

**DEFINING THE MOLECULAR NETWORKS NECESSARY FOR THYMUS FATE AND ORGANOGENESIS**

Kaitlin Alyssa Gutierrez Reeh, Ph.D. Candidate

Supervisory Professor: Ellen R. Richie, Ph.D.

The thymus and parathyroid (PT) glands originate from endodermal progenitors in the bilateral third pharyngeal pouches (3rd pps). By E11.5 during mouse development, cells committed to the thymus lineage express *Foxn1* whereas PT-fated cells express *Gcm2*. While these transcription factors are required for organ-specific differentiation, the exact molecular mechanisms that specify endodermal progenitors to either the thymus or parathyroid lineage are not well defined. *Tbx1* is initially expressed throughout the 3rd pp endoderm, as it is required for segmentation of the pharyngeal apparatus, but is downregulated in the thymus-fated domain by E10.5. Despite the widely held notion that *Tbx1* is required for thymus organogenesis, we have shown that ectopic expression of *Tbx1* in thymic epithelial cells (TECs) suppresses FOXN1, inhibits TEC proliferation and arrests TEC differentiation, suggesting *Tbx1* must be tightly regulated in the 3rd pp endoderm for proper thymus organogenesis to occur. Members of the *miR-17-92* cluster downregulate *Tbx1* in cardiac progenitor cells to permit cardiomyocyte differentiation, and we demonstrated that members of this cluster are expressed in the 3rd pp endoderm and mesenchyme. We find that global or TEC-specific deletion of *miR-17-92* enhances TBX1 expression and reduces FOXN1 in the 3rd pp. Furthermore, global deletion of *miR-17-92* results in an ectopic, hypoplastic thymus lobe, while deletion in TECs results in $TBX1^{+}$ progenitor cells that persist in the fetal thymus. In contrast, overexpression of *miR-17-92* in TECs results in downregulation of TBX1 in the dorsal 3rd pp and surrounding mesenchyme. Therefore, these data suggest that *miR-17-92* plays an essential role in thymus development by regulating *Tbx1* expression in the 3rd pp.

Additionally, previous work from our lab has shown that a genetic deficiency in neural crest cells (NCCs) expands thymus fate in the 3$^{rd}$ pp. We show that NCCs mediate this effect in part by promoting TBX1 expression in the dorsal 3$^{rd}$ pp. Finally, we present evidence consistent with the dual hypothesis that *Fgf8* expression in the ventral 3$^{rd}$ pp promotes thymus fate by restricting TBX1. Based on these results, we generated a working model describing the signaling networks that contribute to thymus fate and 3$^{rd}$ pp patterning.

## TABLE OF CONTENTS

**LIST OF FIGURES**

## LIST OF TABLES

**LIST OF ABBREVIATIONS**

| | |
|---|---|
| AIRE | autoimmune regulator |
| APC | antigen presenting cell |
| BMP | bone morphogenic protein |
| Cldn | Claudin |
| CMJ | corticomedullary junction |
| cTEC | medullary thymic epithelial cell |
| DC | dendritic cell |
| DLL4 | delta-like ligand 4 |
| DN | double negative |
| DP | double positive |
| ETP | early thymic progenitor |
| FGF | fibroblast growth factor |
| Foxn1 | Forkhead box protein N1 |
| Gcm2 | glial cells missing-2 |
| ISH | in situ hybridization |
| K5 | cytokeratin 5 |
| K8 | cytokeratin 8 |
| KGF | keratinocyte growth factor |
| MHCI | major histocompatibility class I |
| MHCII | major histocompatibility class II |
| mTEC | cortical thymic epithelial cell |
| MTS | mouse thymic stroma |
| NCC | neural crest cell |
| PA | pharyngeal arch |
| Plet-1 | placenta expressed transcript-1 |

| | |
|---|---|
| pp | pharyngeal pouch |
| RAG | recombination activating gene |
| SHH | sonic hedgehog |
| SP | single positive |
| SSA | sex steroid ablation |
| TCR | T cell receptor |
| TEC | thymic epithelial cell |
| TEPC | thymic epithelial progenitor cell |
| TRA | tissue restricted antigen |
| $T_{Reg}$ | regulatory T cell |
| TSP | thymus seeding progenitor |

## CHAPTER 1: Introduction

T cells develop in the thymus where multiple stromal cell types form a unique microenvironment that is indispensable for thymocyte maturation. Thymic epithelial cells (TECs) are the major component of the stromal network and provide growth, differentiation and survival signals to thymocytes throughout their differentiation program (1). TECs also present self-peptides that are required to generate naïve T cells that express a self-restricted, yet self-tolerant T cell receptor (TCR) repertoire. T cells that emigrate from the thymus and join the peripheral T cell pool are referred to as naïve T cells, and a constant supply is required to maintain a highly diverse TCR repertoire. Diversity of the TCR is essential for generating effective T cell-mediated immune responses against a broad spectrum of antigens, including pathogens and neoplastic cells. The number of T cells that emigrate from the thymus directly correlates with thymus size and depends on a functional TEC network (2-4). Naïve T cell production is at its peak in young individuals, when the thymus is at its largest. During aging or as a result of stress (i.e. cytoablative therapy), the thymus involutes largely due to degeneration and disorganization of the TEC compartment. The resulting decline in naïve T cell output leads to a homeostatic expansion of memory T cells in the peripheral lymphoid organs. In addition, decreased numbers of naïve T cells from the involuted thymus result in restricted TCR diversity, which severely compromises the ability to respond to newly encountered antigens. Consequently, thymus involution is thought to impair the development of protective immune responses after vaccination and increase susceptibility to new infectious diseases and cancer. In addition, failure to restore thymus function and T cell output is an independent predictor of infection and mortality in allogeneic stem cell transplant recipients (5). Thus, preventing thymus involution and sustaining T cell output would greatly improve human health. There is great interest in identifying effective therapeutic strategies to regenerate the involuted thymus. While several approaches, such as sex steroid ablation (SSA), have been shown to partially restore TEC

cellularity and thymopoiesis, these effects are transient and functional defects were observed in the TEC compartment (6-8). These results suggest that regeneration of a fully functional TEC microenvironment may require activation of specific molecular pathways that drive the differentiation of TEC progenitors during ontogeny. Therefore, this project is focused on identifying the genetic pathways necessary to specify endodermal progenitors to a TEC fate and maintain TEC differentiation in an effort to devise rational therapeutic approaches for thymus regeneration or preservation.

**Thymocyte Maturation is Dependent on TEC Derived Signals**

The thymus is composed of thymocytes (developing T cells) and stromal cells, with thymocytes accounting for greater than 97% of total thymus cellularity. The heterogeneous thymic stromal compartment is composed of TECs, dendritic cells (DCs), endothelial cells, macrophages, fibroblasts and B cells. In addition, the thymic stroma is organized into distinct regions that support different stages of thymopoiesis. These regions consist of phenotypically and functionally distinct stromal cells, which are found in the cortex, medulla, subcapsular region and at the cortico-medullary junction (CMJ).

Early in thymus ontogeny, prior to the development of mature medullary and cortical thymic microenvironments, TEC-derived signals are necessary to support fetal thymopoiesis. The ventral domain of the 3$^{rd}$ pp endoderm expresses the chemokine CCL25 and the dorsal endoderm expresses CCL21 to attract thymus seeding progenitors (TSPs) to the 3$^{rd}$ pp as early as E11.5 (9-11). TSPs upregulate the chemokine receptors, CCR7 and CCR9, and follow a chemotactic gradient to the thymic rudiment (reviewed in (10)). By E11.5, IL-7 is expressed in the ventral, thymus-fated domain of the 3$^{rd}$ pp and its expression promotes the survival, expansion and differentiation of TSPs that migrate into the thymic epithelial microenvironment (12).

In the adult, TSPs migrate from the bone marrow and enter the thymus through vasculature at the CMJ. As these TSPs commit to the thymocyte lineage and subsequently differentiate into functional T cells, they migrate throughout the thymus into different microenvironments (Fig.1). Early thymocyte progenitors in the thymus parenchyma are CD4 and CD8 double negative (DN) cells. DN thymocytes are a heterogeneous population that can be further subdivided into four developmental stages based on the expression of CD44, c-kit and CD25. DN1 cells ($CD44^+c\text{-}Kit^+CD25^-$) are not committed to the T cell lineage and can generate αβ T cells, γδ T cells, B cells, DCs and macrophages (reviewed in (13)). Engagement of the Notch 1 receptor on DN1 thymocytes by delta-like ligand 4 (DLL4) expressed by cortical thymic epithelial cells (cTECs) generates one of the essential signals required for T cell lineage commitment (14). In the absence of DLL4, thymocyte development is arrested at the early DN1 stage (15). Notch signaling promotes the activation of transcription factors (*Gata3*, *Hes1*, *Tcf7*) which are necessary for T-lineage restriction and continued thymocyte maturation (reviewed in (14)). Recombination activating gene 1 (RAG1) and RAG2 are expressed by late DN2 ($CD44^+c\text{-}Kit^+CD25^+$) thymocytes and are required for TCR-β, TCR-γ and TCR-δ gene rearrangement (16, 17). Thymocytes upregulate the IL-7R during the DN2 stage, as IL-7 signaling is necessary to sustain the DN2 thymocyte population as these cells progress to the DN3 stage (18). DN3 thymocytes migrate into the subcapsular region of the thymus and are $CD44^-c\text{-}Kit^-CD25^+$. TEC-derived Notch signaling is essential for the survival of DN3 thymocytes and progression beyond the β-selection checkpoint (19, 20). β-selection ensures that DN3 thymocytes successfully rearrange a TCRβ chain and that it is co-expressed with an invariant pre-TCRα and CD3 polypeptides, forming the pre-TCR complex (reviewed in (14)). Therefore, those thymocytes that are unable to produce a pre-TCR at DN3 undergo apoptosis because they are unable to receive survival signals via the pre-TCR and Notch1. However, those DN3 thymocytes that are signaled via the pre-TCR and Notch, pass through the β-selection checkpoint,

**Figure 1. Thymocyte migration and maturation within the thymus.**

The cortiomedullary junction (CMJ) is denoted by a dashed line and a solid line represents the subcapsule. Thymocytes maturing from double negative (DN) 1-DN4 in the cortex are purple and single positive (SP) thymocytes in the medulla are orange. Thymic epithelial cells (TECs) are star shaped with dark orange medullary TECs (mTECs) and dark purple cortical TECs (cTECs). Thymus seeding progenitors (TSPs) migrate from the adult bone marrow and enter the thymus through vasculature at the CMJ. Once in the thymus, TSPs commit to the thymocyte lineage and differentiate. These early thymocyte progenitors are CD4 and CD8 DN cells and differentiate through four DN stages based on their expression of c-kit, CD44 and CD25 to become DP for both CD4 and CD8. DP thymocytes that form αβTCRs capable of recognizing self-peptide in the context of self-MHC are positively selected in the cortex, downregulate either CD4 or CD8 to become SP thymocytes and migrate into the medulla. Once in the medulla, SP thymocytes undergo negative selection to ensure that autoreactive T cells do not circulate throughout the periphery. Those thymocytes that pass negative selection exit the thymus at the CMJ and enter the periphery as self-restrictive, yet self-tolerant CD4 or CD8 SP T cells.

**Figure 1. Thymocyte migration and maturation within the thymus.**

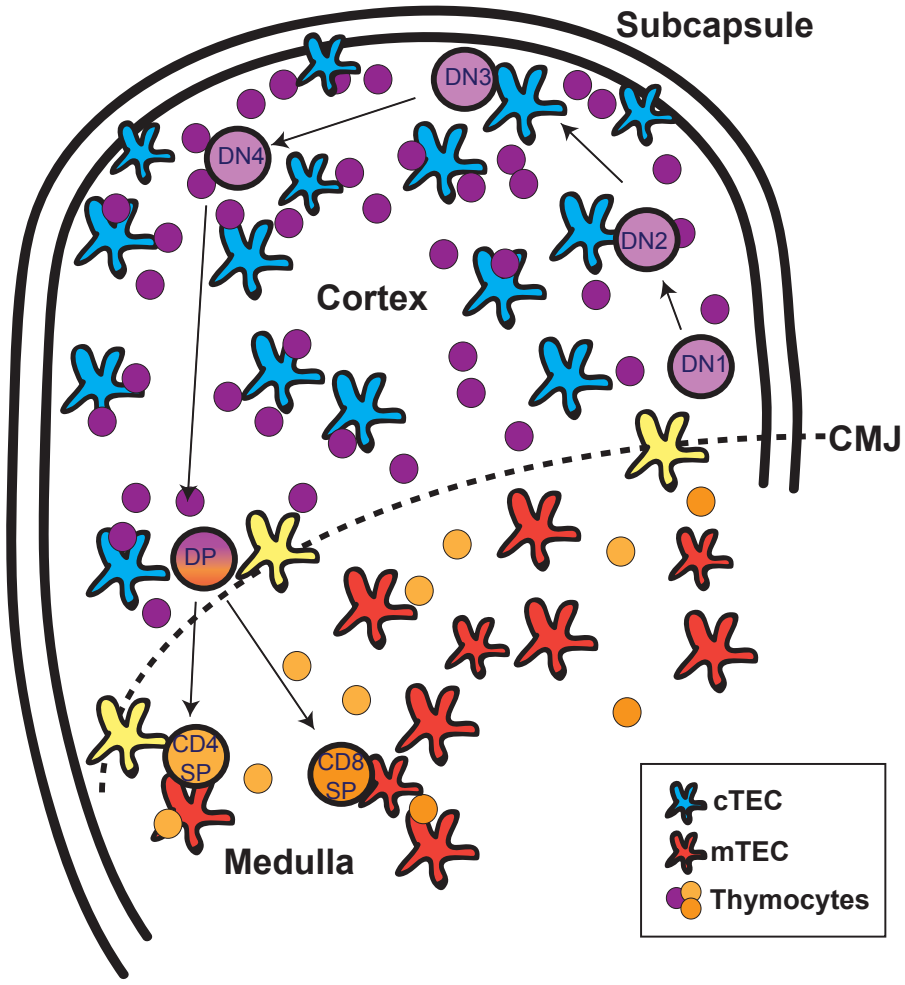

downregulate CD25 and become DN4 ($CD44^-c\text{-}Kit^-CD25^-$) thymocytes that are committed to the αβ as opposed to γδ T cell lineage. DN4 thymocytes undergo a proliferative burst (eight to nine cell divisions) and upregulate both CD4 and CD8 to become double positive (DP) thymocytes which constitute ~85% of total thymocytes (21, 22). TCRα gene rearrangement is initiated at the DP stage. TCRα and TCRβ polypeptides form TCRαβ heterodimers that along with non-covalently linked CD3 polypeptides are expressed at low levels on DP thymocytes.

Positive selection tests the ability of newly formed αβTCRs on DP thymocytes to recognize self-peptide in the context of self-MHC molecules (reviewed in (23) and (24)). The majority of DP thymocytes fail positive selection either because they do not express an αβTCR, or the expressed αβTCR does not recognize self peptide-MHC complexes with low affinity. In either case, these cells are not signaled to survive and undergo apoptosis (death by neglect). Only thymocytes that express a TCR capable of recognizing self peptide-MHC presented by cTECs are rescued from programmed cell death. In order to test the affinity of TCRs on DP thymocytes, cTECs present self-peptides in the context of MHC class 1 (MHCI) or MHC class II (MHCII) molecules. Cortical TECs have unique proteolytic pathways for generating peptides to be presented by MHC. Peptides presented in the context of MHCI are processed by the thymoproteosome, which contains a unique catalytic subunit exclusively found in cTECs, called β5t (25). Mice lacking β5t have a defect in positive selection of MHCI restricted $CD8^+$ thymocytes (25). Self-peptides are also presented in the context of MHCII molecules expressed on cTECs. In contrast to other antigen presenting cells (APCs), cTECs have the ability to endogenously process peptides using a process called macroautophagy, which is dependent upon lysosomal and serine proteases (reviewed in (23)). Deficiency in macroautophagy or in cathespsin L impairs positive selection of $CD4^+$ T cells (reviewed in (23)). The expression of unique peptide generating

machinery by cTECs is consistent with the notion that cTECs play an indispensable role in presenting a diverse and distinct set of peptides to positively select self-restricted DP thymocytes. After being positively selected, DP thymocytes are signaled to downregulate either CD4 or CD8 to become SP thymocytes that are restricted to MHCII or MHCI, respectively (reviewed in (24)). In addition, single positive (SP) thymocytes upregulate chemokine receptors such as CCR7 in response to chemokines (CCL19, CCL21) produced by TECs, which facilitates their migration into the medulla (26).

Central tolerance is established in the medulla where many self-reactive T cell clones are deleted during the process of negative selection. Medullary thymic epithelial cells (mTECs) have the unique ability to present a vast array of self-antigens termed tissue-restricted antigens (TRAs) that are otherwise expressed only in peripheral tissues. SP thymocytes that express TCRs that recognize self-antigen in the context of MHC with high affinity undergo apoptosis, thus preventing most autoreactive T cells from entering the periphery. While mTECs express a wide array of TRAs, the frequency at which each TRA is expressed is very low, reducing the likelihood of thymocyte-APC interactions (27, 28). Therefore, thymocytes must migrate quickly and efficiently throughout the medullary region of the thymus to maximize the frequency at which they encounter APC presentation of TRA (29).

The ability of mTECs to express a subset of TRAs is mediated by the transcription factor *autoimmune regulator* (AIRE) (30). AIRE binds to histone 3 on the lysine 4 residue (H3K4) and interacts with other transcriptional regulators to promote activation of “silent” genes that are otherwise lineage restricted (31, 32). Mice and humans deficient in *Aire* fail to eliminate autoreactive T cells during thymopoiesis and develop autoimmune polyendocrinopathy-candidiasis-ectodermal dystrophy (APECED) (30, 33). Presentation of TRAs to developing thymocytes in the medulla is not only restricted to the mTEC stromal population. Dendritic cells are also capable of presenting self-antigen in the context of MHC

to thymocytes, despite the fact that they are *Aire*$^{-/-}$. This is because mTECs have the unique ability to transfer self-antigen to DCs (34, 35).

Negative selection ensures that most cytotoxic CD8 and CD4 helper T cells do not bind to, and recognize self-peptide with high affinity, generating an autoimmune reaction. However, mTEC-mediated testing of TCR affinity is also important for regulatory T cell ($T_{Reg}$) development. $T_{Reg}$ cells are a subset of T cells that function to negatively regulate T cell immune responses that occur in response to autoimmune disorders, chronic infection or allergic reactions (36). Regulatory T cells are generated when SP thymocytes recognize self-peptide with high affinity, but not high enough to induce apoptosis (23). Therefore, the medulla not only provides an environment for the elimination of autoreactive T cells, but also promotes the maturation of T cells necessary for dampening peripheral immune responses and preventing self-reactivity.

SP thymocytes that survive both positive and negative selection emigrate from the thymus and once in the periphery, naïve $CD4^+$ and $CD8^+$ T cells circulate throughout the blood and lymphatic system. After encountering APCs that present foreign peptide-MHC complexes in secondary lymphoid organs, peripheral T cells undergo clonal expansion and differentiate into either helper $CD4^+$ or cytotoxic $CD8^+$ T cells to mediate their effector functions. However, for this to occur, cTECs and mTECs are required throughout the thymocyte maturation process to generate self-tolerant, yet self-restrictive T cells.

**Thymocyte Derived Signals are Important for TEC Maturation**

The progression of thymocytes from early thymic progenitors (ETPs) to functionally competent $CD4^+$ or $CD8^+$ T cells is a non-cell autonomous process that depends on appropriate signals from TECs. Conversely, several studies have shown that thymocytes provide indispensable signals for TEC survival and differentiation (37-39). Mouse models that display early blocks in thymocyte maturation have been used to study the contribution

of thymocyte-derived signals to cTEC and mTEC maturation (40, 41). RAG2/common $\gamma_c$-deficient and hCDε transgenic mice have a very early block in thymocyte maturation, specifically at the DN1 stage (40, 41). Consequently, there is a failure in cTEC differentiation and these mice lack a three-dimensional TEC network. However, if thymocyte maturation progresses beyond DN1 to DN3, as in the RAG2$^{-/-}$ model, these mice form three-dimensional cortical regions as well as medullary islets that fail to differentiate. These models clearly demonstrate that developing thymocytes provide signals that are required to generate mature cTECs and mTECs in the postnatal thymus. However, we have shown that the initial stages of TEC differentiation in the fetal thymus occur independently of thymocyte-derived signals. *Ikaros* is a transcription factor that is required for commitment to the lymphoid lineage and mice null for this transcription factor have a significant delay in B and T cell development due to a deficiency of thymus seeding hematopoietic progenitors at early fetal stages (42). When thymus organogenesis was studied in *Ikaros*$^{-/-}$ mice, Klug et al. found that the fetal thymus was capable of organizing into cortical and medullary regions at E15.5, despite the fact that there was a delay in thymocyte development (43). These data demonstrate that initial thymus organogenesis is independent of lymphoid-derived signals (41, 44).

**Involution**

The thymus undergoes gradual and progressive involution during aging. Acute thymus involution occurs as a result of cytoablative therapy, severe viral infection and pregnancy (45). Although the exact mechanisms that govern thymus involution are unknown, this process is in large part due to atrophy of the TEC compartment (7). As the thymus involutes, thymopoiesis declines. The resulting decrease in naïve T cell output restricts TCR diversity in the peripheral T cell pool, which in turn compromises the immune system's ability to respond to newly encountered antigens. Thus, thymus involution is

associated with increased susceptibility to infectious disease and cancer, poor responses to vaccines as well as increased autoimmunity.

Since thymus involution negatively impacts overall health, there has been considerable interest in restoring the involuted thymus to a functional state that supports robust thymopoiesis. SSA is a well-characterized approach that restores cellularity and organization of the involuted thymus in aging humans and mice. However, this effect is transient, as old, regenerated thymi may not be functionally competent compared to a young thymus (6). Specifically, regenerated thymi fail to form discrete medullary regions capable of expressing a full complement of TRAs (6).

Other approaches have been taken to regenerate the involuted thymus. For example, exogenous administration of keratinocyte growth factor (KGF) and IL-7 to old mice has been shown to increase TEC cellularity and thymopoiesis. During thymopoiesis, IL-7 is important for thymocyte survival and maturation, and IL-7 as well as IL-7 receptor (IL-7R) knockout mice exhibit significantly reduced total thymus cellularity (46, 47). Treatment with exogenous IL-7 results in an expansion of the early DN subsets and increased thymocyte cellularity in some, but not all studies (reviewed in (7)). Both KGF (also known as FGF7) production by developing thymocytes and FGFR2IIIb (FGF7 receptor) expression by TECs is required for thymocyte differentiation (48). Administration of KGF after cytoablative therapy results in increased total thymus cellularity as well as an expansion in the peripheral T cell pool (reviewed in (7)). However, similar to SSA, IL-7 or KGF administration only transiently restores thymus cellularity.

It is clear that the methods being used to rejuvenate the aged thymus are not restoring the full developmental program within the TEC progenitor population. Thus, a more promising approach would be to recapitulate the signaling pathways active during embryonic development to ensure proper functionality of TECs. However, in order to

generate TECs from fetal progenitors, it is important to understand the pathways that regulate their development during ontogeny.

**Overview of Thymus Organogenesis**

The pharyngeal region of the developing embryo is segmented into a series of bilateral arches that develop in an anterior to posterior manner. The pharyngeal arches (PAs) are comprised of pharyngeal pouches (pps) (endoderm) and pharyngeal clefts (ectoderm) separated by mesoderm-derived mesenchyme (Fig.2). The single layer endoderm of the first pp gives rise to the auditory tube, the second pp will develop into the palatine tonsil, and the fourth pp develops into the ultimobrachial body. Additionally, each third pp generates a shared primordium which gives rise to one thymus lobe and one PT gland (49).

To conclusively determine if the thymus originates from endodermal and/or ectodermal contributions, a series of experiments were performed in which E8.5-E9.0 3$^{rd}$ pp endoderm and ectoderm were transplanted under the kidney capsule of a *Foxn1*$^{nu/nu}$ (nude) mouse (50). This study found that 3$^{rd}$ pp endoderm, not ectoderm, was capable of giving rise to a thymus that could organize into cortical and medullary regions as well as support the maturation of functionally competent T cells. In addition, this study suggests that cells comprising the 3$^{rd}$ pp endoderm have already committed to either a thymus or PT fate very early in ontogeny.

Thymus fate is specified in the ventral region of the 3$^{rd}$ pp as early as E9.5-E10.5 (50), in a process that relies on endodermal-mesenchymal crosstalk (51). While the thymus- and PT-specific domains of the 3$^{rd}$ pp are not morphologically distinguishable at E11.5, organ specification is revealed by expression of the transcription factors *Forkhead box protein N1* (*Foxn1*) in the ventral, thymus-fated domain and *glial cells missing-2* (*Gcm2*) in the dorsal, PT-fated domain (52, 53) (Fig.3B). Therefore, these markers are useful to detect

**Figure 2. Pharyngeal morphology.**

The pharyngeal arches (PAs) are divided into three germ layers; endoderm (green), ectoderm (blue) and mesenchyme (yellow). The endodermal and ectodermal layers separate the pharyngeal pouches (pps) and pharyngeal clefts. Mesoderm- and neural crest-derived mesenchyme form the core of the PAs. The thymus and parathyroid originate from the 3$^{rd}$ pp endoderm.

**Figure 2. Pharyngeal morphology.**

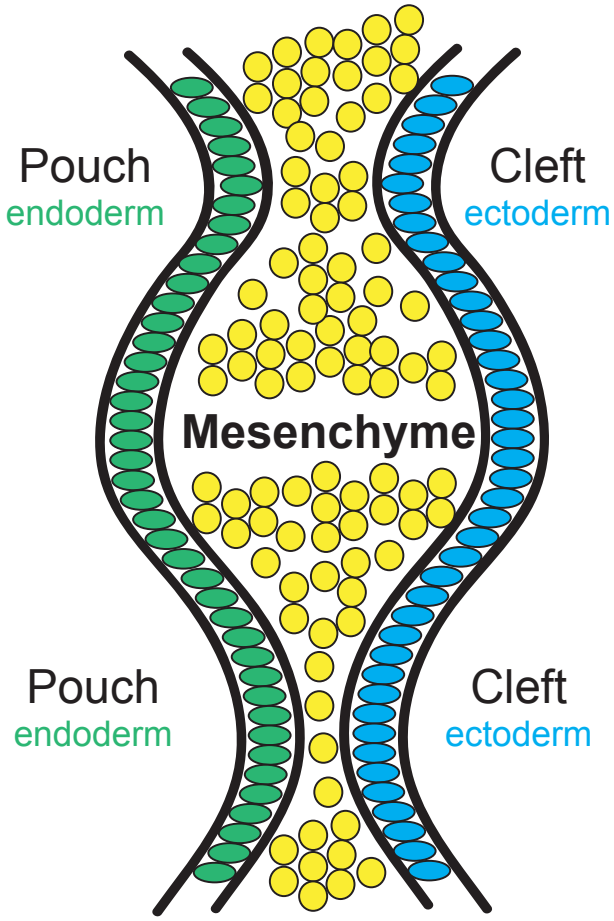

**Figure 3. Thymus organogenesis.**

(**A**) Coronal representation of the pharyngeal arches at E9.5. The thymus and parathyroid originate from the bilateral 3rd pp endoderm. (**B**) Sagittal representation of 3rd pp patterning in the E11.5 endoderm. The ventral domain of the 3rd pp gives rise to the thymus (green) and the dorsal domain gives rise to parathyroid (red). Although not morphologically distinguishable, cells fated to become thymus express *Foxn1* and those cells fated to become the parathyroid express *Gcm2*. Neural crest cells are represented in blue. (**C**) By E12.5, the thymus and parathyroid detach from the pharynx and begin to separate form one another. (**D**) The thymus and parathyroid migrate to their final locations. The thymus is located anterior to the heart and the parathyroid is adjacent to the thyroid.

**Figure 3. Thymus organogenesis.**

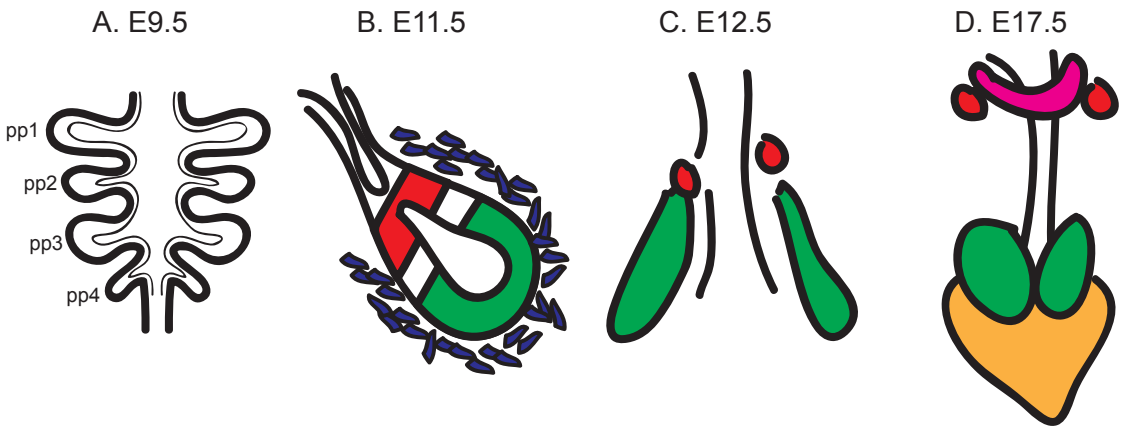

early patterning of the 3rd pp. *Foxn1* is required for the proliferation and differentiation of TECs and expression of *Gcm2* is necessary for the survival and development of the PT gland (54). Since neither transcription factor is required to establish organ fate, other molecular signaling networks are necessary to initiate cell fate acquisition.

Morphological identification of thymic lobes and PT glands is apparent beginning at E12.5 as the thymus and PT separate from the pharynx and one another, and begin to migrate to their final locations (Fig.3C,D). The thymus migrates ventrally and medially until it is just anterior to the heart and the PT migrates caudally into the neck to its final location next to the thyroid gland (Fig.3D). By E12.5-E13.5, cortical and proto-medullary regions are apparent in the thymic primordium and MHCII expression on TECs is initiated (55-57).

In order to identify TEC subsets, cytokeratins can be used to distinguish cortical from medullary TECs. By E12.5, the initial emergence of cortical and medullary thymic epithelial cell lineages is first observed and can be distinguished from one another by the expression of cytokeratin 8 (K8) and K5, respectively. TECs that are $K5^+$ tend to localize to the middle of the lobe (medulla) and express lower levels of K8, with $K5^-K8^+$ cells expressed towards the outer region of the lobe (cortex) (43, 55). As development progresses, progenitor-like cells that co-express K5 and K8, downregulate either K5 or K8, suggesting that these cells are committing further to either an mTEC or cTEC lineage (43, 55). By E17.5, the fetal thymus consists of distinct cortical and medullary regions that are $K8^+K5^-$ and $K8^-K5^+$, respectively, with only the cells at the CMJ being $K5^+K8^+$.

**Neural Crest and Mesoderm-derived Mesenchyme Contribute to Thymus Organogenesis**

Neural crest cells (NCCs) are a multipotent population of stem/progenitor cells that delaminate from the dorsal neural tube and migrate ventrally in discrete streams. NCCs give rise to numerous derivatives including, endocrine, mesenchymal and adipose cells, as

well as neurons, cartilage and skin (58). NCCs surround the 3rd pp by E10 and form the mesenchymal capsule that condenses around the developing thymic primordium (59, 60). Studies have shown that thymus fate is established prior to NCCs reaching the pouch and that NC depletion results in thymus aplasia or hypoplasia (61).

NCCs play an indispensible role in various processes during thymus organogenesis. Specifically, NCCs contribute to pouch patterning, supply essential growth factors that support the proliferation and outgrowth of TECs as well as contribute to thymus vasculature (62-65). This multipotent population of cells is capable of differentiating into pericytes and contributes to the thymus vasculature at E14.5 (66). Pericytes function to maintain vessel integrity and dysregulation of NC-epithelial interactions results in a delay in thymus vascularization (66). In addition, NCCs are required for the timely separation of the thymus and PT gland as well as the proper migration of the thymic primordium (63).

The transcription factor, *Pax3* is required for the survival, proliferation and differentiation of NCCs (67-69). A homozygous point mutation in the *Pax3* gene (*Splotch*), results in embryonic lethality by E13.5 due to numerous developmental defects (67, 68). In addition, these mice are characterized as athymic, suggesting a role for NCCs in thymus development. However, Griffith et al. found that *Pax3*$^{Sp/Sp}$ mutants were not athymic, but rather had severely ectopic, hyperplastic thymic lobes when compared to control littermates (70). Furthermore, when 3rd pp patterning was analyzed at E11.5, they found an expansion in the *Foxn1* domain as well as a significant reduction in *Gcm2* expression (70). This suggests that NCCs are not only important in thymus morphogenesis, but may play a role in patterning the 3rd pp and influence cell fate decisions.

Although not well studied, mesoderm derived mesenchyme in the pharyngeal arches also plays an important role in thymus organogenesis. The T-box transcription factor, *Tbx1*, is expressed by mesodermally-derived mesenchymal cells, and loss of *Tbx1* results in a complete failure in the segmentation of the pharyngeal apparatus (71). Consequently, the

3rd pp never forms, thus abrogating thymus development. Furthermore, the mesodermal expression of *Tbx1* is required for the patterning and proliferation of the pharyngeal endoderm (71), thus providing further evidence that mesoderm-derived mesenchyme provides additional, unknown factors that are necessary for proper development of the 3rd pp.

**Growth Factors and Morphogens Play Essential Roles in Thymus Organogenesis**

*Fibroblast growth factors*

During thymus development, the NCCs supply several fibroblast growth factors (FGFs) that are important to 3rd pp patterning, proliferation, outgrowth and eventual organ-specific migration. At E12.5, the NC mesenchymal capsule that surrounds the thymic primordium expresses *Fgf7* and *Fgf10*, which promote TEC proliferation (72, 73). In addition, TEC expression of FGF receptor, *FgfR2IIIβ*, persists in the postnatal thymus, as does thymocyte expression of *Fgf7* and *Fgf10* (48, 74, 75). Embryonic deletion of *FgfR2IIIβ* on TECs causes a block in TEC proliferation and differentiation, resulting in thymus hypoplasia and an arrest in thymocyte development (72). Interestingly, the *Fgf10* (72), and not *Fgf7 (76)*, deletion model recapitulates the phenotype observed in *FgfR2IIIβ*$^{-/-}$ mice, suggesting that *Fgf10* and *Fgf7* may function differently during thymus development. However, their continued expression in the postnatal thymus suggests a role for FGF signaling in TEC maintenance. Furthermore, exogenous administration of FGF7 is capable of transiently restoring the involuted thymus (reviewed in (7)), providing additional evidence that FGF signaling is important in TEC maturation and homeostasis.

*Fgf8* is another member of the FGF family that is implicated in embryonic thymus development. *Fgf8* is expressed in the ventral 3rd pp endoderm, but is almost completely absent from the pouch by E11.5 (77). Mice harboring a hypomorphic *Fgf8* allele display variable thymic phenotypes ranging from thymus aplasia to hypoplasia (78, 79). However,

these mice die in utero as a result of multiple complications including; aberrant cardiac development, craniofacial defects and hypoplastic pharyngeal arches (78, 79). The majority of these phenotypes may be secondary to the PA hypoplasia, suggesting that *Fgf8* is important for proper development of tissues derived from the PAs and NCCs (78).

*Bmp and SHH*

Morphogens are signaling molecules that act across a concentration gradient to influence the cell fate and patterning of developing tissues. *Bone morphogenic protein 4* (*Bmp4*) is a member of the TGFβ superfamily and functions to promote thymus development early in ontogeny. At E10.5, *Bmp4* is expressed in the arch mesenchyme, however is absent from the 3$^{rd}$ pp endoderm until E11.5 (80). At this time, *Bmp4* expression is restricted to the ventral, thymus-fated domain of the pouch endoderm and mesenchyme (80). *Bmp4* expression expands throughout the E12.5 primordium and is expressed in the adjacent mesenchymal capsule, suggesting *Bmp4* is necessary for thymus outgrowth (80).

To define in what capacity BMP4 acts in thymus and PT organogenesis, Gordon et al. performed a series of experiments in which *Bmp4* was deleted from either the 3$^{rd}$ pp endoderm or surrounding NC-mesenchyme. Pouch patterning was not altered in any of the mutants, and thymus-PT differentiation and migration were unaltered in mutants that had *Bmp4* deleted from either the NCCs or TECs (81). However, simultaneous deletion of *Bmp4* in both the NCCs and TECs resulted in incomplete capsule formation, a significant delay in organ separation and failure of both organs to migrate to their appropriate locations (81). Interestingly, both *Bmp2* and *Bmp4* are required for myocardial differentiation, as deletion arrests cardiac cells in a progenitor stage (82). Therefore, the mild thymus phenotype observed when *Bmp4* is deleted in the endoderm and NC-derived mesenchyme may be attributable to the redundant function of *Bmp2* in pouch patterning and thymus organogenesis.

Inhibition of BMP signaling using an antagonist, results in phenotypes similar to what is seen in the deletion models. Noggin is a secreted protein that antagonizes BMP signaling and its expression is restricted to the dorsal domain of the 3rd pp, suggesting it is necessary to inhibit thymus fate and allow for the establishment of PT fate (83, 84). When a Noggin transgene regulated by the *Foxn1* promoter is ectopically expressed in TECs, the inhibition of *Bmp* signaling results in hypoplastic, cystic thymic lobes that fail to migrate (83). This suggests that BMP signals are necessary for the development and migration of the thymic lobes.

There is evidence that BMP and FGF signaling networks act in concert to promote 3rd pp patterning and thymus development. Neves et al. demonstrated that sequential *Bmp-Fgf* signaling in chick is required for *Foxn1* and *Gcm2* expression in the 3rd and 4th pps. Mesenchymal production of *Bmp4* is required within a 24-hour period for 3rd and 4th pp endoderm development (85). However, beyond this point expression of *Bmp4* from the mesenchyme was no longer needed to promote thymic epithelial differentiation. Rather, expression of *Fgf10* from the mesenchyme was needed to support late-stage epithelial differentiation. Neves et al. proposed a model in which a signal from the endoderm is required to recruit somatopleural mesenchyme to the 3rd and 4th pps to induce a *Bmp4-Fgf10* signaling cascade that promotes patterning of the pouches into thymus and PT domains and supports their subsequent differentiation. Interestingly, they hypothesize that endodermal expression of *Fgf8* may be this inductive signal, given its role in early thymus ontogeny.

Sonic hedgehog (SHH) is another morphogen that is critical for 3rd pp patterning. SHH is expressed throughout the PAs, but is not detected in proximity to the 3rd pp until E10.5 when it is located in the endoderm closest to the pharynx (86). At E11.5, *Shh* expression extends into the ventral region of the first and second pps, however is no longer detected in the third or fourth pps (86). The SHH receptor Patched (*Ptc1*) is more widely

expressed. Until E11.5, *Ptc1* is restricted to the opening of the third and fourth pps and dorsal mesenchyme, from which point *Ptc1* expression expands in the mesenchyme, but remains absent from the most ventral regions of the 3rd and 4th pps (86).

SHH acts in opposition to BMP and is required for PT development (86). *SHH*$^{Null}$ mutants fail to express *Gcm2*, resulting in aberrant 3rd pp patterning and aparathyroidism (86). Given that SHH is no longer present in the mesenchyme to oppose BMP signaling, there is an expansion of BMP4 towards the pharynx (86). Interestingly, the expansion of *Bmp4* in the SHH null mutants is concomitant with an expansion of *Foxn1* throughout the 3rd pp and into the pharynx (86). This suggests that SHH signaling is required for PT development and in its absence, thymus fate expands throughout the pouch.

**Thymic Epithelial Progenitor Cells**

It is well established that the fetal thymus contains bipotent progenitors capable of giving rise to both cortical and medullary TECs (55, 87, 88). Thymic epithelial progenitor cells (TEPCs) were first characterized in a study using chimeric mice to define the role of the *Foxn1*$^{nu}$ (*nude*) gene in thymus organogenesis (88). Thymus development is arrested at an early stage in the *Foxn1*$^{nu/nu}$ model and these mice have a small, highly cystic thymic rudiment. In the presence of wildtype cells, the *nude* epithelium is unable to differentiate into mature TEC subsets, suggesting that the *nude* gene acts cell autonomously. Furthermore, in the adult chimeras, a small population of *nude* cells that failed to express mature TEC markers (*Foxn1*, MHCII, MTS10) was able to persist, suggesting that the *nude* rudiment contains TECs that are arrested at a primitive differentiation stage (88). Interestingly, these TECs expressed antigens identified by two monoclonal antibodies, mouse thymic stroma 24 (MTS24) and MTS20. These antigens were also expressed on a rare subset of mTECs in the adult thymus, further suggesting that these cells might be a progenitor population of TECs.

Later studies showed that MTS24 was expressed throughout the 3rd pp endoderm and the frequency of MTS24$^+$ TECs significantly declines with age and becomes restricted to the medullary region of the thymus (89). To address whether or not MTS24$^+$ cells were truly TEC progenitors, these cells were isolated and transplanted into recipient mice. Upon transplantation, MTS24$^+$ cells were able to differentiate and generate a thymic rudiment capable of attracting and supporting lymphocyte maturation (55, 89). This supported the notion that these cells were bipotent progenitors capable of generating cTECs and mTECs. To further characterize the TEPC, Depreter et al. found that MTS20/24 bound an orphan protein, placenta expressed transcript (Plet)-1. The expression pattern of Plet-1 is congruent with MTS20/24 in the 3rd pp and throughout thymus development (90). In addition, Plet-1 expression is detected in stem-like pancreas and mammary cells (90), therefore identifying Plet-1 as a novel protein that can be used to detect progenitor populations.

Additional molecules that are indicative of differentiation status and distinguish cTECs and mTECs have also been identified. Early in ontogeny, TECs express not only Plet-1, but also Claudins (Cldns) 3 and 4, CD205 and β5t (90-93). Cldn3/4 expression is associated with mTECs and CD205 as well as β5t are used to identify cTECs. However, at early developmental stages, these molecules also identify progenitor populations within the thymus. In the same study that defined Plet-1 positive cells as bipotent progenitors, Depreter et al. found that the tight junction proteins, Cldn4 and Cldn7 could also be potential TEPC markers. Interestingly, Cldn3/4 is expressed in the developing 3rd pp endoderm as well as by mTECs in the adult thymus (91). In addition, Hamazaki et al. found that Cldn3/4 positive cells eventually give rise to terminally differentiated Aire$^+$ mTECs (91), suggesting that these molecules identify progeny of the mTEC lineage. Similarly, studies have shown that CD205 cells and β5t positive cells identify the earliest progenitors of cTEC and mTEC lineages (91, 92). However, as development continues, their expression becomes restricted

to the cortical sublineage. Given that Cldn3/4, CD205 and β5t are all expressed as early as E11.5 and become lineage restricted throughout thymus development, suggests that bipotent progenitors are capable of expressing both cTEC and mTEC markers early in development, but are differentially regulated later in organogenesis. These data, as well as others, have shown evidence suggestive of a progenitor population within the adult thymus that is capable of generating medullary and cortical lineages (94, 95).

To discern if there is a different population of TEPCs within the adult versus fetal thymus, recent studies have employed the use of stem cell surface markers and cell culture to identify a population of self-renewing adult TEPCs that may be phenotypically different from that of fetal progenitors, but capable of giving rise to differentiated TEC lineages (96, 97). Specifically, $MHCII^{Lo}Sca^{+}$ cells isolated from the adult thymus were able to give rise to terminally differentiated TECs (96, 97). In addition, these and other studies have shown that adult TEPCs are capable of persisting in the presence of low to negative levels of *Foxn1* (96, 98). However, these reports do not agree on whether or not restoration of *Foxn1* levels is necessary for TEC maturation. Therefore, with the identification of a potentially rare population of adult TEPCs that are capable of giving rise to a functional thymus, further work needs to be done to define what molecular pathways govern adult TEPC maintenance and if this stem population is functionally distinct from that of fetal TEPCs.

**Transcriptional Regulation of Thymus Organogenesis**

Thymus development depends on complex and continuous interactions between differentiating endoderm, thymocytes, endothelial and mesenchymal cells. Failure in any component of this multicellular crosstalk can result in a multitude of developmentally aberrant phenotypes. While the molecular signaling networks that specify 3$^{rd}$ pp cell fate have yet to be defined, several transcription factors have been identified that are important

in the early stages of thymus organogenesis. These transcriptional regulators are discussed below and are summarized in Table 1.

*Foxn1*

*Foxn1* is a key transcription factor that is nonredundant and critical for TEC differentiation and proliferation. *Foxn1* expression is first detected in the 3$^{rd}$ pp at ~E11.25, and is restricted to the ventral, thymus-fated domain of the endoderm (54). During later stages of fetal development, *Foxn1* is widely expressed by both cTECs and mTECs. However, the amount and frequency at which TECs express *Foxn1* declines with age, suggesting a correlation between *Foxn1* levels and involution. The loss of *Foxn1* causes a reduction in TEC organization and proliferation and indirectly results in a decline in T cell output (99). Mice that have a hypomorphic *Foxn1* allele maintain normal levels of *Foxn1* throughout fetal TEC development, but expression is significantly reduced by one week postnatally (99). Specifically, TECs that express higher levels of *Foxn1* (MHCII$^{Hi}$UEA-1$^{Hi}$ mTECs) were more sensitive to *Foxn1* modulation (99). Given that reduction in *Foxn1* is an early event in thymus involution, this model phenocopies age-related thymus involution, but at an accelerated rate. The fact that fluctuating levels of *Foxn1* can impact TEC maturation is further supported by the use of a revertible hypomorphic *Foxn1* allele. Nowell et. al demonstrated that while *Foxn1* was not required for TEC fate commitment, it is required for divergence into either cortical or medullary TEC sublineages and that reducing the levels of *Foxn1* alters gene expression, which ultimately, affects the terminal differentiation and function of TECs (57). Interestingly, the genes that were affected are known regulators of thymic epithelial commitment and differentiation; such as *Pax1*, *MHCII* and *Dll4*, all of which were shown to be either directly or indirectly downstream of *Foxn1*.

**Table 1. Transcriptional regulation of thymus development.**

Description of the expression pattern and thymus phenotypes of transcription factors implicated as regulators of thymus organogenesis.

**Table 1. Transcriptional regulation of thymus development.**

| Transcription Factor | Location of Expression | Mutant Phenotype |
|---|---|---|
| Foxn1 | E11.25-restricted to ventral domain of 3rd pp<br>Expressed by TECs | Small, highly cystic thymic rudiment that contains undifferentiated, MTS24+ TEPCs |
| Tbx1 | E9.5-throughout 3rd pp endoderm<br>E10.5-restricted to dorsal domain of 3rd pp | Complete failure in segmentation of the pharyngeal endoderm, thymus never develops |
| Hoxa3 | E10.5-throughout 3rd pp endoderm and surrounding mesenchyme<br>E11.0-downregulated in 3rd pp endoderm and surrounding mesenchyme<br>E13.5-absent from 3rd pp endoderm and surrounding mesenchyme | Early block in 3rd pp patterning, delay in Foxn1 and Gcm2 expression, thymus aplasia or hypoplasia |
| Pax1 | E9.5- 3rd pp endoderm | Reduced thymocyte cellularity |
| Pax9 | E9.5- 3rd pp endoderm | Thymus hypoplasia and a failure of thymus-PT separation |
| Eya-1 | E10.5-throughout 3rd pp endoderm and surrounding mesenchyme | 3rd pp endoderm fails to detach from the pharynx, failure in pouch patterning, thymus aplasia |
| Six-1 | E10.5-throughout 3rd pp endoderm and surrounding mesenchyme | Athymic |
| Foxg1 | E10.0- ventral tip and proximal dorsal region of the 3rd pp<br>E11.5- ventral domain of 3rd pp<br>Expressed by TECs | Yet to be defiend |
| Isl1 | E9.0- ventral domain of 3rd pp endoderm<br>E10.0-ventral domain of 3rd pp endoderm<br>Expressed by TECs | Embryonic lethal at E9.5-E10.5 |
| Nkx2-5/6 | E9.0- 3rd pp endoderm<br>E10.0-ventral domain of 3rd pp endoderm | Aberrant pharyngeal endoderm development |

Furthermore, upregulation of *Foxn1* in the involuted thymus is sufficient to restore the function of key regulatory genes that promote TEC proliferation and differentiation (100). In contrast to SSA methods of thymus rejuvenation, this study also showed that the restored thymus was comparable in both stromal architecture and genetic profile to that of a young thymus (100). Furthermore, previous studies have also shown that when *Foxn1* is expressed in TEPCs, it promotes the differentiation of both cortical and medullary TEC lineages (87). Taken together, these experiments demonstrate that small changes in *Foxn1* levels can have profound effects on TEC differentiation and function.

Numerous studies have described the indispensible role *Foxn1* has throughout thymus development; beginning from onset of expression in progenitor cells at E11.25, its maintained expression to ensure TEC differentiation, as well as its decline at the onset of thymus involution. However, it is evident that *Foxn1* is a hallmark of thymus fate, and does not specify endodermal progenitors to thymus fate. Therefore, additional mechanisms and key regulatory factors must be required for cell fate decisions.

*Hox-Pax-Eya-Six Signaling Network*

The *Hox*, *Pax*, *Eya*, *Six* gene network is highly conserved from *Drosophila to* vertebrates. Each gene is expressed, at some point during ontogeny, throughout the 3$^{rd}$ pp, and mutations in any of these genes results in similar phenotypic abnormalities, including thymus and PT aplasia or hypoplasia.

*Hoxa3*, a member of the Homeobox protein family, is expressed by NCCs as they migrate throughout the PAs (101-103). By E10.5 *Hoxa3* is expressed in the endoderm of the 3$^{rd}$ and 4$^{th}$ pps as well as in the arch mesenchyme surrounding the two pouches (101-103). Detailed *in situ* hybridization (ISH) analysis of *Hoxa3* expression revealed that at E10.5, *Hoxa3* is strongly expressed throughout the 3$^{rd}$ PA mesenchyme and endoderm, but its expression is downregulated in the endoderm and mesenchyme at E11.0 and E12.0,

respectively, until it is completely absent by E13.5 (104). NCC migration is unaffected in *Hoax3* mutant mice and there is no defect in pp formation (101-103). However, there is an early block in 3rd pp patterning, which results in an aplastic or hypoplastic thymic phenotype as well as a hypoplastic PT that fails to migrate (101-103).

A recent study performed experiments to determine the expression pattern and timing of 3rd pp region-specific markers in *Hoxa3* null mutants. Temporal and spatial expression of thymus- and PT-specific markers revealed that *Hoxa3* is required for *Gcm2* expression to be maintained beyond E10.5 and its absence causes *Tbx1* expression to be significantly downregulated, although never extinguished in the presumptive PT-fated domain (104). When thymus-specific markers were analyzed, *Foxn1* expression was not detected until E12.0 (104). Tissue specific deletion of *Hoxa3* in the 3rd pp endoderm resulted in delayed expression of *Foxn1* coupled with thymus and PT ectopia and hypoplasia (104). The thymus and PT phenotype was similar in the NC deletion of *Hoxa3*, but there was a failure in organ separation and migration (104). Compound deletion of *Hoxa3* in the endoderm and NCCs phenocopied *Hoxa3* null mutants (104). These data suggest that *Hoxa3* contributions to thymus and PT development are tissue specific and required for proper patterning, organogenesis and morphogenesis.

The *Pax1/9*, *Eya1*, *Six1/4* signaling network is highly conserved from drosophila to vertebrates. During embryonic development, each transcription factor is differentially expressed in the ectoderm, endoderm and/or mesenchyme and mutations in any of the genes results in a range of thymus phenotypes (103). Specifically, the 3rd pp endoderm fails to detach from the pharynx in *Eya1*$^{-/-}$ embryos and *Gcm2* and *Foxn1*, are never expressed in the endoderm (105). Consequently, the thymus and parathyroid never form in these mutants. In addition, a mutation in *Pax1* results in reduced thymocyte cellularity, while *Pax9* mutants have a more severe phenotype, characterized by thymus hypoplasia and a failure of thymus-PT separation (reviewed in (106)). Interestingly, the thymus and kidneys are

absent in *Six1*$^{-/-}$ mice and they exhibit craniofacial abnormalities reminiscent to what is seen in mice with mutations in the transcription factors *Tbx1*, *Pax1* and *Eya1* (107). As described in all of these mutants, the severe thymus and PT phenotypes may be attributable to the fact that the 3$^{rd}$ pp was never patterned into distinct thymus and PT domains. However, none of the transcription factors discussed have been implicated in the establishment of thymus cell fate.

A comprehensive ISH analysis was performed to identify potential transcriptional targets that are expressed in the presumptive thymus-fated domain at and prior to E9.5 (108). Interestingly, several of the genes identified are expressed by cardiac progenitor cells and have a role in cardiac development. These common genes, as identified by the ISH analysis, are *Nkx2-5*, *Nkx2-6* and *Isl1*. Expression of *Nkx2-5*, *Nkx2-6* and *Isl1* is required for PE formation and all are expressed within the 3$^{rd}$ pp endoderm as well as have a role in postnatal TEC development (108-110). Specifically, *Nkx2-5* positive cells contribute to the TEC lineage (110) and *Isl1* is expressed in the thymus by late fetal and postnatal TECs (108).

In the same study, analysis of *Foxg1* expression revealed that it is initially expressed at E10.0 in the most ventral region of the 3$^{rd}$ pp and its expression is maintained in the same location at later stages, but is also detected in a discrete region of the dorsal domain. Our work has shown that at E11.5, FOXG1 expression overlaps with, and is independent of, FOXN1 (111). Similar to *Isl1*, *Foxg1* is expressed in late fetal and adult TECs (108). Additional studies need to be performed to determine if and how these genes contribute to fate specification of the 3$^{rd}$ pp.

**The Conundrum of Tbx1**

The exact role of *Tbx1*, a T-box transcription factor, during thymus organogenesis has been contested. *Tbx1* is expressed throughout the pharyngeal endoderm and arch

mesenchyme at E7.5, but is not expressed by NC-derived mesenchyme (112). Deletion or mutation of *Tbx1* results in cardiac outflow defects, thymus and PT hypoplasia as well as craniofacial abnormalities (113). Furthermore, homozygous deletion of *Tbx1* in mouse models phenocopies the 22q11.2 deletion (DiGeorge) syndrome, with thymus aplasia as a hallmark, thus implicating it as the gene responsible for DiGeorge syndrome (114-116). Based on these data, the prevailing thought in the literature is that *Tbx1* is required for thymus organogenesis, as loss or haploinsufficiency of *Tbx1* results in thymus aplasia or hypoplasia. However, conditional over expression of *Tbx1* results in cardiac hypertrophy, outflow tract defects and thymus hypoplasia (117). Therefore, this suggests that *Tbx1*-attribuatble phenotypes may be dose dependent, further complicating the role of *Tbx1* during thymus organogenesis.

Importantly, *Tbx1* is required for segmentation of the pharyngeal endoderm, as the pharyngeal apparatus fails to form in *Tbx1*$^{-/-}$ mice (112, 114, 115, 118, 119). Given that the loss of *Tbx1* abrogates 3$^{rd}$ pouch formation, it is reasonable to hypothesize that the athymic phenotype observed in DiGeorge syndrome is secondary to the loss of *Tbx1*, and attributable to the fact that the 3$^{rd}$ pouch never formed. Furthermore, temporal deletion of *Tbx1* reveals that loss of *Tbx1* expression at E8.5 abrogates 3$^{rd}$ pp formation, providing additional evidence that athymia is the result of a failure in pouch formation (120).

Furthermore, the expression pattern of *Tbx1* in the wildtype 3$^{rd}$ pp is interesting in that it is initially expressed throughout the pouch, but is downregulated by E10.5 in the ventral, thymus-fated domain and restricted to the dorsal, PT-fated domain (112, 121, 122). SHH is an upstream regulator of *Tbx1* (123, 124) and is required for *Gcm2* expression (121). However, *Tbx1* is expressed in 3$^{rd}$ pp endoderm in *Gcm2* deficient mice, suggesting that *Shh* is upstream of *Tbx1* and that *Gcm2* is downstream of *Tbx1* during PT organogenesis. Taken together, these data suggest that *Tbx1* is necessary of PT development and may antagonize thymus organogenesis.

Therefore, the first aim of this thesis addresses the hypothesis that *Tbx1* negatively regulates thymus fate and must be suppressed during thymus organogenesis. As discussed in Chapter 3, we found that when ectopically expressed in the thymus-fated domain of the 3rd pp, TBX1 suppresses FOXN1, inhibits TEC proliferation and arrests TEC differentiation at a very early progenitor stage. However, it does not reverse thymus cell fate. Our results refute the previously held notion that *Tbx1* is required for proper development of the thymus and clearly demonstrate that *Tbx1* is antagonistic to thymus organogenesis.

Given the notion that SHH and BMP act in opposition to pattern the PT and thymus in the 3rd pp, respectively, we can now add an additional factor, *Tbx1*, to the molecular signaling networks necessary for thymus development. Based on the literature and our published results, we have developed a model in which *Bmp4*-mediated expression of *Foxn1*, in addition to the downregulation of *Tbx1* in the ventral domain of the 3rd pp, is required for thymus organogenesis (Fig.4). Although these data strongly support our hypothesis, the molecular mechanisms necessary to downregulate *Tbx1* in the ventral domain of the 3rd pp to allow for the establishment of thymus cell fate, have yet to be defined.

Therefore, the second aim of this thesis is to identify the genetic pathways necessary to downregulate *Tbx1* expression in the 3rd pp to allow for the establishment, proliferation and differentiation of TEC progenitors.

**Figure 4. Model of molecular pathways that establish thymus cell fate in the 3rd pp endoderm.**

Model system of molecular signaling networks necessary for 3rd pp patterning and thymus cell fate. Bold lines indicate those pathways that are discussed and tested in this dissertation.

**Figure 4. Model of molecular pathways that establish thymus cell fate in the 3rd pp endoderm.**

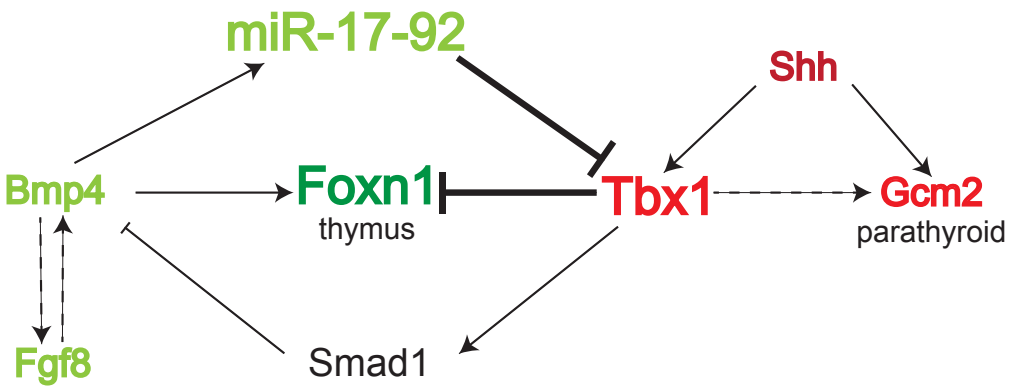

**Molecular Mechanisms that Regulate *Tbx1* in the 3rd pp Endoderm**

*The miR-17-92 cluster*

MicroRNAs (miRNAs) are a class of highly conserved, small, non-coding RNAs (ncRNA) that function to post-transcriptionally regulate gene expression (125). The first miRNA was discovered during a genetic screen studying larval development in *C. elegans*, and thousands more have since been identified in vertebrates (126, 127). Genes that encode miRNAs begin as primary transcripts in a stem-hairpin loop conformation (pri-miRNA). The RNAse III enzymes, Drosha and Dicer process the pri-miRNA transcript in the nucleus and cytoplasm, respectively to generate mature miRNA duplexes that are 18-24 nucleotides in length. Either the 5' or 3' end of the miRNA duplex is incorporated into the RNA-induced silencing complex (RISC), binds the 3' untranslated region (UTR) of its target and post-transcriptionally silences gene expression (reviewed in (128)). A single miRNA is capable of silencing numerous genes through imperfect base pairing, thus allowing them to regulate several developmental and physiological processes.

The *miR-17-92* cluster is comprised of six members: *miR-17*, *miR-18a*, *miR-19a, miR-20a*, *miR-19b-1* and *miR-92a-1*, and is found within an 800 base pair region on chromosome 13 (129). There is strong evidence implicating *miR-17-92* as an important regulator in hematopoietic and solid tumorigenesis as well as in immune, cardiovascular and neurodegenerative diseases. Although additional studies have uncovered roles for the cluster during normal developmental and aging processes, how this miRNA functions throughout multiple developmental pathways in various organ systems is under investigation.

The *mir-17-92* cluster is highly expressed throughout the embryo and has a significant impact on the normal development of several organs. Specifically, it contributes to the proliferation and branching of the lung epithelium, is required for B cell maturation and is required for cardiomyocyte differentiation (reviewed in (130)). Interestingly, *miR-17-92* is

the first miRNA cluster to be implicated in a human developmental syndrome. Loss of functional *miR-17-92* results in Feingold syndrome; a condition in which patients have numerous skeletal abnormalities, microcephaly as well as varying degrees of learning disabilities (131). Mice lacking *miR-17-92* recapitulate the phenotypes of Feingold syndrome, thus making it a good model system to understand its role in the disease as well to define the role of *miR-17-92* in development of other organ systems.

*The miR-17-92 cluster and Tbx1*

A recent report demonstrated that *Tbx1* is expressed in cardiac progenitor cells and must be downregulated to allow for the differentiation of cardiomyocytes (82). Interestingly, they found that *miR-17-92* directly binds the 3' UTR of *Tbx1* to silence its expression (132). Furthermore, they reported that *Bmp2* and *Bmp4* expression are required to initiate the *miR-17-92*-mediated silencing of *Tbx1* to promote cardiomyocyte differentiation. Given the role of *Bmp4* in thymus organogenesis coupled with our results showing that ectopic expression of *Tbx1* arrests TEC differentiation, we hypothesize that a similar *Bmp2/4-miR-17-92*-mediated mechanism regulates *Tbx1* expression in the 3$^{rd}$ pp endoderm.

Additional data has shown that TBX1 binds SMAD1 and suppresses *Bmp4* signaling, suggesting a regulatory loop (133). Based on these data and our results showing that *Tbx1* is indeed regulated by *miR-17-92* in the 3$^{rd}$ pp endoderm, we have developed a model in which *Tbx1* is regulated by a *Bmp-miRNA*-mediated pathway to specify thymus fate in the 3$^{rd}$ pp (Fig.4). Chapter 5 of this thesis will focus on the role of *miR-17-92* regulation of *Tbx1* in the 3$^{rd}$ pp endoderm and the subsequent development of the fetal thymus.

## CHAPTER2: Materials and Methods

### Mice

We generated a conditional *Tbx1* knock-in strain by targeting a *Tbx1* inducible expression cassette to the endogenous *Rosa26* locus to generate a $R26^{iTbx1}$ allele. In this *Tbx1* inducible cassette, a full-length mouse *Tbx1* cDNA and an IRES-GFP were inserted downstream of a floxed stop cassette (vector provided by Dr. A. McMahon). Expression of the $R26^{iTbx1}$ allele was activated in TECs by crossing $R26^{iTbx1}$ females with $Foxn1^{Cre}$ males (134). $R26^{iTbx1/+}$ and $R26^{+/+}$ littermate controls were maintained on a mixed C57Bl/6 genetic background at the MD Anderson Cancer Center Science Park in accordance with the guidelines set forth by the Association for the Accreditation of Laboratory Animal Care. Timed pregnancies were set up in the evening and monitored daily thereafter. The day of vaginal plug was considered embryonic day 0.5. Morphological cues and somite staging were used to determine embryonic stage. Yolk sac DNA was genotyped using:
Rosa26 forward 5'TTGCAATACCTTTCTGGGAGTT-3',
Rosa26 reverse 5'-AACCCCAGATGACTCCTATCCT-3' and
β-galactosidase reverse 5'-GACAGTATCGGCCTCAGGAAG-3'.
All experiments were performed in accordance with the MD Anderson Animal Care and Use Committee.

The *miR-17-*, $miR\text{-}17\text{-}92^{OE}$ , $Pax3^{Sp}$ and $Tbx1^{Fgf8}$ mouse models have been previously described and were obtained from the Jackson Laboratory (Bar Harbor, ME). The $Foxn1^{Cre}$ mice were gifted from the Manley Lab at the university of Georgia (Athens, GA).

**Histochemistry and Immunohistochemistry**

Embryos intended for either OCT or paraffin embedding were dissected into cold PBS and age-matched by somite counting. Those harvested for frozen sections were fixed in filtered 4% paraformaldehyde (PFA) dissolved in phosphate buffered saline solution (PBS) for 15 min (E11.5), 30 min (E13.5) or 40 minutes (E15.5). After fixation, the embryos were washed three times, for five minutes in PBS and placed in 20% sucrose (dissolved in PBS) overnight at 4°C. The next day, embryos were removed from the sucrose, embedded in OCT and stored at -80°C until ready for sectioning. Sagittal or transverse serial sections of the embryonic tissue were cut at 7µm on a Thermo Shandon Cryostat (Cryotome SME, SN:CS3094B0110) onto Superfrost Plus microscope slides (Fisher Scientific, Catalog Number: 12-550-15). When ready for analysis, slides were placed on the bench top and allowed to warn to room temperature for 5 minutes. They were then washed for 5 minutes in slide mailers containing PBST (PBS with 0.05%Triton X-100, BioRad, Catalog Number: 161-0407) at room temperature. The primary antibody mixture was prepared as follows: primary antibody at the appropriate dilution, 5% donkey serum and 0.05% Triton X-100 in PBS. 120µl of the primary antibody mix was added to each slide, coverslipped with parafilm and incubated overnight at 4°C in a humidified chamber. The next day, slides were rinsed three times, at 5 minutes per wash in PBST. The secondary antibody solution contained: host-specific secondary antibody diluted at 1:400 in 0.05% Triton X-100 in PBS. 120µl of the secondary antibody solution was applied to each slide, coverslipped and incubated in the dark for 1 hour at room temperature. Slides were washed in PBST two times, for five minutes, then incubated with 4',6-diamidino-2-phenylindole (DAPI) for 3 min at room temperature. After DAPI staining, three, five minute PBS washes in slide mailers were performed in preparation for mounting. Finally, slides were mounted with ProLong® Gold antifade reagent (Life Technologies) and coverslipped for imaging.

Embryos collected for paraffin embedding were fixed for a period of 1 hour to overnight (depending on the tissue size) in 4% PFA (prepared as described above). After PFA fixation, embryos were washed for five minutes in PBS, then dehydrated in an ethanol gradient as follows: 30%, 50%, 70%, 80%, 90%, 95%, then 100%. Each wash step was done at 4°C for 30 minutes, with the last 100% EtOH wash going overnight at 4°C. Embryos were permeabilized with xylenes and embedded in paraffin in accordance with general embedding protocols. Serial sections were cut at 7μm on a Leica ThermoShandon Finesse 325 microtome and allowed to dry on a plate warmer overnight at 37°C, then stored at 4°C until ready for analysis. Slides were allowed to warm to room temperature, placed in slide mailers, dewaxed in xylene and rehydrated through a methanol gradient as follows: two, five minute xylene washes, one minute in each wash step: 100% MeOH, 100% MeOH, 95% MeOH, 70% MeOH and cold tap water. Then slides were subjected to an antigen retrieval to reverse PFA crosslinks. Slides were transferred from tap water directly into slides mailers containing AR buffer (10mM $Na_3C_6H_5O_7 \bullet 2H_2O$, pH 6, 0.05% Tween 20) in a boiling (95°C - 100°C) water bath for 30 minutes. The amount of time in the AR buffer can be adjusted to lengths between 20 and 60 minutes. Remove slide mailers from the boiling water bath and allow slides to slowly cool to room temperature in the AR buffer (approximately 15 minutes). Prior to adding the primary antibody mixture, wash slides in 0.05% PBST for 1 minute. Prepare primary antibody mixture as follows: primary antibody at the appropriate dilution and 10% donkey serum into 0.05% Triton X-100 in PBS. Add 120μl of the primary antibody mix to each slide, coverslip with parafilm and incubate overnight at 4°C in a humidified chamber. The next day, slides were washed three times, five minutes each on a rocker. Dilute secondary antibody in PBST and add 120μl per slide, coverslip and incubate at room temperature for 30 minutes to 1 hour in the dark. Repeat wash steps in the dark, and then add DAPI for three minutes as described above. Finally, slides were rinsed in PBS for two, five-minute washes and mounted using ProLong Gold.

Paraffin embedded tissues collected for hematoxalyn and eosin (H&E) staining were processed according to standard techniques. Primary antibodies used were goat anti-Foxn1 (1:200, Santa Cruz, G-20), rabbit anti-Tbx1 (1:100, Abcam), rabbit anti-Gcm2 (1:200, Abcam), rabbit anti-Foxg1 (1:50, Abcam), rat anti-BrdU (1:10, Serotec), goat anti-β5t (1:200, MBL), rat anti-Ly75 (1:100, Abcam), K14 (1:400, Covance), Biotinylated UEA1 (1:200, Vector), rabbit anti-Aire-1 (1:50 Santa Cruz, M-300), rabbit anti-Claudins 3 and 4 (1:200, Invitrogen), K5 (1:400, Covance), Plet-1 (kindly provided by Dr. Claire Blackburn), Ikaros (1:100, Santa Cruz, M-20). All secondary antibodies were conjugated with DyLight 488 (Jackson Immunoresearch).

BrdU (300µl of 10mg/ml) was injected by the intraperitoneal (IP) route into pregnant females and embryos were harvested after a 90 minute chase. Cells from serial sections were counted based on expression of FOXN1, GCM2, TBX1, and/or BrdU using Cell Profiler (Broad Institute) or Imaris (BITPLANE). Images were taken on a Leica DM600b using LAS X Software.

**Flow Cytometry**

Embryonic TEC analysis was adapted from the Gray et al. protocol (135). For TEC analysis, fetal thymi were dissected out of the embryo into cold RPMI (ThermoScientific) containing 5% fetal calf serum and processed as described. Then, the thymi were incubated in 0.125% Collagenase (Sigma) and 0.1% DNase (Roche) for three 10 minute periods in a 37°C water bath until the tissue was completely digested. Specifically, after each incubation period, the tissue was gently aspirated using a 1 mL pipette and supernatant was collected in a separate 50 mL conical containing FACS wash buffer (PBS pH 7.2, 0.005M EDTA, 2% fetal calf serum). The single cell suspensions were spun down at 1250 rpm for 4 minutes to generate a cell pellet. The supernatant was discarded and

cells were re-suspended in 200µl -2000µl, depending on the size of the cell pellet and total cellularity was calculated using a Countess (Invitrogen).

For analysis of thymocyte subsets, fetal thymi were pressed through a 70µm strainer (Fisher). Single cell suspensions were centrifuged at 1500 rpm for 5 minutes as cellularity was calculated as described above. Cells were resuspended in FACS wash buffer and aliquoted into single color control and data tubes, and then stained with fluorochrome-conjugated antibodies in FACS buffer for 20 minutes on ice. After incubation with antibodies, cells were washed in 1 mL of FACS wash buffer, vortexed, spun down as described above and re-suspended in PBS for analysis. Propidium iodide (Invitrogen) was added (0.5 µg/ml) to each sample prior to analysis to exclude dead cells. Anti-CD326 (clone G8.8) conjugated to PE/Cy7, anti-I-A/I-E (clone M5/114.15.2) and anti-CD25 (clone PC61) conjugated to Pacific Blue, anti-CD326 (Clone G8.8) conjugated to allophycocyanin and anti-CD117 (clone 2 B8) conjugated to allophycocyanin -Cy7 were purchased from Biolegend. Anti-CD44 (clone IM7) conjugated to allophycocyanin, anti-CD8α (clone 53-6.7) conjugated to PE-Cy7, anti-CD45 (clone 30-F11) conjugated to PerCp-Cy5.5 were purchased from eBioscience. Anti-CD4 (clone RM4-5) conjugated to Qdot® 605 was purchased from Invitrogen. To exclude erythrocytes, granulocytes, dendritic cells, macrophages and NK cells from the thymocyte analyses, the following antibodies, all conjugated to PE-Cy5 were purchased form eBioscience: TER-119, CD11c (cloneN418), CD11b (clone M1/70), NK-1.1 (clone PK136) and Ly-6G (clone RB6-8C5). Cells were analyzed or sorted on a FACS Aria II (BD Science). Data were analyzed using FlowJo software (Tree Star).

**RNA Isolation, cDNA Synthesis and Real-time Quantitative Reverse Transcriptase Polymerase Chain Reaction (qRT-PCR)**

FACS sorted *R26*$^{iTbx1}$ and control TECs from a given litter were pooled and lysed in Trizol (Ambion) and stored at -80°C until ready for RNA isolation. RNA was isolated using a protocol adopted from the Ehrlich lab (The University of Texas, Austin, TX). The cells in Trizol were removed from -80°C and 2µl of linear acrylamide (Ambion) was added to each tube, followed by 200µl of cholorform. Each sample was shaken vigorously for 15 seconds and incubated on ice for 10 minutes. Then the cell samples were centrifuged at 13,000 rpm for 15 minutes at 4°C. During the 15-minute spin, 2µl of linear acrylamide was added to new, labeled tubes and the upper, translucent layer of the chloroform mixture was added to the new tube containing the linear acrylamide. As much of the upper, translucent layer was transferred as possible, while avoiding contamination from the middle layer. Then, 500µl of isopropanol was added to each tube, shaken vigorously for 15 seconds, then stored at -20°C overnight.

The following day, the samples were removed from the freezer and centrifuged at 13,000 rpm for 15 minutes at 4°C. The supernatant was removed using a pipette, without disturbing the pellet. Then, 1mL of 70% ethanol/DEPC water was added to each tube. The tubes were gently inverted and centrifuged at 7,500 rpm for 10 minutes at 4°C. The alcohol was removed using a pipette, and the pellet was allowed to air dry. Finally, the cell pellet was re-suspended in 5µl of RNase-free DEPC water and stored at -80°C for cDNA synthesis.

First-strand cDNA was synthesized using a SuperScript® III First-Strand cDNA synthesis kit (Invitrogen) according to the manufactuer's protocol. TaqMan® Gene Expression Master Mix (Applied Biosystems) and TaqMan primers (Applied Biosystems) were used for quantitative reverse transcriptase PCR (qRT-PCR) analysis of *Foxn1*, *Tbx1* and *α-tubulin* (endogenous control). Samples were analyzed using a LightCycler® 480 (Roche). In each experiment, comparators were set to a value of 1. All experiments were repeated 3 times and analyzed using the ΔΔCt method.

Primer Sequences:

*Foxn1*: Mm00433946_m1

*Tbx1*: Mm00448848_m1

*α-tubulin*: Mm00846967_g1

**In Situ Hybridization**

The dissection station and all dissection tools were wiped down with RNase Off (Ambion) prior to harvesting embryos. Embryos were dissected into cold DEPC (diethylpyrocarbonate)-treated PBS and fixed in 4% PFA (DPEC PBS) overnight. The next day, tissue was washed in PBS, dehydrated in an ethanol gradient, permeabilized using xylenes and embedded in paraffin, as previously described. However, all of these steps were performed in RNase-free conditions. Serial sections were cut at 14μm on a Leica ThermoShandon Finesse 325 microtome that had been treated with RNase off and then slides were allowed to dry on a plate warmer overnight at 37°C, then stored at 4°C until ready for analysis.

Prior to beginning the in situ, slide mailers were soaked in 1M NaOH overnight, rinsed with DEPC water and autoclaved. Slides were allowed to warm to room temperature on a bench top that had been thoroughly wiped down with RNase wipes. Tissue sections were then dewaxed in two, 10 minute xylene washes followed by rehydration steps in an ethanol/DEPC PBS gradient: 100%, 100%, 90%, 70%, 30%. Slides were incubated in each ethanol wash for two minutes at room temperature then washed in DEPC PBS for 5 minutes. 200μl of hybridization solution containing 0.5μg/mL of dig-labeled riboprobe was applied to each slide and then coverslipped using parafilm. Slides were incubated overnight in a humidified chamber with 2X SSC (DEPC) and formamide (in the bottom of the chamber) at 65°C.

The following day, slides were removed from the humidified chamber, transferred into slide mailers containing prewarmed 0.5X SSC, 20% formamide and washed at 65°C for 20 minutes. This step was repeated for a total of three washes. While slides were incubating at 65°C, 1X NTE solution was warmed to 37°C and after the third SSC/formamide wash, slides were then rinsed in 1X NTE for 15 minutes. Slides were washed for 30 minutes in pre-warmed NTE containing 10µg/mL RNase A (Sigma) at 37°C to minimize background, then washed in NTE alone for 15 minutes at 37°C. After the NTE washes were complete, slides were once again washed in pre-warmed 0.5X SSC, 20% formamide for a total of four 20 minute washes at 65°C. Washes can be extended to one hour each, if necessary. Subsequently, slides were washed for 30 minutes in 2X SSC at room temperature. During this time, a 1% blocking solution was prepared by dissolving blocking powder in MAB at 55°C. Slides were incubated in slide mailers containing the 1% blocking solution in MABT for one hour at room temperature. During this hour, anti-Dig-AP antibody diluted to a concentration of 1:100 in 1% blocking solution/MABT was incubated on ice. Finally, the slides were placed in a humidified chamber containing MAB and 200µl of the antibody solution was added to each slide and coverslipped using parafilm. The humidified chamber containing slides was incubated at 4°C overnight.

At the beginning of day 3, the parafilm coverslips were removed and the slides were placed in mailers and washed in TBST at room temperature for the following amounts of time: 10 minutes, 20 minutes then six, 1 hour washes. After the last TBST wash, slides were washed for 10 minutes in AP buffer at room temperature. During the 10 minute AP wash, enough BM Purple to add 200µl to each slide was allowed to warm to room temperature in the dark. In a humidified chamber containing distilled water, 200µl of BM Purple was added to each slide and coverslipped with parafilm. The humidified chamber was placed at room temperature in the dark and monitored daily until the color reaction was complete. Each day, the slides were washed in AP buffer for 10 minutes and new BM

purple solution was added. Once the color reaction was complete, the staining process was stopped by rinsing slides in PBS. Tissue sections were fixed in 4% PFA for 20 minutes then washed for 1 minute in PBS containing 5μM EDTA at 4°C. Slides were counterstained with nuclear fast red, then dehydrated along a methanol/PBS gradient: 30%, 50%, 70%, 90%, 100%, 100%. Each methanol wash was performed at room temperature for 5 minutes. Finally slides were placed in xylene for 5 minutes and mounted with cytoseal and a glass coverslip for imaging. Images were captured using an Aperio (Scan Scope) and an Olympus bright field microscope.

The following probes were used for ISH analysis: *miR-17*, *miR-19a* and *miR-92a* (Exiqon) and *Fgf8* and *Bmp4* (kindly provided by Dr. Virginia Bain).

ISH Solutions:

1. 20X SSC- 175g NaCl, 88g $Na_3C_6H_5O_7 \bullet 2H_2O$ (sodium citrate dehydrate), add DEPC water to 1L
2. 10X NTE- 292g NaCl, 100mL 1M Tris (pH 7.5), 100mL 0.5M EDTA, add DEPC water to 1L and autoclave
3. AP Buffer- 1mL 5m NaCl, 2.5mL 1M $MgCl_2$, 50μl Tween-20, 2.5mL 2M Tris (pH 9.75), 2mM Levamisole, add water to 50mL
4. MAB- 5.8g Maleic acid, 4.4g NaCl, pH to 7.5 using NaOH, add water to 500mL, autoclave
5. MABT- Add 0.1% Tween-20 to MAB
6. 10X TBST (make fresh solution each time)- 8g NaCl, 0.2g KCl, 25mL 1M Tris (pH 9.75), add water to 99 mL then add 1mL of Tween-20
7. Rnase A (10mg/mL) – Dissolve 0.01g of Rnase A in 900μl of 0.01M sodium acetate (pH 5.2) at 100°C for 15 minutes. Allow to cool to room temperature, add 100μl of 1M Tris

8. Hybridization Buffer- 25mL formamide, 12.5 mL 20X SSC (DEPC), 5.0mL 50% dextran sulfate, 6.5mL DEPC water, 50µl Heparin (50µg/µl), 50 µl Tween-20, 400µl 1M $Na_3C_6H_5O_7 \bullet 2H_2O$, 0.005g tRNA powder/ Filter sterilize, aliquot and store at -80°C

**Statistics**

Prism 6.0 (GraphPad version 6.0b; Sand Diego, CA) and Microsoft Excel were used for statistical analyses. We used a Student's *t* test to evaluate differences between controls and mutants regarding the number of cells expressing FOXN1, GCM2, TBX1 and/or BrdU. A *p*-value <0.05 was considered statistically significant.

## Chapter 3: Ectopic TBX1 suppresses thymic epithelial cell differentiation and proliferation during thymus organogenesis

Note this chapter is based on: Reeh, K. A., K. T. Cardenas, V. E. Bain, Z. Liu, M. Laurent, N. R. Manley, and E. R. Richie. 2014. Ectopic TBX1 suppresses thymic epithelial cell differentiation and proliferation during thymus organogenesis. *Development* 141: 2950-2958. With permission from the copyright holder.

### INTRODUCTION

By E11.5, the thymus- and parathyroid-fated domains can be recognized by *Foxn1* and *Gcm2* expression, respectively. However, although these transcription factors regulate differentiation, they do not specify thymus versus parathyroid fate (57, 87, 121). A *Hox-Pax-Eya-Six* cascade is implicated upstream of thymus specification, but has not been directly linked to the establishment of thymus fate (106). Additional transcription factors with restricted expression patterns in the 3$^{rd}$ pp have been identified, but their role in thymus fate is not yet established (108). Thus, the transcription factors and molecular pathways that specify thymus fate and regulate thymus organogenesis are not yet defined.

Earlier reports suggested that the T-box transcription factor TBX1 is essential for thymus organogenesis because thymus aplasia is a characteristic feature of *Tbx1* homozygous deletion mutants (40, 114, 121, 136). However, TBX1 is required for segmentation of the pharyngeal apparatus and in its absence, the pharyngeal pouches do not develop (112, 114, 115, 118, 119). Therefore, the athymia observed in the absence of *Tbx1* is a secondary consequence of defective pouch formation. As a result, the potential role of *Tbx1* in thymus organogenesis cannot be determined from analysis of *Tbx1* null embryos. In the pharyngeal region, Tbx1 is expressed in arch mesenchyme and in pouch endoderm, but not by NCCs (112). Thymus hypoplasia was reported in a transgenic line expressing a *Tbx1* transgene in the *Tbx1* expression domain (117). Since the *Tbx1*

transgene was widely expressed in mesenchyme and endoderm, the mechanism(s) leading to thymus hypoplasia are unclear. By E10.5 *Tbx1* expression in the 3rd pp is restricted to the parathyroid domain and excluded from the thymus domain (112, 122, 137), suggesting that *Tbx1* may be necessary for parathyroid formation, but antagonistic to thymus development. This notion is supported by reports showing that *Tbx1* is a downstream target of SHH signaling (123, 124) and that *Foxn1* expression is expanded in the 3rd pp of *Shh* null mice (86).

To test the hypothesis that *Tbx1* expression in 3rd pp endoderm suppresses thymus fate and/or TEC differentiation, we generated a novel mouse strain in which a stop-floxed *Tbx1* allele was knocked into the ubiquitously expressed *Rosa26* locus. We used *Foxn1*$^{Cre}$ to activate *Tbx1* expression in the thymus fated domain of the 3rd pp. Here we show that ectopic *Tbx1* expression in the ventral 3rd pp suppresses *Foxn1* expression, alters patterning of organ specific domains, inhibits TEC proliferation and blocks TEC differentiation at an early progenitor stage, but does not reverse thymus fate. The results support the hypothesis that *Tbx1* negatively regulates TEC growth and differentiation and that extinction of *Tbx1* expression in 3rd pp endoderm is a prerequisite for thymus organogenesis.

## RESULTS

### Foxn1$^{Cre}$ activates ectopic expression of the R26$^{iTbx1}$ allele in the ventral domain of the 3rd pp

*Tbx1* is expressed throughout 3rd pp endoderm at E9.5, but by E10.5 is restricted to the dorsal, parathyroid fated domain (112, 121, 122, 138). *Foxn1* expressing cells are present in the dorsal 3rd pp and extend into pharyngeal endoderm in the absence of SHH, a positive regulator of *Tbx1* expression (86, 123, 124). Taken together, these data suggest that TBX1 antagonizes thymus development. Therefore, we used a gain-of-function

approach to test this hypothesis. *Tbx1* cDNA and an IRES-GFP tag were inserted into a modified *Rosa26* targeting vector containing a floxed stop cassette to generate a knock-in strain hereafter referred to as $R26^{iTbx1}$ (Fig. 5). This allele activates expression of both *Tbx1* and *EGFP* after Cre-mediated deletion of the stop cassette.

We used $Foxn1^{Cre}$ to activate ectopic *Tbx1* expression in the ventral, thymus fated domain of the 3rd pp beginning at ~E11.25 (134). Thymus fate is specified in 3rd pp endoderm as early as E9.5-E10.5 prior to expression of *Foxn1*, which is essential for TEC differentiation and proliferation (reviewed in (51, 106)). Therefore, $Foxn1^{Cre}$ activates expression of the $R26^{iTbx1}$ allele in ventral 3rd pp endoderm after the cells commit to a thymus fate and are beginning to differentiate. Immunohistochemical (IHC) analysis of GFP expression in the $Foxn1^{Cre/+}$;$R26^{iTbx1/+}$ 3rd pp verified the predicted ectopic expression of $R26^{iTbx1}$ in the ventral, but not in the dorsal domain and confirmed the absence of a GFP signal in $Foxn1^{Cre/+}$;$R26^{+/+}$ controls (Fig. 6). Continued expression of the $R26^{iTbx1}$ allele in fetal thymi throughout ontogeny was confirmed by FACS analysis of GFP expression, which also verified restriction of the GFP signal to $EpCAM^{+}$ $CD45^{-}$ TECs (Fig. 6).

**Ectopic TBX1 expression suppresses FOXN1 but does not alter GCM2 expression**

We asked whether ectopic expression of *Tbx1* in the ventral domain altered patterning of the 3rd pp at E11.5. IHC staining of serial sections from $Foxn1^{Cre}$;$R26^{+/+}$ controls confirmed that endogenous TBX1 is restricted to the dorsal, parathyroid fated domain (Fig. 7A), whereas FOXN1 is restricted to the ventral, thymus fated domain (Fig. 7A, 7C). FOXN1 and TBX1 co-expressing cells were not found in the control 3rd pp. In contrast to the restricted expression of TBX1 in the control 3rd pp at this stage, we found an increased number of TBX1 positive cells located in both the ventral and dorsal regions of the

**Figure 5. Generation of *Rosa26Tbx1* conditional knock-in mice.**

(**A**) Schematic illustration of the *Rosa26* genomic wild-type (WT) locus, targeting vector and targeted knock-in (KI) locus. Black triangles represent the loxP sites. The black bar represents the 5' probe used for the Southern Blot screen. Arrows represent the primers used for the PCR screen for the targeting event, which amplify a 1.2 kb PCR product from the KI allele, but not the wild-type allele. (**B**) Southern blot analysis of genomic DNA from Neo resistant ES cell lines after electroporation. The genomic DNA samples were digested with Hind III and hybridized with the 5' probe shown in S1A. The 5' probe hybridizes with a 4.3 kb band from the Rosa26 WT allele and a 3.6 kb band from the $R26^{iTbx1}$ allele. (**C**) PCR genotyping analysis of genomic DNA from $R26^{iTbx1}$ strain in which a 298bp band represents the WT allele and a 456bp band represents the mutant allele.

**Figure 5. Generation of *Rosa26Tbx1* conditional knock-in mice.**

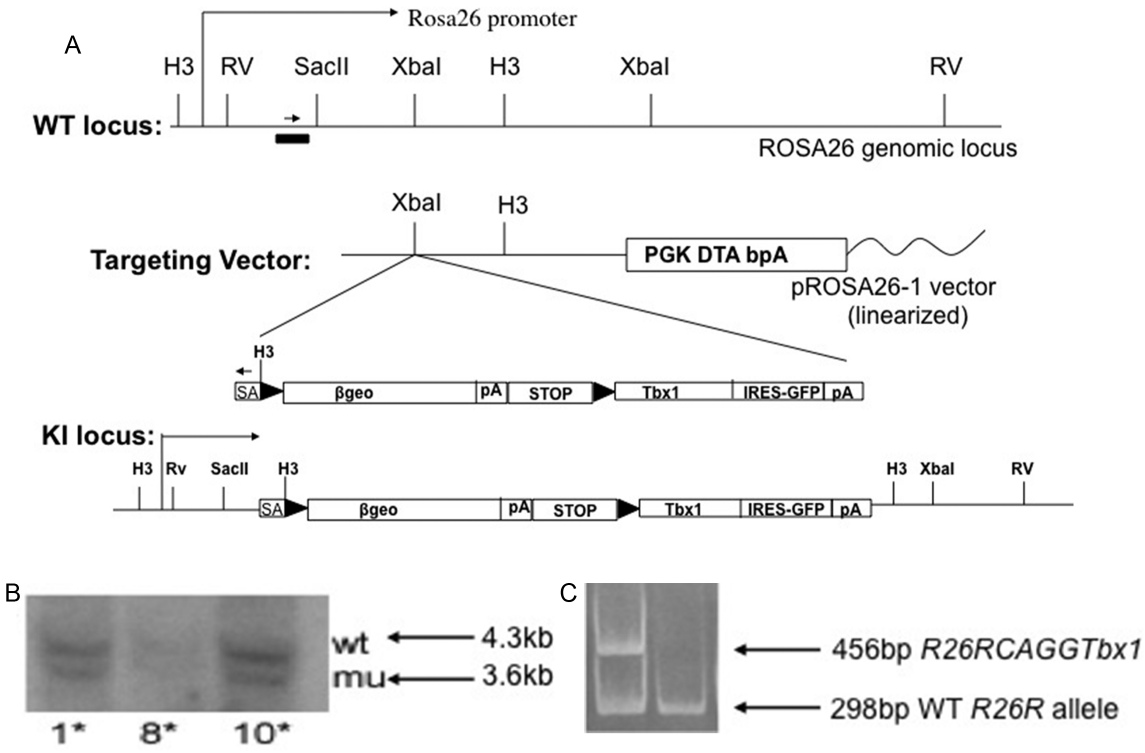

**Figure 6. Ectopic *Tbx1* is expressed in the thymus-fated domain of the 3rd pp and in TECs, as reflected by GFP expression.**

(**A,B**) Representative IHC stains of sagittal sections from E11.5 3rd pp show GFP expression in the *R26*$^{iTbx1}$ mutant (**B**) but not the control (**A**) and verifying ectopic expression of *Tbx1* in the ventral, but not dorsal, domain of the pouch. (**C**) FACS analysis of E15.5 control and *Foxn1Cre;R26*$^{iTbx1/+}$ thymi showing electronic gates set around EpCAM$^{+}$ CD4$^{5-}$ TECs (red), CD45$^{+}$ thymocytes (blue) and EpCAM$^{-}$CD45$^{-}$ non-TEC stromal cells (green). (**D**) Histograms showing GFP expression in the corresponding TEC, thymocyte and non-TEC stromal cell subsets. The GFP signal in *Foxn1Cre;R26*$^{iTbx1/+}$ TECs confirms continued expression of the *R26*$^{iTbx1}$ allele in mutant TECs. The data also confirm that the GFP signal is restricted to EpCAM$^{+}$ CD45$^{-}$ TEC subset in the mutant thymus and is not detected in control TECs.

**Figure 6. Ectopic *Tbx1* is expressed in the thymus-fated domain of the 3rd pp and in TECs, as reflected by GFP expression.**

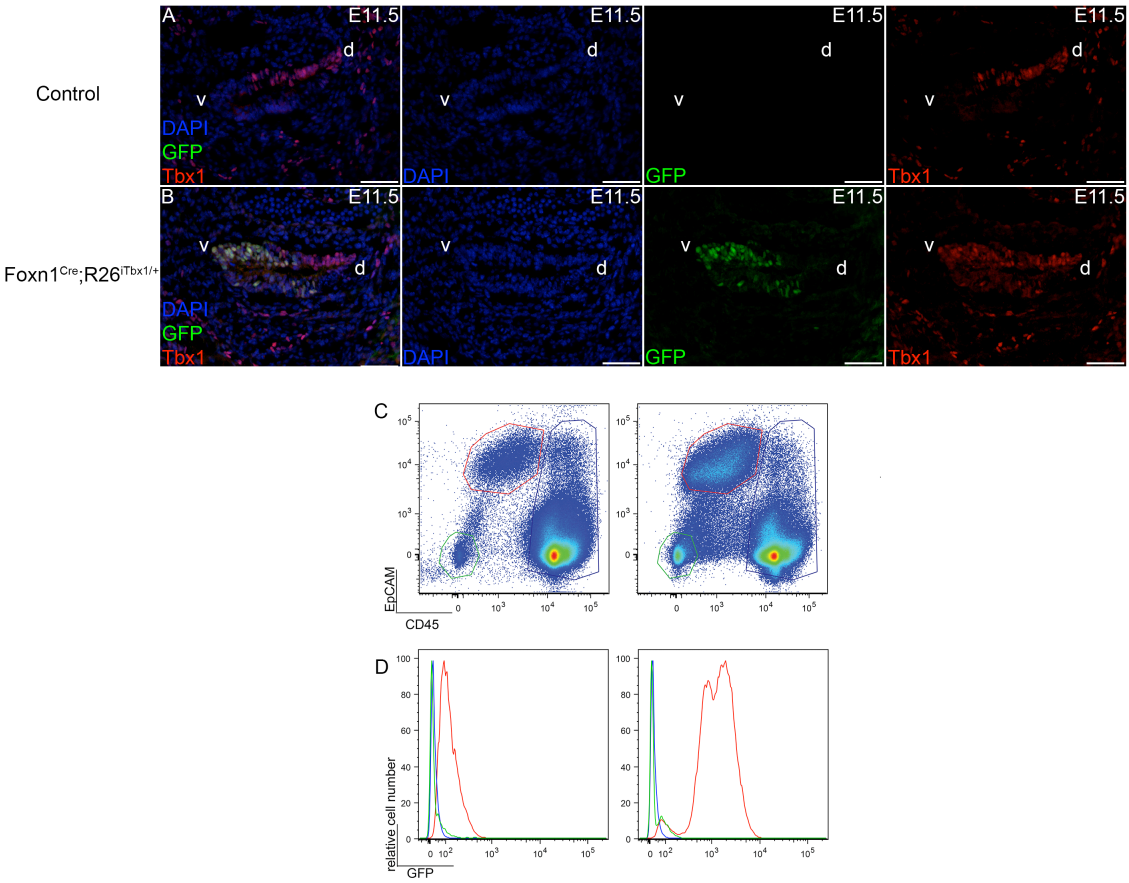

**Figure 7. Ectopic TBX1 in the ventral 3rd pp reduces the number of FOXN1 positive cells.**

(**A-D**) Representative IHC stains of sagittal sections from 3rd pp of *Foxn1Cre;R26*$^{+/+}$ control and *Foxn1Cre;R26*$^{iTbx1/+}$ E11.5 embryos. (**A, B**) TBX1 (red) is restricted to the dorsal parathyroid-fated domain of the control, but is present throughout the mutant 3rd pp. Note the marked reduction in FOXN1 positive cells (green) in the mutant 3rd pp. A few cells in the mutant 3rd pp are FOXN1 positive and co-stain for TBX1 (yellow). (**C**) GCM2 (red) is present in parathyroid-fated cells in the dorsal domain of the control 3rd pp. (**D**) Ectopic TBX1 does not affect localization or frequency of GCM2 positive cells in the mutant 3rd pp. Scale bars: 50 μm (**E**) Bar graph of the percentage ± SD of 3rd pp cells that are positive for FOXN1, TBX1 or GCM2 (n = 4 control and 4 *Foxn1Cre;R26*$^{iTbx1/+}$ 3rd pps). **P<0.02.

**Figure 7. Ectopic TBX1 in the ventral 3rd pp reduces the number of FOXN1 positive cells.**

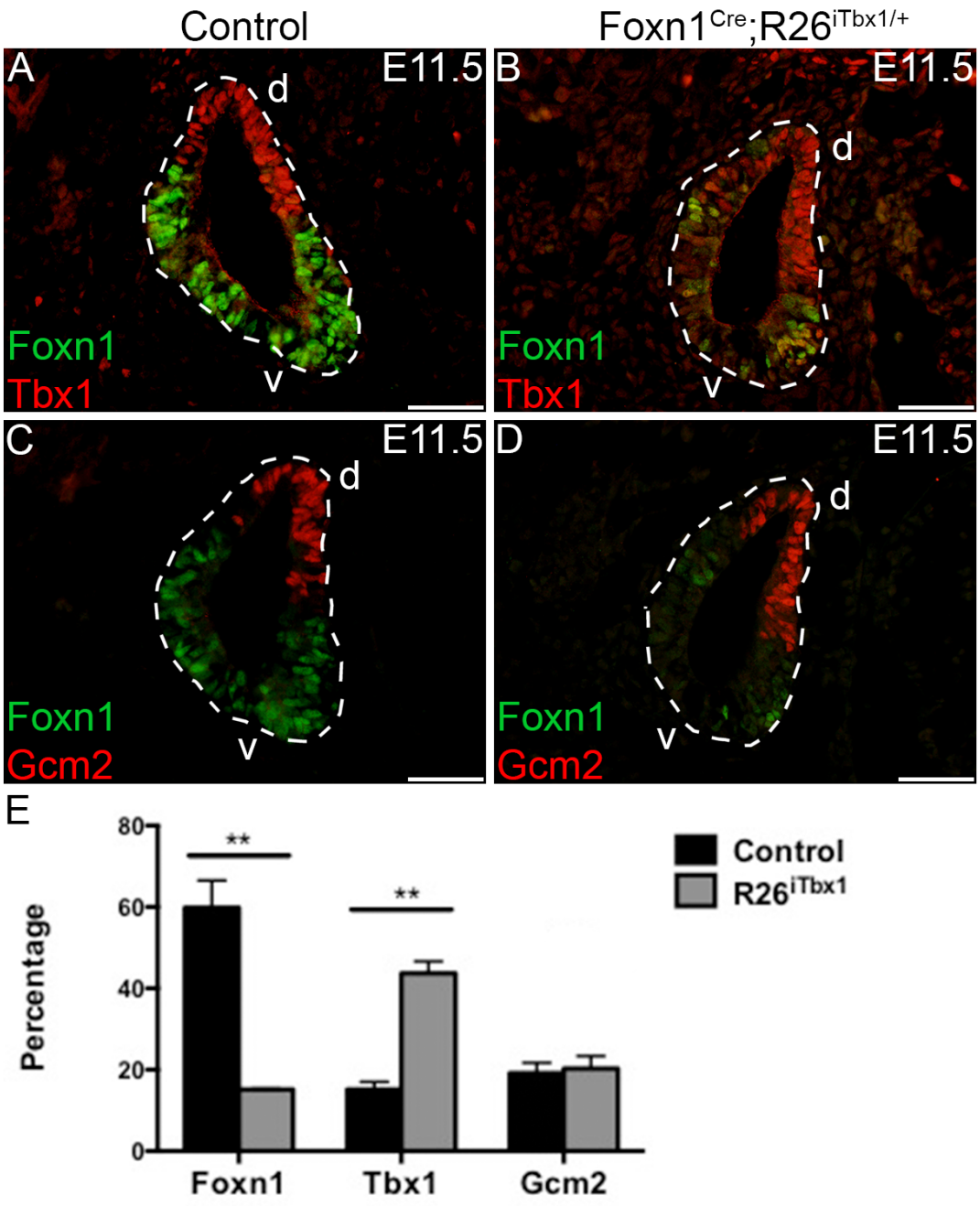

*Foxn1*$^{Cre}$;*R26*$^{iTbx/+}$ 3rd pp (Fig. 7B, E). The presence of ectopic TBX1 protein in the ventral 3rd pp is consistent with the GFP staining pattern observed in the *Foxn1*$^{Cre}$;*R26*$^{iTbx/+}$ 3rd pp (Fig. 5). Ectopic TBX1 in the ventral domain resulted in a profound and rapid reduction in the frequency of 3rd pp cells containing detectable levels of FOXN1 (Fig. 7B, D, E).

*Gcm2* was previously proposed to be a downstream target of *Tbx1* (121, 139r1223). However, ectopic *Tbx1* expression had no discernable effect on the number or localization of GCM2 positive cells (Fig. 7D, E). GCM2 was localized to the dorsal, anterior region of the control 3rd pp, and this restricted expression pattern was maintained in the *Foxn1*$^{Cre}$;*R26*$^{iTbx/+}$ 3rd pp. Therefore, these data demonstrate that ectopic expression of *Tbx1* is not sufficient to induce *Gcm2* expression in the ventral domain of the 3rd pp, suggesting that additional regulators are involved in controlling *Gcm2* expression.

**Ectopic TBX1 expression in the E11.5 3rd pp does not reverse thymus fate**

Owing to the severe reduction in FOXN1 positive cells and failure to expand GCM2, the majority of cells in the ventral domain of the *Foxn1*$^{Cre}$;*R26*$^{iTbx/+}$ 3rd pp express neither FOXN1 nor GCM2 (Fig. 7B, D, E). To determine if these cells are no longer committed to a thymus fate, we examined expression of additional factors that are expressed by thymus specified cells. We previously reported that at E11.5, thymus-, but not parathyroid-fated cells in the 3rd pp express IL7, a cytokine that is essential for thymocyte differentiation and survival (12, 140). Moreover, IL-7 is expressed by immature TECs in the thymic rudiment of FOXN1 deficient nude (*Foxn1*$^{nu/nu}$) mice (12). Therefore, IL7 is a *Foxn1* independent marker of thymus fated cells. Quantitative RT-PCR analysis demonstrated comparable levels of *IL-7* mRNA in 3rd pp cells of *Foxn1*$^{Cre}$;*R26*$^{iTbx/+}$ and control embryos (Fig. 8A).

**Figure 8. Ectopic TBX1 does not affect expression of IL-7 or FOXG1 in the ventral 3rd pp.**

(**A**) Real-time quantitative PCR analysis shows equivalent *IL7* mRNA levels in 3rd pp dissected from E11.5 control or *Foxn1Cre;R26*$^{iTbx1/+}$ embryos. (n = 6 control and 6 *Foxn1Cre;R26*$^{iTbx1/+}$) (**B**) Representative IHC stain showing a sagittal section of E11.5 3rd pp. FOXG1 (red) and FOXN1 (green) are co-expressed in the ventral domain; DAPI (blue). (**C**) Representative IHC stain of a sagittal section of mutant 3rd pp showing abundant FOXG1 in the ventral domain despite the severe reduction in FOXN1. (**D, E**) Single color images of FOXN1 staining. Scale bars: 50 μm.

**Figure 8. Ectopic TBX1 does not affect expression of IL-7 or FOXG1 in the ventral 3rd pp.**

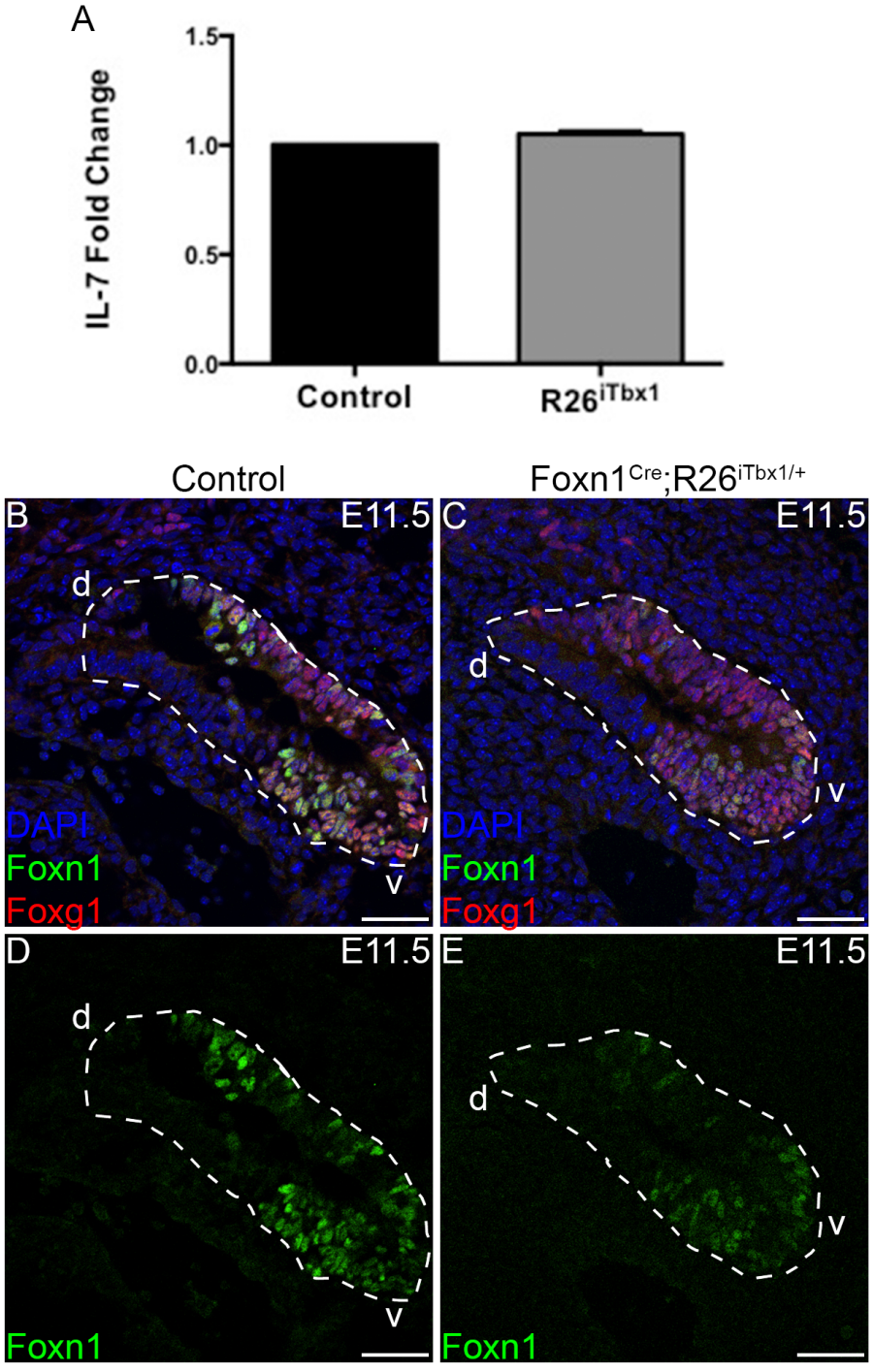

FOXG1 is a transcription factor that is initially expressed in the ventral domain of the 3rd pp by E10.5, preceding *Foxn1* (108). Similar to *IL7*, *Foxg1* is expressed in the *Foxn1*$^{nu/nu}$ thymic rudiment (Wei and Condie, unpublished data). IHC analysis of serial sections in the control 3rd pp showed that FOXG1 overlaps with FOXN1 in the ventral domain and is excluded from the dorsal, GCM2 domain (Fig. 8B, D). Interestingly, FOXG1 is abundantly expressed by the FOXN1 negative cells in the *Foxn1*$^{Cre}$;*R26*$^{iTbx/+}$ ventral 3rd pp domain (Fig. 8C). The robust expression of IL-7 and FOXG1 in the *Foxn1*$^{Cre}$;*R26*$^{iTbx/+}$ ventral 3rd pp demonstrates that ectopic expression of *Tbx1* does not repress or reverse thymus fate, but instead is selectively acting through repression of *Foxn1*.

**Ectopic TBX1 expression reduces proliferation of GCM2-negative cells in the ventral 3rd pp**

Despite the severely reduced levels of *Foxn1* expression in the 3rd pp of *Foxn1*$^{Cre}$;*R26*$^{iTbx/+}$ embryos, thymic primordia formed, detached from the pharynx and migrated to a normal position above the heart in a timely manner (Fig. 9) (51). These data are consistent with the conclusion that cells in the ventral 3rd pp remain specified to a thymus fate after ectopic *Tbx1* expression. However, *Foxn1*$^{Cre}$;*R26*$^{iTbx/+}$ fetal thymi are severely hypoplastic throughout ontogeny and remain so in the postnatal period (Fig. 9 and data not shown). The hypoplastic phenotype is not surprising given that FOXN1 is essential for TEC proliferation (57, 99, 141, 142).

To determine the cellular mechanism(s) by which ectopic TBX1 expression results in thymus hypoplasia, we analyzed the frequency of proliferating and apoptotic cells in the ventral domain of the 3rd pp. Due to the paucity of FOXN1 positive cells caused by ectopic TBX1, we determined the percentage of BrdU incorporating cells in GCM2 positive

**Figure 9. Thymic lobes are hypoplastic throughout ontogeny in *Foxn1Cre;R26*$^{iTbx1/+}$ embryos.**

(**A-F**) H&E stained transverse sections show that *Foxn1Cre;R26*$^{iTbx1/+}$ thymic lobes are smaller than controls at each developmental stage. Asterisks indicate thymic lobes. (**A, B**) E12.5 (**C, D**) E14.5; (**E, F**) E17.5. Scale bars: 50 μm.

**Figure 9. Thymic lobes are hypoplastic throughout ontogeny in *Foxn1$^{Cre}$;R26$^{iTbx1/+}$* embryos.**

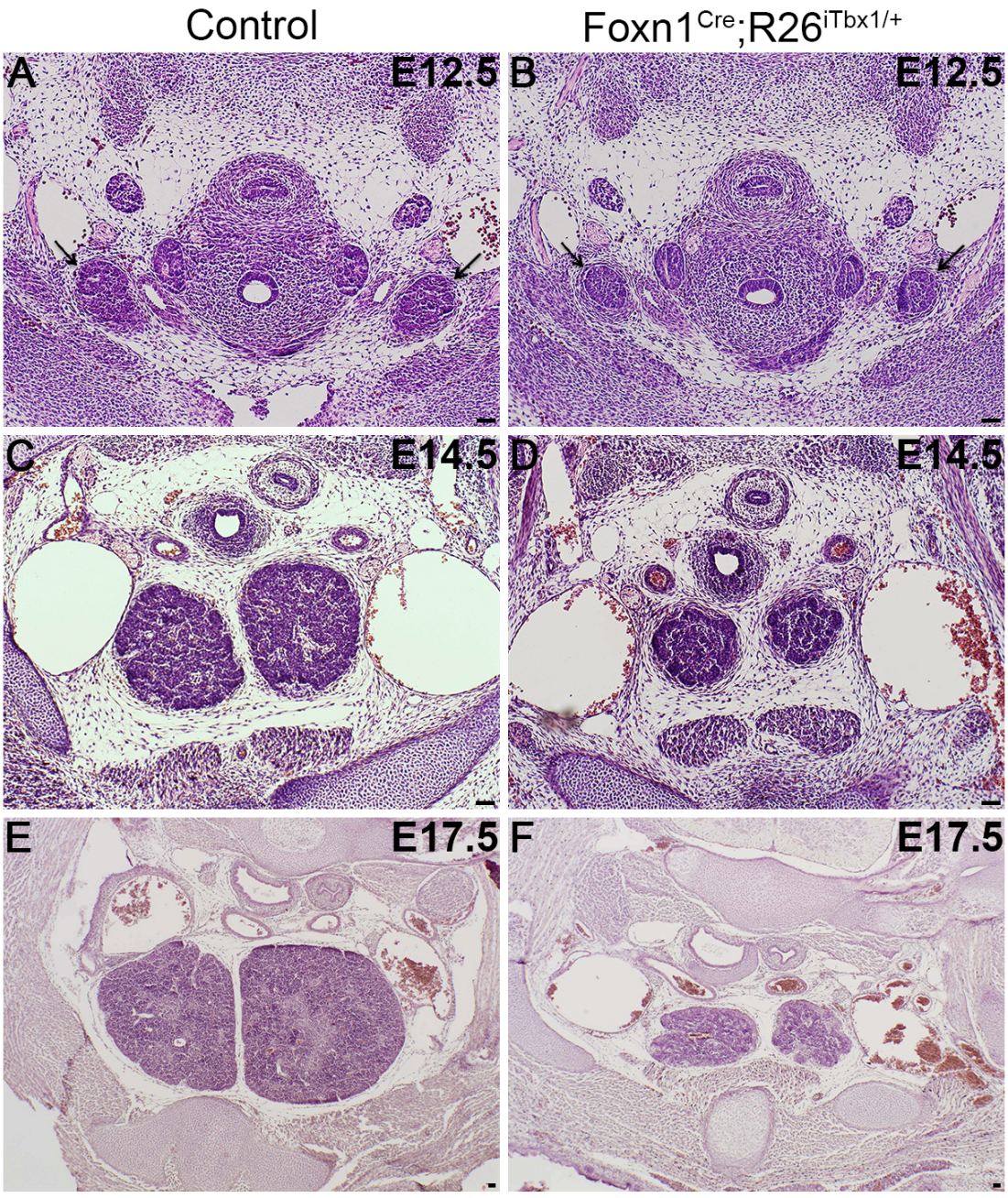

compared to GCM2 negative 3rd pp domains. Ectopic *Tbx1* expression decreased the frequency of proliferating cells in the GCM2-negative domain (Fig. 10A-C). In contrast, we found no difference in the frequency of proliferating GCM2-positive cells. To determine if ectopic *Tbx1* expression enhanced apoptosis in the 3rd pp, we stained sections for cleaved caspase 3. No difference was observed in the frequency of apoptotic 3rd pp cells in *Foxn1*$^{Cre}$;*R26*$^{iTbx/+}$ compared to control embryos (data not shown). These data demonstrate that TEC proliferation, but not survival, is compromised by ectopic expression of *Tbx1* in the thymus fated domain.

**TEC differentiation is impaired by ectopic TBX1 expression**

Given that FOXN1 is required for TEC differentiation (57, 87, 88, 99, 143), we predicted that this process would be impaired in *Foxn1*$^{Cre}$;*R26*$^{iTbx/+}$ thymi. To test this hypothesis, we first assessed expression of MHC Class II (MHCII), an early differentiation marker that is expressed on wildtype TECs beginning at E12.5 in a *Foxn1* dependent manner (57, 99, 144, 145). Whereas most TECs in E15.5 control thymi expressed high levels of MHCII, there was a five to ten fold reduction in the frequency of MHCII$^{hi}$ TECs in *Foxn1*$^{Cre}$;*R26*$^{iTbx/+}$ mutants, indicating an early block in TEC differentiation (Fig. 11A). We isolated TECs by cell sorting into MHCII$^{hi}$ and MHCII$^{neg\text{-}lo}$ populations for qRT-PCR analysis using the sort gates shown in Figure 11A. As previously reported (99), MHC II$^{hi}$ TECs from controls expressed higher levels of *Foxn1* transcripts than MHCII$^{lo}$ TECs (Fig. 11B). Neither TEC subset isolated from control thymi expressed significant levels of *Tbx1* (Fig. 11C). In contrast, both MHCII$^{hi}$ and MHCII$^{neg\text{-}lo}$ TECs from *Foxn1*$^{Cre}$;*R26*$^{iTbx/+}$ thymi expressed very low levels of *Foxn1* and high levels of *Tbx1* mRNA (Fig. 11B, C). These data are consistent with the notion that TBX1 suppression of *Foxn1* causes decreased TEC differentiation.

**Figure 10. Proliferation is reduced in the *Foxn1$^{Cre}$;R26$^{iTbx1/+}$* thymus-fated 3$^{rd}$ pp domain.**

(**A, B**) BrdU (10 mg/ml) was injected into pregnant females 1.5 hrs prior to obtaining E11.5 embryos. IHC staining for BrdU (teal) identifies proliferating cells in the GCM2 positive (red), parathyroid fated domain and the GCM2 negative thymus fated domain of the 3$^{rd}$ pp from control (**A**) and *Foxn1Cre;R26$^{iTbx1/+}$* (**B**) embryos. Scale bars: 50 μm. (**C, D**) Bar graphs showing the frequency of BrdU labeled cells that are GCM2 negative or GCM2 positive. Data show percentage ± SD for 8 control and 8 *Foxn1Cre;R26$^{iTbx1/+}$* 3$^{rd}$ pps. **P<0.005.

**Figure 10. Proliferation is reduced in the *Foxn1$^{Cre}$;R26$^{iTbx1/+}$* thymus fated 3$^{rd}$ pp domain.**

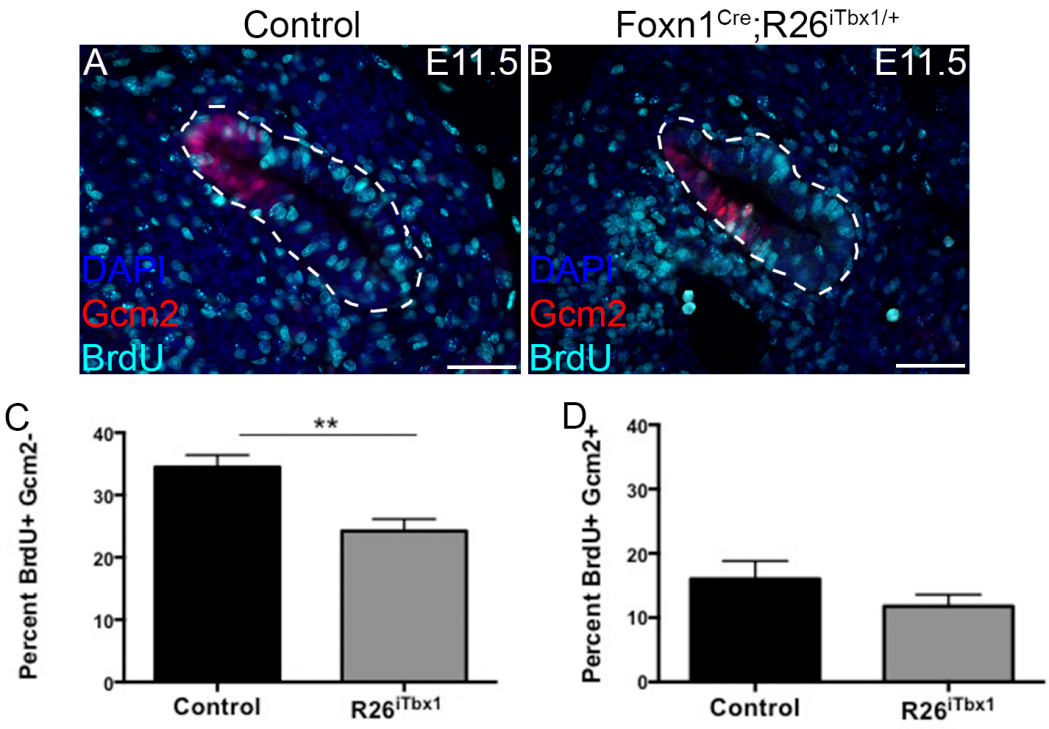

**Figure 11. Ectopic TBX1 blocks TEC differentiation and suppresses *Foxn1* expression.**

(**A**) Flow cytometric analysis of MHC class II expression on $EpCAM^{+}$ $CD45^{-}$ control and *Foxn1Cre;R26*$^{iTbx1/+}$ TECs. Note that the majority of control TECs are $MHCII^{hi}$ whereas most *Foxn1Cre;R26*$^{iTbx1/+}$ TECs are $MHCII^{neg\text{-}lo}$ (**B,C**) Representative bar graphs of qRT-PCR analysis showing *Foxn1* (**B**) or *Tbx1* (**C**) expression in E15.5 control and *Foxn1Cre;R26*$^{iTbx1/+}$ TECs. $MHCII^{hi}$ and $MHCII^{neg\text{-}lo}$ were obtained by FACS sorting using the indicated gates.

**Figure 11. Ectopic TBX1 blocks TEC differentiation and suppresses *Foxn1* expression.**

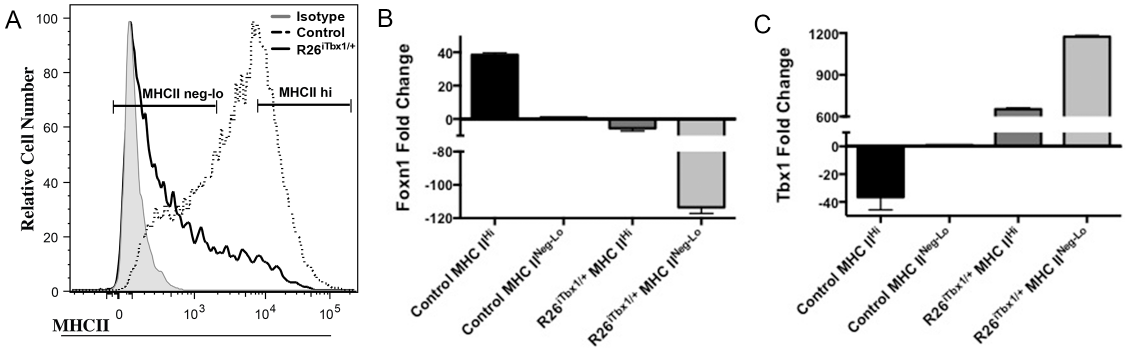

**FOXN1-positive TECs express cTEC and mTEC markers, and segregate from TBX1 positive TECs**

By E15.5, a small number of FOXN1 positive TECs were present in the *Foxn1*$^{Cre}$;*R26*$^{iTbx/+}$ thymi; these TECs had low TBX1 levels, presumably due to down regulation of or failure to activate *R26*$^{iTbx}$. IHC analysis revealed that this small number of FOXN1 positive TECs localize predominantly to the central region of each lobe (Fig. 12B), whereas FOXN1 expressing TECs are distributed throughout control thymi at E15.5 (Fig. 12A). Most TECs in *Foxn1*$^{Cre}$;*R26*$^{iTbx/+}$thymic lobes continued to express high levels of TBX1 and low to undetectable levels of FOXN1. These cells were concentrated towards the outer region of each lobe (Fig. 12B). A similar pattern of TBX1 and FOXN1 expression was observed at E17.5 (Fig. 13).

To determine if TECs in *Foxn1*$^{Cre}$;*R26*$^{iTbx/+}$ thymi were committed to either cTEC or mTEC lineages, we analyzed additional lineage specific TEC markers. The thymoproteosome subunit, b5t as well as the surface receptor, CD205 are expressed in a FOXN1-dependent manner at early stages of cTEC differentiation (92, 144, 146). As expected, the majority of cTECs in the control thymus were positive for both CD205 and b5t (Fig. 12C, E). In contrast, only a subset of TECs in *Foxn1*$^{Cre}$;*R26*$^{iTbx/+}$ thymi expressed b5t or CD205. TECs expressing these markers were primarily found in the center of each lobe, where FOXN1 positive cells were also located (Fig 12D, F).

K14 expression and binding of the lectin, *Ulex europeaus* agglutinin 1 (UEA-1) are markers that distinguish mTEC subsets (147). Both K14 positive and UEA-1 binding mTECs were present in the developing medullary regions of control thymi (Fig. 12G, I). However, only exceedingly rare cells expressed either of these mTEC markers in the *Foxn1*$^{Cre}$;*R26*$^{iTbx/+}$ thymic lobes (Fig. 12H, J). Furthermore, the mutant TECs failed to express the nuclear protein Aire (autoimmune regulator), which regulates transcription of tissue restricted antigens and is a marker for mTEC maturation (Fig. 12J) (32, 148, 149). Claudin (Cldn) 3

**Figure 12. A small number of FOXN1-positive TECs are present in the center of *Foxn1$^{Cre}$;R26$^{iTbx1/+}$* fetal thymic lobes.**

(**A-J**) Representative IHC stains of transverse sections from control and *Foxn1Cre;R26$^{iTbx1/+}$* E14.5 or E15.5 thymic lobes show distinct patterns of TEC localization. (**A**) FOXN1 positive (green) TECs are dispersed throughout the control thymus and TBX1 positive cells are not found. (**B**) The small number of FOXN1 positive TECs (green) in *Foxn1Cre;R26$^{iTbx1/+}$* mutants localize to the center of each lobe and generally segregate away from the abundant TBX1 positive TECs (red) that are concentrated in the outer region of the each lobe. (**C-F**) Only a few of the mutant TECs are positive for β5t and CD205 that mark the cTEC lineage (green), and these cells localize primarily in the center of each lobe where FOXN1 positive cells are found (see Fig. 6B). (**G-J**) Markers of the mTEC lineage (UEA-1, Aire and K14) are readily detectable in control thymic lobes but rarely present in *Foxn1Cre;R26$^{iTbx1/+}$* lobes. Scale bars: 50 μm.

**Figure 12. A small number of FOXN1-positive TECs are present in the center of *Foxn1$^{Cre}$;R26$^{iTbx1/+}$* fetal thymic lobes.**

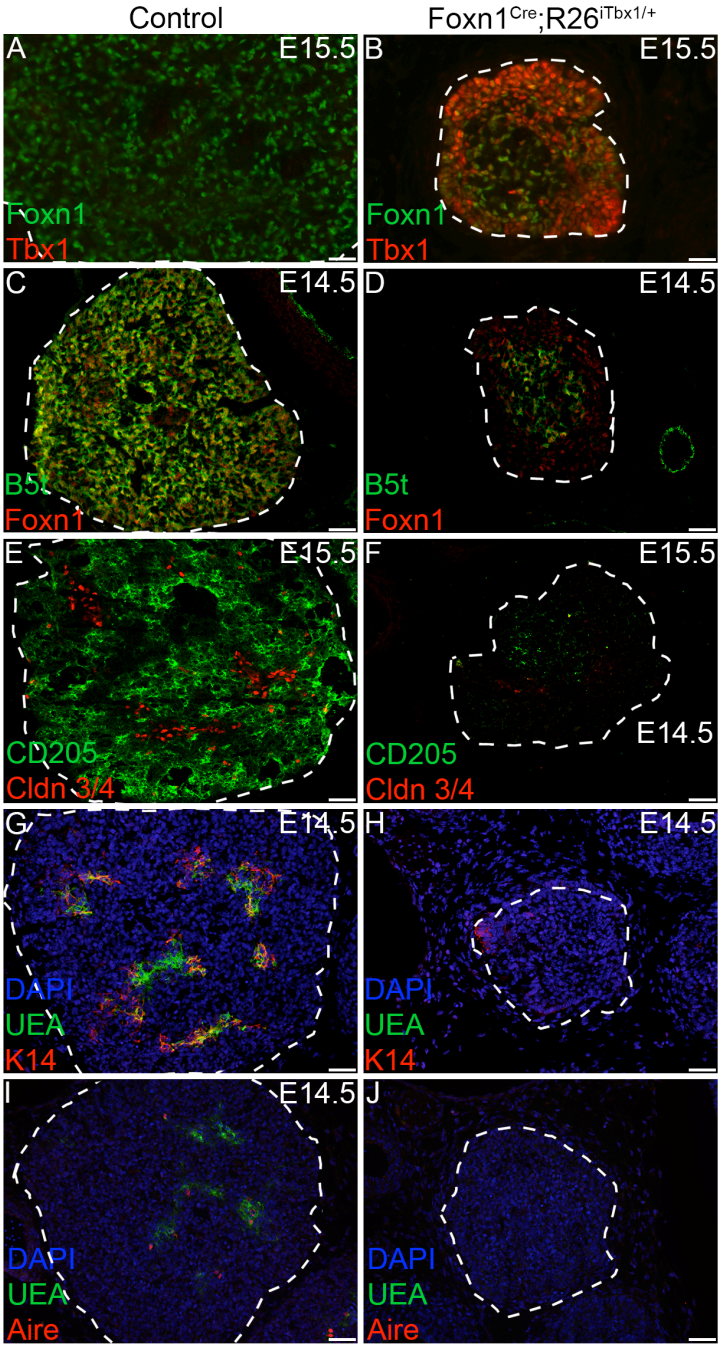

**Figure 13. Thymocytes co-localize with TECs expressing low levels of FOXN1 in E17.5 *Foxn1$^{Cre}$;R26$^{iTbx1/+}$* thymic lobes.**

Representative IHC stains of serial transverse sections showing co-stains for FOXN1 and TBX1 (**A,C**) and for IKAROS and TBX1 (**B,D**) in control (**A,C**) and *Foxn1$^{Cre}$;R26$^{iTbx1/+}$* (**B,D**) E17.5 thymic lobes.

**Figure 13. Thymocytes co-localize with TECs expressing low levels of FOXN1 in E17.5 *Foxn1*$^{Cre}$;*R26*$^{iTbx1/+}$ thymic lobes.**

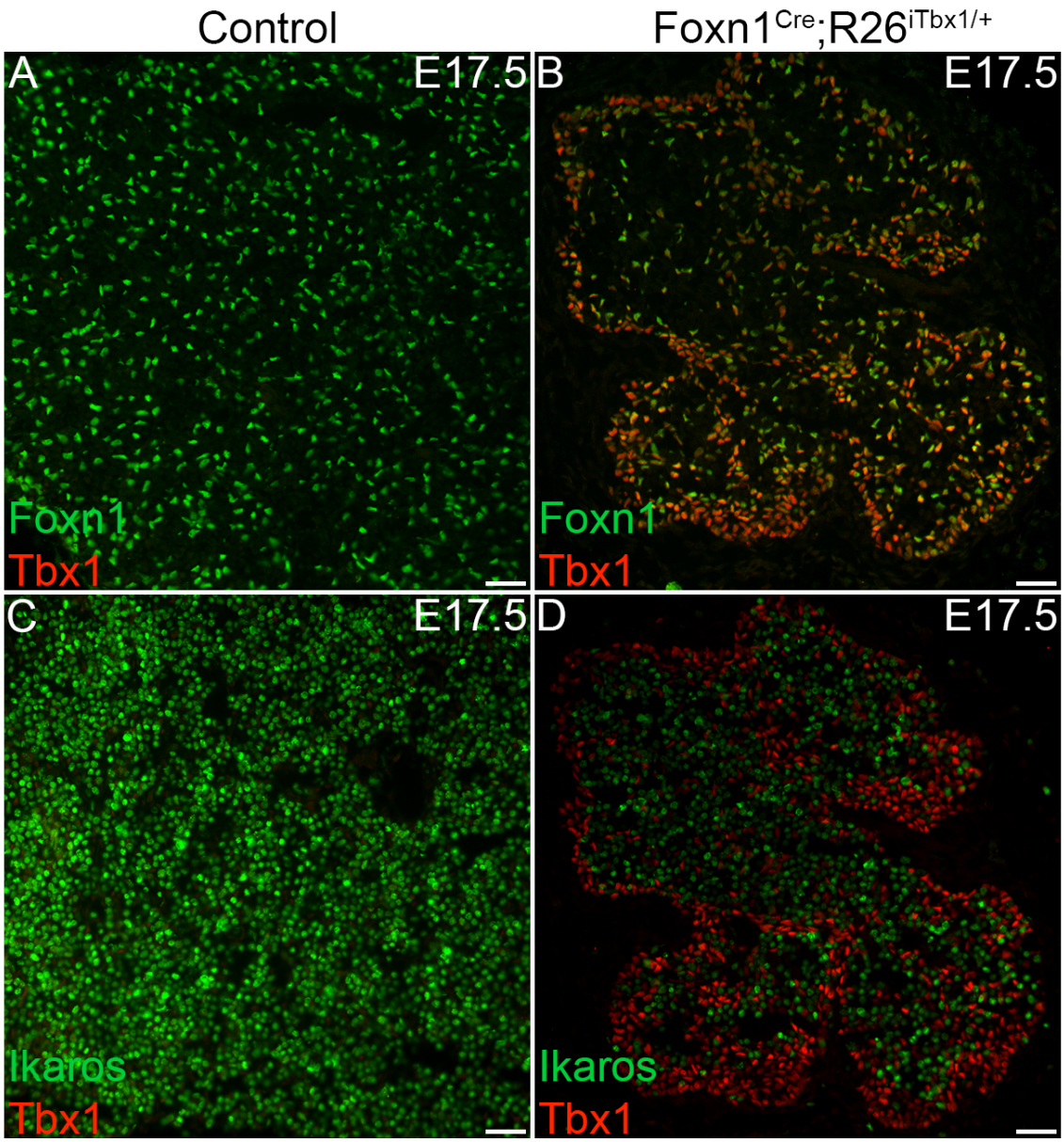

and Cldn 4 are expressed on TEC precursors that are committed to the mTEC lineage (91). There was a paucity of Cldn3/4 positive TECs in *Foxn1*$^{Cre}$;*R26*$^{iTbx/+}$ thymi (Fig. 12F). Interestingly, the few Cldn3/4 positive precursors were positioned towards the outer region of the thymic lobes where TECs expressing higher levels of TBX1 and lower levels of FOXN1 are found. Taken together, these data suggest that ectopic TBX1 compromises differentiation of both cTEC and mTEC lineages.

**Ectopic TBX1 results in an accumulation of early TEC progenitors**

PLET-1 is a cell surface protein expressed by founder cells in the 3$^{rd}$ pp that give rise to both cTEC and mTEC lineages (87, 89, 90, 150, 151). A relatively high frequency of TECs in both *Foxn1*$^{Cre}$;*R26*$^{iTbx/+}$ and control thymic rudiments express PLET-1 at E12.5 (Fig. 14A, B), consistent with previously published data (57). The frequency of PLET-1 positive TECs decreases during ontogeny as TECs undergo differentiation and proliferation (57). Thus, PLET-1 expression is confined to a rare subset of TECs in control thymi by E14.5 (Fig. 14C). In striking contrast, a higher frequency of PLET-1 positive cells persists at E14.5 in the *Foxn1*$^{Cre}$;*R26*$^{iTbx/+}$ thymi (Fig. 14D). Furthermore, the PLET-1 positive cells in the mutant thymi are found in the outer region of the lobes, similar to the localization pattern observed for TBX1 expressing cells (Fig. 14D). These data are consistent with ectopic TBX1 expression blocking TEC differentiation at an early progenitor stage. Flow cytometric analysis confirmed an increased frequency of PLET-1 positive cells in E15.5 *Foxn1*$^{Cre}$;*R26*$^{iTbx/+}$ compared to control thymi (Fig. 14E). However, the absolute number of PLET-1 positive cells was comparable in *Foxn1*$^{Cre}$;*R26*$^{iTbx/+}$ and control thymi (Fig. 14F, G). The maintenance of the same number of PLET-1 positive TECs in the hypoplastic *Foxn1*$^{Cre}$;*R26*$^{iTbx/+}$ thymi at late stages of ontogeny is more consistent with TBX1 blocking differentiation of existing progenitors, rather than reverting differentiated TECs to a progenitor state.

**Figure 14. *Foxn1*$^{Cre}$*;R26*$^{iTbx1/+}$ fetal thymi contain a high frequency of TEC progenitors.**

(**A-D**) Representative IHC stains of transverse sections from control and *Foxn1Cre;R26*$^{iTbx1/+}$ E12.5 or E14.5 thymic lobes showing Plet-1 (red) and K5 (green) positive cells. Note the high frequency of Plet-1 positive TEC progenitors in the outer region of *Foxn1Cre;R26*$^{iTbx1/+}$ thymic lobes (**D**). Scale bars: 50 μm (**E**) FACS plots showing MHC II and Plet-1 expression on EpCAM+ CD45- control and *Foxn1Cre;R26*$^{iTbx1/+}$ TECs. Numbers in each quadrant show percentage of cells. (**F, G**) Bar graphs showing the frequency (**F**) or number (**G**) of Plet-1 positive cells in E14.5 control and *Foxn1Cre;R26*$^{iTbx1/+}$ thymic lobes. Data show mean ± SD for 4 control and 4 *Foxn1Cre;R26*$^{iTbx1/+}$ thymic lobes. **P<0.001.

**Figure 14. *Foxn1*$^{Cre}$;*R26*$^{iTbx1/+}$ fetal thymi contain a high frequency of TEC progenitors.**

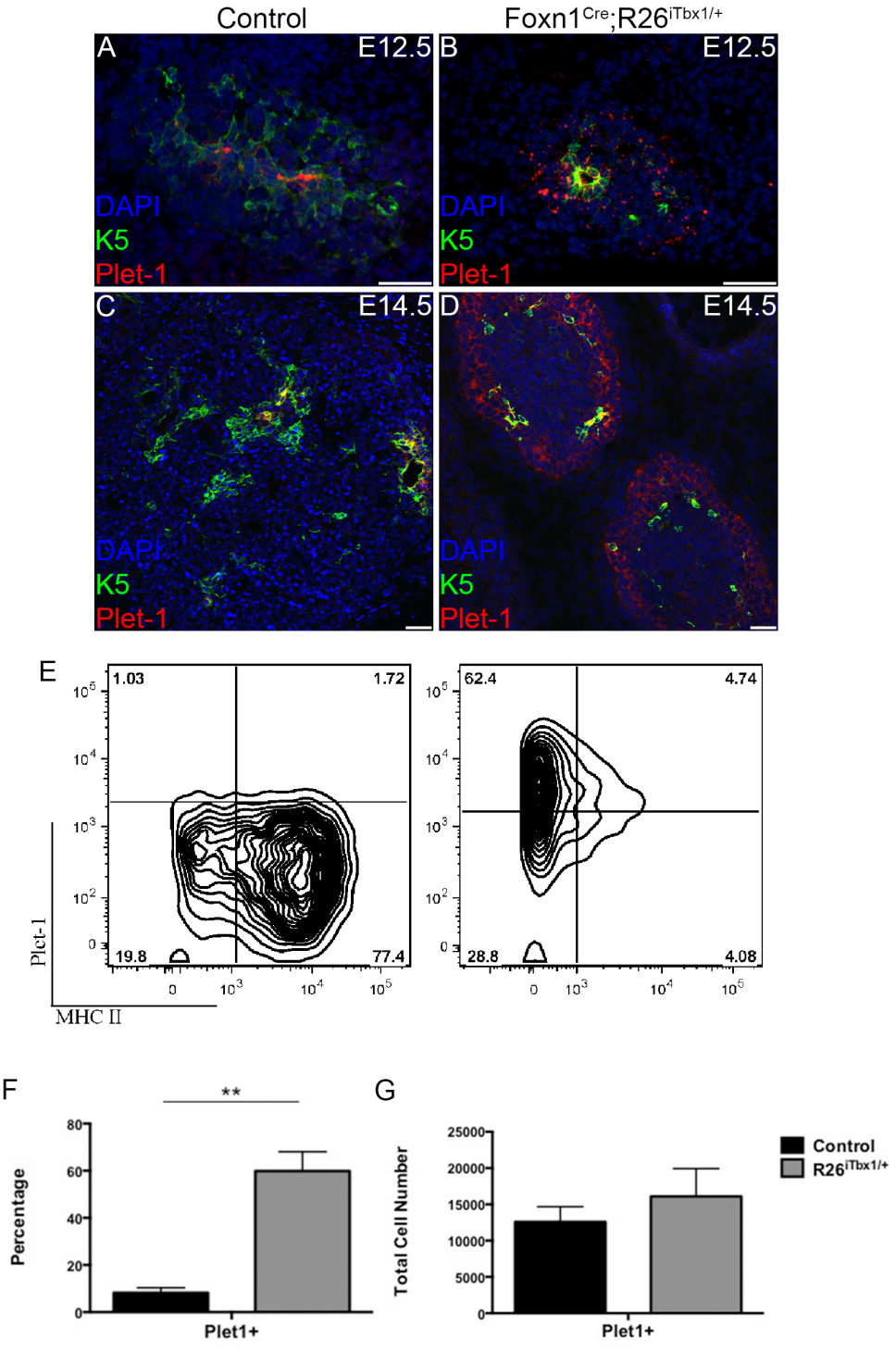

**Thymocyte development and localization is altered in the *Foxn1$^{Cre}$;R26$^{iTbx/+}$* thymic microenvironment**

TECs are required for thymocyte proliferation, survival and differentiation (152-155). Given the profound arrest in TEC development resulting from ectopic *Tbx1* expression, we expected to find defects in thymocyte development. Total thymocyte cellularity was decreased by ~5 fold in in E15.5 *Foxn1$^{Cre}$;R26$^{iTbx/+}$* compared to control thymi (Fig. 15A). Flow cytometric analyses were performed to assess thymocyte differentiation. At this developmental stage, thymocytes have not yet differentiated beyond the immature CD4 and CD8 double negative (DN) precursor subset (Fig. 15B). Expression of c-kit and CD25 distinguishes DN subsets at sequential maturation stages, referred to as DN1 through DN4. Flow cytometric analysis revealed a partial block at the DN3 to DN4 transition in *Foxn1$^{Cre}$;R26$^{iTbx/+}$* thymi (Fig. 15C). The reduction in thymocyte cellularity, together with the partial differentiation arrest at the DN3 stage suggest that the aberrant TEC microenvironment in *Foxn1$^{Cre}$;R26$^{iTbx/+}$* thymi fails to provide adequate growth and differentiation signals to support normal thymocyte development. IHC analysis of E14.5 thymi revealed that thymocytes, identified by expression of the Ikaros transcription factor (156), were distributed throughout the control thymic lobes (Fig. 15D). In contrast, the scarce thymocytes present in *Foxn1$^{Cre}$;R26$^{iTbx/+}$* fetal thymus lobes were concentrated in the central region in juxtaposition to TECs expressing higher levels of FOXN1 (compare Figs. 12B and 15E). This spatial relationship emphasizes the importance of TEC-thymocyte crosstalk in T cell development.

**Figure 15. Thymocyte localization, cellularity and development are aberrant in *Foxn1$^{Cre}$;R26$^{iTbx1/+}$* fetal thymi.**

(**A, B**) Representative IHC stains of transverse sections from control and *Foxn1Cre;R26$^{iTbx1/+}$* E15.5 thymic lobes show that thymocytes identified as Ikaros positive (green) are scattered through control thymic lobes, but are restricted to the central region of mutant lobes where FOXN1 positive cells are found (see Fig. 6B). Scale bars: 50μm. (**C**) Bar graph of the number ± SD of thymocytes recovered from control (n = 2) and *Foxn1Cre;R26$^{iTbx1/+}$* (n = 3). (**D**) FACS plots showing that most E15.5 thymocytes are CD4 or CD8 double negative (DN) cells. (**E**) FACS plots showing the distribution of DN subsets based on c-kit and CD25 expression. Note the partial block at the DN3 (c-kit$^{-}$CD25$^{+}$) to DN4 (c-kit$^{-}$CD25$^{+}$) developmental transition in *Foxn1Cre;R26$^{iTbx1/+}$* thymocytes.

**Figure 15. Thymocyte localization, cellularity and development are aberrant in *Foxn1$^{Cre}$;R26$^{iTbx1/+}$* fetal thymi.**

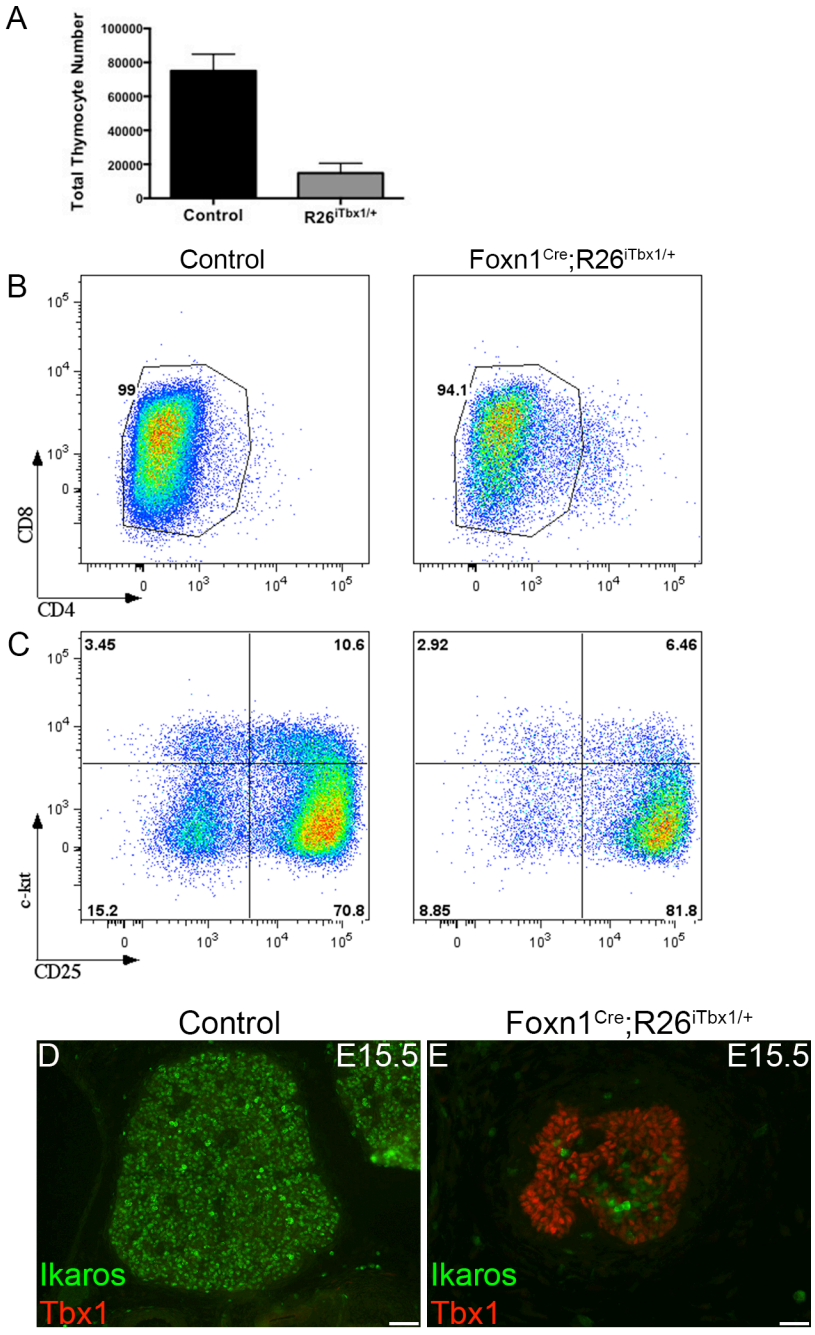

## CONCLUSIONS

The molecular events that specify thymus fate and regulate TEC development have yet to be fully delineated. Previous reports suggested that TBX1 promotes thymus development based on the thymic aplasia or hypoplasia in patients with 22q11.2 deletion (DiGeorge) syndrome, in which loss or haploinsufficiency of *Tbx1* is the primary defect (40, 114, 121, 136). However, the failure of pharyngeal pouch formation in *Tbx1* deletion mutants (112, 114, 115, 118, 119) suggests that the thymus phenotype in *Tbx1* mutants is likely secondary to defects in pharyngeal pouch formation and does not reflect a role for *Tbx1* in wildtype thymus organogenesis. Our current results clearly demonstrate that TBX1 can suppress *Foxn1* expression, preventing both TEC proliferation and differentiation. These data, combined with the down regulation of *Tbx1* in the ventral domain during pouch formation (112, 121, 122), support the conclusion that TBX1 is a negative regulator of thymus development.

### *Ectopic expression of TBX1 in ventral 3$^{rd}$ pp endoderm suppresses FOXN1*

All of the defects in TEC maturation and proliferation observed in *Foxn1$^{Cre}$;R26$^{iTbx/+}$* thymi are consistent with the suppression of *Foxn1* expression, which is known to promote these processes. Down regulation of *Foxn1* occurred as early as E11.5, almost immediately upon ectopic expression of *Tbx1*. The inverse pattern of FOXN1 and TBX1 protein levels in E15.5 *Foxn1$^{Cre}$;R26$^{iTbx/+}$* TECs is further evidence that TBX1 negatively regulates *Foxn1* expression. TBX1 may shut down *Foxn1* expression by an indirect rather than direct mechanism, since there is not an obvious TBX binding site in the *Foxn1* promoter (BLAT; UCSC Genome Bioinformatics). These findings are consistent with the report of Bain, et al. showing that ectopic activation of SHH signaling in 3$^{rd}$ pp endoderm both induces *Tbx1* expression and represses *Foxn1* (V.E.B. and N.R.M., unpublished).

The few FOXN1 positive TECs present in these mutants appear to be the progeny of 3rd pp progenitors that failed to effectively express ectopic TBX1, as these cells have very low or undetectable levels of TBX1. This failure could be due to inefficient or late deletion of the stop codon in the *R26*$^{iTbx1}$ allele, or due to secondary shutdown of the Rosa26 locus. These FOXN1 positive cells tend to aggregate in the center of the lobe, forming a microenvironment that supports differentiation of a small number of thymocytes, with variable efficiency.

*Ectopic TBX1 expression does not reverse thymus fate*

By E11.5, most cells in the wildtype 3rd pp have acquired either a thymus or parathyroid fate, and express either *Foxn1* or *Gcm2* (54). In contrast, the reduction of FOXN1 positive cells in the *Foxn1*$^{Cre}$;*R26*$^{iTbx/+}$ 3rd pp, coupled with the lack of a compensatory expansion of *Gcm2* expression, results in a sizeable domain containing cells that fail to express either marker. However, as *Foxn1* is not required to establish thymus fate, these cells could still retain thymus fate specification. This appears to be the case, as these ventral cells do express *IL7* and FOXG1, both of which are expressed by thymus fated cells independently of *Foxn1*–mediated regulation (12, 108) and B.G. Condie, personal communication). These data also demonstrate that ectopic *Tbx1* cannot reverse thymus fate after it is established, since *Foxn1*$^{Cre}$ is expressed in 3rd pp cells that are already committed to a thymus fate. The down regulation of *Tbx1* in the ventral domain during pouch outgrowth at E9-9.5, prior to expression of thymus-specific markers, raises the possibility that this down regulation is essential to establish thymus fate. Activation of *R26*$^{iTbx1}$ in 3rd pp endoderm at an earlier developmental stage will be required to test whether TBX1 can block initial thymus fate commitment.

*Ectopic TBX1 expression arrests TEC differentiation at an early progenitor stage*

TEC differentiation is arrested at a PLET-1 positive stage in *Foxn1* null (nude) mutants (88, 90). *Plet*-1 expressing TECs have been shown to contain a TEC progenitor activity in transplant experiments at both early and later stages of fetal thymus development (89, 150). These data strongly suggest that PLET-1 likely marks a very early stage of committed thymus progenitor cells (reviewed in (106). The loss of FOXN1 in *Foxn1*$^{+/Cre}$;*R26*$^{+/iTbx1}$ fetal thymi was associated with a marked increase in the frequency of PLET-1 positive TECs. However, the number of PLET-1 positive TECs was comparable in mutant and control fetal thymi. These data indicate that ectopic TBX1 results in arrested differentiation of PLET-1 positive progenitors, rather than induction of their proliferation or reversal of a differentiated phenotype to a progenitor-like state.

*Ectopic TBX1 expression uncouples FOXN1 and MHC Class II expression*

Previous studies have suggested that *Foxn1* directly or (more likely) indirectly regulates *MHC Class II* expression. MHC Class II levels are severely downregulated on TECs from *Foxn1*$^{\Delta/\Delta}$ mutants (99, 157). Furthermore, a direct relationship was observed between the frequency of MHC Class II positive TECs and *Foxn1* levels in an allelic series of strains expressing progressively lower levels of *Foxn1* (57). Therefore, we were surprised to find that the minor fraction of MHCII$^{hi}$ *Foxn1*$^{Cre}$;*R26*$^{iTbx/+}$ TECs expressed exceedingly low levels of *Foxn1* mRNA. The mechanism responsible for this finding is not clear, but this result does indicate that FOXN1 levels alone are not sufficient to determine *MHC Class II* levels. It is possible that ectopic *Tbx1* in *Foxn1*$^{Cre}$;*R26*$^{iTbx/+}$ mutants disrupts the normal regulatory pathway linking *Foxn1* and *MHC Class II*. Regardless of the mechanism, *Foxn1* and *MHC Class II* expression are uncoupled by ectopic *Tbx1* expression in TECs.

*Ectopic TBX1 expression does not induce GCM2 expression*

GCM2 is a transcription factor that marks the parathyroid fated domain of the 3rd pp and is required for parathyroid survival and differentiation (54, 121, 158). *Tbx1* and *Gcm2* expression domains overlap in the dorsal 3rd pp, and previous reports suggested that *Gcm2* may be a downstream target of *Tbx1*, based on microarray data in *Tbx1* null mutants (139), or on the persistence if *Tbx1* expression in *Gcm2* null mutants (121). However, our data show that ectopic expression of TBX1 was not sufficient to induce an expansion of *Gcm2* expression into the ventral 3rd pp. This result is consistent with the finding that expression of a constitutively active allele of *Smo* throughout the 3rd pp expanded the *Tbx1* expression domain ventrally, but did not expand *Gcm2* expression (V.E.B. and N.R.M., unpublished). Thus, activation of additional positive regulators and/or suppression of negative regulators must be involved in regulating parathyroid fate specification and/or *Gcm2* expression during 3rd pp patterning.

## Chapter 4: The *miR-17-92* cluster regulates *Tbx1* expression in 3rd pharyngeal pouch endoderm

### INTRODUCTION

Factors that specify thymus versus PT fate have not yet been identified. Although several labs have identified transcription factors within the endoderm or mesenchyme that have temporal expression patterns consistent with a role in organ specification, these candidates have not been shown to control thymus or PT fate. Thus, identifying factors that establish thymus fate would facilitate *in vitro* and *in vivo* approaches to specify endoderm progenitors to a TEC fate in order to generate or maintain a functional thymus.

The transcription factor, *Tbx1*, is an example of one such factor that is implicated in 3rd pp organ specification. At E10.5, *Tbx1* is expressed in the PT-fated domain, but silenced in the ventral, thymus-fated domain (112, 121, 122), suggesting that *Tbx1* must be suppressed during thymus organogenesis. We have shown that ectopic expression of the *Tbx1* allele in the ventral domain of the 3rd pp inhibits FOXN1 expression leading to a block in TEC differentiation, resulting in severely hypoplastic thymus lobes that have an accumulation of TEC progenitors (111). Therefore, we wanted to determine what mechanisms must be present to downregulate *Tbx1* in the ventral domain of the 3rd pp at E10.5, thus permitting proper thymus organogenesis to occur.

Evidence from other labs suggests that BMP morphogens may also play a critical role in establishing TEC fate and/or promoting TEC differentiation (80, 81, 83). Specifically, loss of *Bmp* signaling in the 3rd pp endoderm and NC-derived mesenchyme results in a delay in thymus and PT separation as well as incomplete migration of the thymic anlage (81). Furthermore, transgenic expression of *Noggin*, a *Bmp* inhibitor, results in hypoplastic, cystic thymic lobes (83). Interestingly, *Bmp2* and *Bmp4* promote differentiation of cardiac progenitor cells by activating *miR-17-92,* which suppresses the expression of *Tbx1* (82).

Furthermore, an additional study has shown that TBX1 binds SMAD1 to suppress *Bmp4* signaling, suggesting a regulatory loop (133). Based on these findings, we propose a model pathway in which *Bmp2/4* activates *miR-17-92* expression, which in turn downregulates *Tbx1* in the 3rd pp (Fig.4). We hypothesize that this feedback loop is required for thymus fate specification and/or TEC differentiation.

MicroRNAs (miRNAs) are highly conserved, short non-coding RNAs that post-transcriptionally modify gene expression (125). Through imperfect Watson Crick base pairing, miRNAs are capable of silencing numerous genes by binding complementary seed sequences in the 3' UTR of target mRNA. Interestingly, miRNAs are differentially expressed within tissues at specific times during development, thus adding additional complexity to their roles throughout normal developmental and aging processes. While the cellular functions of some miRNAs have been defined in T cell development (159), their role in thymus organogenesis has yet to be defined. To address this, we have used both loss-of-function (LOF) and gain-of-function (GOF) genetic models to test the hypothesis that *miR-17-92* plays a role in suppressing *Tbx1* expression in the developing 3rd pp endoderm to promote thymus cell fate.

## RESULTS

### Expression of *miR-17-92* family members in 3rd pp endoderm

The expression of *miR-17-92* cluster members has been investigated in various tissues (82, 130, 132, 160). However, the timing and expression pattern of *miR-17-92* within the 3rd pp endoderm has not yet been reported. Therefore, we first addressed this question by using *in situ* hybridization (ISH). Given that miRNAs are approximately twenty-two nucleotides in length and transiently expressed, this presents a unique challenge when trying to define their expression pattern. We used miRNA *in situ* probes that employ locked nucleic acid (LNA) technology (Exiqon), in which the sugar ring is locked in the 3' endo

conformation, significantly increasing the probe's affinity for short, specific RNA sequences. Based on reports studying the frequency at which each member is detected, we chose to analyze the expression pattern of *miR-17*, *miR-19a* and *miR-92a* in wildtype 3rd pp endoderm at E10.5 and E11.5.

Wildtype C57BL/6J embryos were harvested at each time point, processed for ISH analysis and sectioned to obtain both 3rd pps in their entirety. Our preliminary data indicate that at E10.5, *miR-17* is detected in the dorsal domain of the 3rd pp as well as in the surrounding mesenchyme (Fig.16A). However by E11.5, *miR-17* is expressed in the ventral domain of the 3rd pp, and is no longer detected in the dorsal domain as was seen at E10.5 (Fig.16F). Next, we analyzed the expression pattern of *miR-19a* within in the developing endoderm. The expression pattern of *miR-19a* is different from that of *miR-17* at E10.5, in that it is expressed in the ventral region of the 3rd pp and is not detected in the mesenchyme (Fig.16B). At E11.5, *miR-19a* is still expressed in the ventral domain, however not as highly as was seen at E10.5 (Fig.16G). We also analyzed expression of *miR-92a* and found it to be widely expressed throughout the 3rd pp endoderm and surrounding mesenchyme at E10.5, but restricted to the ventral domain at E11.5 (Fig.16C,H). It is interesting to note that *miR-17-92* is not only detected in the 3rd pp endoderm, but also in the adjacent mesenchyme. Given that *Tbx1* is expressed in non-NC-derived mesenchyme (112) and that the 3'UTR of *Tbx1* contains *miR-17-92* seed sequences (82), it is not surprising that expression of this cluster is also detected in the mesenchyme.

Additionally, the Martin lab generated a *miR-17-92-LacZ* transgenic mouse line to analyze the expression of *pri-miR-17-92* during heart development (132). Although these mice are no longer available, Dr. Martin kindly provided images of the E11.5 3rd pp from their studies. In wildtype embryos, *pri-miR-17-92-LacZ* is expressed in the ventral domain of the 3rd pp (data not shown, personal communication). Furthermore, the *miR-17-92* cluster is

**Figure 16. Expression of *miR-17-92* family members in 3rd pp endoderm.**

(**A-J**) ISH analysis of (**A, F**) *miR-17*, (**B, G**) *miR-19a* and (**C, H**) *miR-92a* expression in the 3rd pp endoderm of C57BL/6J at (**A-E**) E10.5 and (**F-J**) E11.5. (**D, I**) Positive control is *Fgf8*. (**E, J**) Negative control is a scrambled probe. Arrows indicate examples of miR signal. v, ventral. d, dorsal. Scale Bars: 50 μm.

**Figure 16. Expression of *miR-17-92* family members in 3rd pp endoderm.**

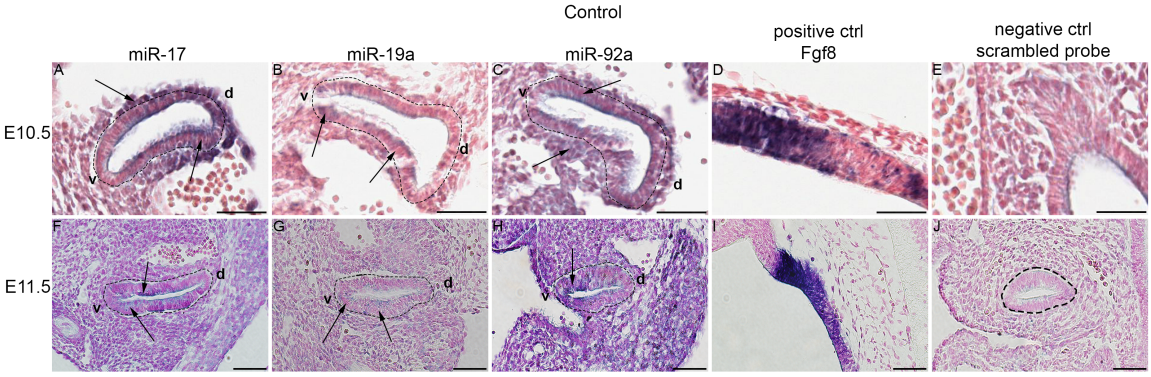

also expressed in the mesenchyme adjacent to the ventral domain of the pouch and extends towards the thymus-PT boundary. However, its expression does not reach completely into the mesenchyme surrounding the dorsal domain.

Although preliminary, our results describing the expression pattern of *miR-17*, *miR-19a* and *miR-92a* in wildtype 3rd pp endoderm are consistent with the results from the Martin lab using the *pri-miR-17-92-LacZ* reporter line. Therefore, these results bolster the conclusion that *miR-17-92* is expressed in the developing 3rd pp endoderm and adjacent mesenchyme.

**Global deletion of *miR-17-92* reduces the frequency of FOXN1 positive cells at E11.5**

Based on our model shown in Figure 4, we predicted that global deletion of *miR-17-92* would result in an incomplete downregulation of Tbx1 in the 3rd pp, thus leading to an increased frequency of TBX1 positive cells in the ventral domain of the 3rd pouch endoderm. To test this prediction, we used *miR-17-92$^{Null}$* embryos to determine if the absence of the *miR-17-92* cluster affects 3rd pp patterning and thus thymus organogenesis. Mice null for *miR-17-92* die shortly after birth and have craniofacial abnormalities, cardiac defects and lung hypoplasia (161). We obtained *miR-17-92$^{Null}$* embryos from the Martin lab at Baylor College of Medicine and serial sagittal sections from control and *miR-17-92$^{Null}$* embryos were cut for IHC analysis of region-specific markers throughout the pouch.

Given our evidence that *Tbx1* regulates *Foxn1* expression (111) and the finding that *miR-17-92* downregulates *Tbx1* in cardiac progenitors during cardiomyocyte differentiation (132), we hypothesized that TBX1 expression would be increased in the 3rd pp of *miR-17-92$^{Null}$* mice. Not surprisingly, we observed an increase in the TBX1 expression domain that expanded towards the ventral region of the 3rd pp, whereas it remained restricted to the dorsal domain in the control (Fig.17). Although TBX1 was ectopically located in the 3rd pouch, it was not detected throughout the endoderm into the ventral tip as was seen in the

**Figure 17. Global deletion of *miR-17-92* reduces the frequency of FOXN1 positive cells at E11.5.**

(**A-D**) Representative IHC stains of sagittal sections from 3rd pp of *miR-17-92*$^{Null}$ and control E11.5 embryos. (**A, B**) Loss of *miR-17-92* expression does not affect the localization or frequency of GCM2 positive cells (red). (**C-D**) TBX1 (red) is restricted to the dorsal, parathyroid-fated domain of the control, but is moderately expanded into the ventral domain of the *miR-17-92*$^{Null}$ 3rd pp. (**B, D**) Note the reduction in FOXN1 positive cells (green) and the absence of cells that are FOXN, GCM2 or TBX1 positive (yellow arrows) in the *miR-17-92*$^{Null}$ 3rd pp. v, ventral. d, dorsal. Scale Bars: 50 μm.

**Figure 17. Global deletion of *miR-17-92* reduces the frequency of FOXN1 positive cells at E11.5.**

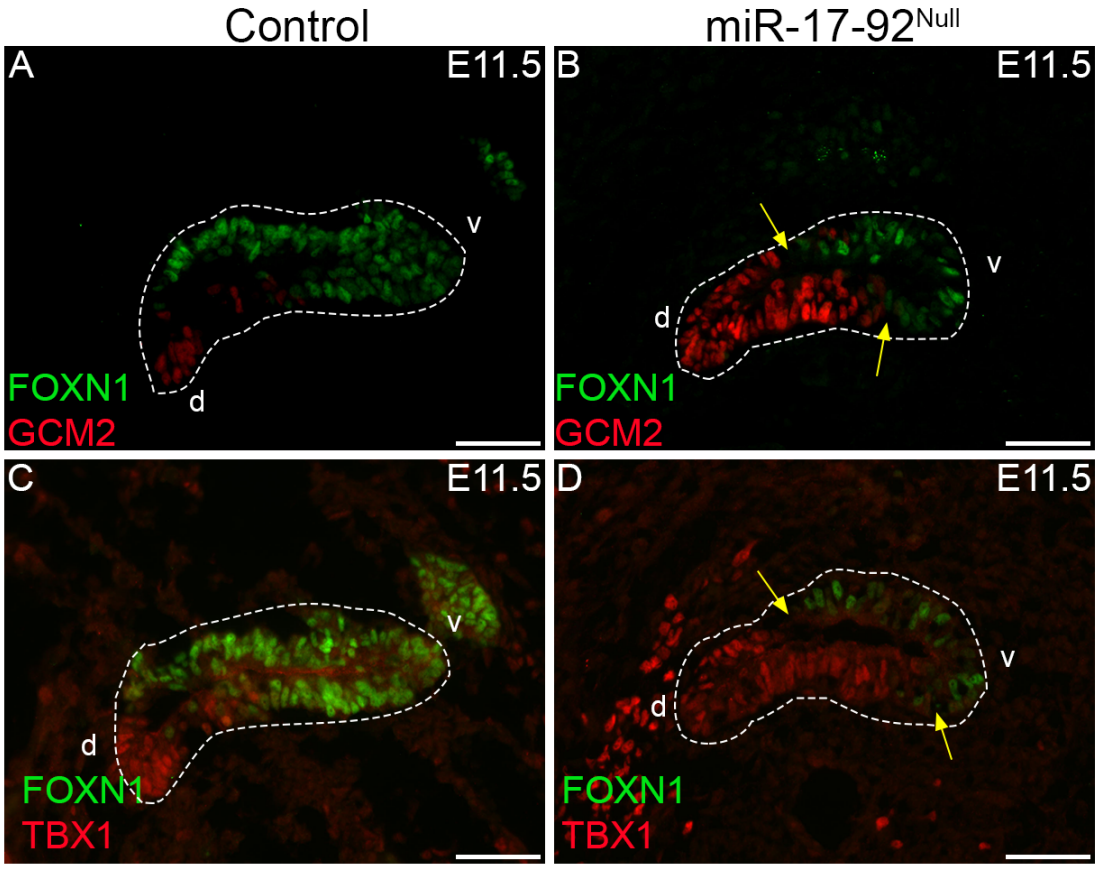

*Foxn1*$^{Cre}$;*R26*$^{iTbx/+}$ model (Fig.17C,D). This suggests that while *miR-17-92* plays a role in regulating *Tbx1* expression, additional mechanisms are necessary to suppress its expression in the ventral domain of the 3rd pp. Furthermore, we noted an increase in the mesenchymal staining intensity of TBX1 surrounding the mutant 3rd pouch when compared to littermate controls (Fig.17C-D), indicating that *miR-17-92* may also function to regulate TBX1 in non-endodermal-derived tissues. Furthermore, despite global deletion of the *miR-17-92* cluster, the 3rd pp developed and was similar in size to *miR-17-92* sufficient littermate controls (Fig.17). Interestingly, FOXN1 expression was downregulated in the mutant 3rd pp at E11.5 (Fig.17B,D). Therefore, this result is consistent with our model that TBX1 indirectly regulates the expression of FOXN1 in the ventral domain of the 3rd pp endoerm.

The transcription factor GCM2 is required for the differentiation of PT fated cells and is expressed in the dorsal domain of the 3rd pp at E11.5 (54, 121). It has been suggested that *Tbx1* regulates *Gcm2* expression because mice lacking *Tbx1* fail to express *Gcm2* (139). Furthermore, since *Tbx1* expression is not altered in *Gcm2*$^{-/-}$ mice, *Gcm2* is thought to be a downstream target of *Tbx1* (121, 139). Based on these data, we would expect GCM2 expression to phenocopy that of TBX1 in the *miR-17-92*$^{Null}$ embryos. However, GCM2 expression was unaltered in the mutant embryos at E11.5 when compared to control littermates, suggesting that *Gcm2* may not be a direct downstream target of *Tbx1*. These data seemingly contradict the conclusion from gene expression studies in *Tbx1* null mice (139). However, given that pharyngeal segmentation does not occur in the absence of *Tbx1*, the loss of *Gcm2* expression in *Tbx1* null mice is likely secondary to the absence of 3rd pp formation.

By E11.5, the wildtype 3rd pp is patterned into distinct regions of FOXN1 positive thymus-fated cells and TBX1/GCM2 positive PT-fated cells. At this stage of development, organ fate has been specified in most 3rd pp cells and there are very few, if any, organ-specific cells that comingle at the boundary between the thymus and PT fated cells.

However, in the *miR-17-92*$^{Null}$ 3$^{rd}$ pp, there was not a clear demarcation between the thymus and PT boundary, with several thymus- or PT-specific cells comingling (Fig.17). Furthermore, when *miR-17-92* is globally deleted, there are a number of cells at the thymus-PT boundary that do not express FOXN1, GCM2 or TBX1 (yellow arrows), suggesting that organ-specific cell fate is delayed or defective or that there may be a reversal in cell identity.

These results suggest that global deletion of *miR-17-92* increases the TBX1 expression domain into the ventral region of the 3$^{rd}$ pp and reduces FOXN1 expression. Furthermore, the absence of *miR-17-92* results in a small population of cells that presumably, have yet to assume organ-specific fate given that they do not express either thymus- or PT-specific markers. Taken together, these data support our model in which *miR-17-92* mediates downregulation of *Tbx1* in the 3$^{rd}$ pp. These data also demonstrate a role for *miR-17-92* in regulating *Tbx1* expression in mesenchyme adjacent to the 3$^{rd}$ pp.

**Global deletion of *miR-17-92* impairs thymus organogenesis**

Given that *Foxn1* is required for TEC proliferation and differentiation (57, 87, 88, 99, 142), we hypothesized that thymus development would be inhibited as a result of the reduced frequency of FOXN1 positive cells seen at E11.5 in the *miR-17-92*$^{Null}$ embryos. To test this premise, we analyzed the location of thymic lobes as well as TEC differentiation in E14.5 *miR-17-92*$^{Null}$ and littermate control embryos. The left thymic lobe was absent in the first *miR-17-92*$^{Null}$ embryo we examined (Fig.18B). However, the right thymic lobe was present, but severely ectopic, being located 60μm beneath the jaw and adjacent to the thyroid. In addition, the right lobe was extremely hypoplastic when compared to the control. It has been shown that during mouse embryogenesis, there is left-right asymmetry, with the right side having the developmental advantage (81). Specifically, the 3$^{rd}$ pp on the right side of the animal is larger than the left and separates from the pharynx prior to the left 3$^{rd}$ pp

**Figure 18. Global deletion of *miR-17-92* impairs thymus organogenesis.**

(**A-F**) Representative IHC stains of transverse sections from control and *miR-17-92*$^{Null}$ E14.5 thymic lobes show that the absence of *miR-17-92* results in an ectopic and hypoplastic thymus phenotype. (**A,B**) 10X image demonstrates *miR-17-92*$^{Null}$ left thymic lobe is absent (as indicated by an asterisk) and the right thymic lobe is severely ectopic and hypoplastic as compared to the control. (**C,D**) FOXN1 positive cells are present in both the *miR-17-92*$^{Null}$ and control thymic lobes. (**E, F**) TEC differentiation is not altered in the *miR-17-92*$^{Null}$ thymic lobe as reflected by K8 expression in cortical TECs and K5 expression in medullary TECs. Oe, oesophagus. Tr, trachea. Lx, larynx. Th, thyroid. Scale Bars: 50 μm.

**Figure 18. Global deletion of *miR-17-92* impairs thymus organogenesis.**

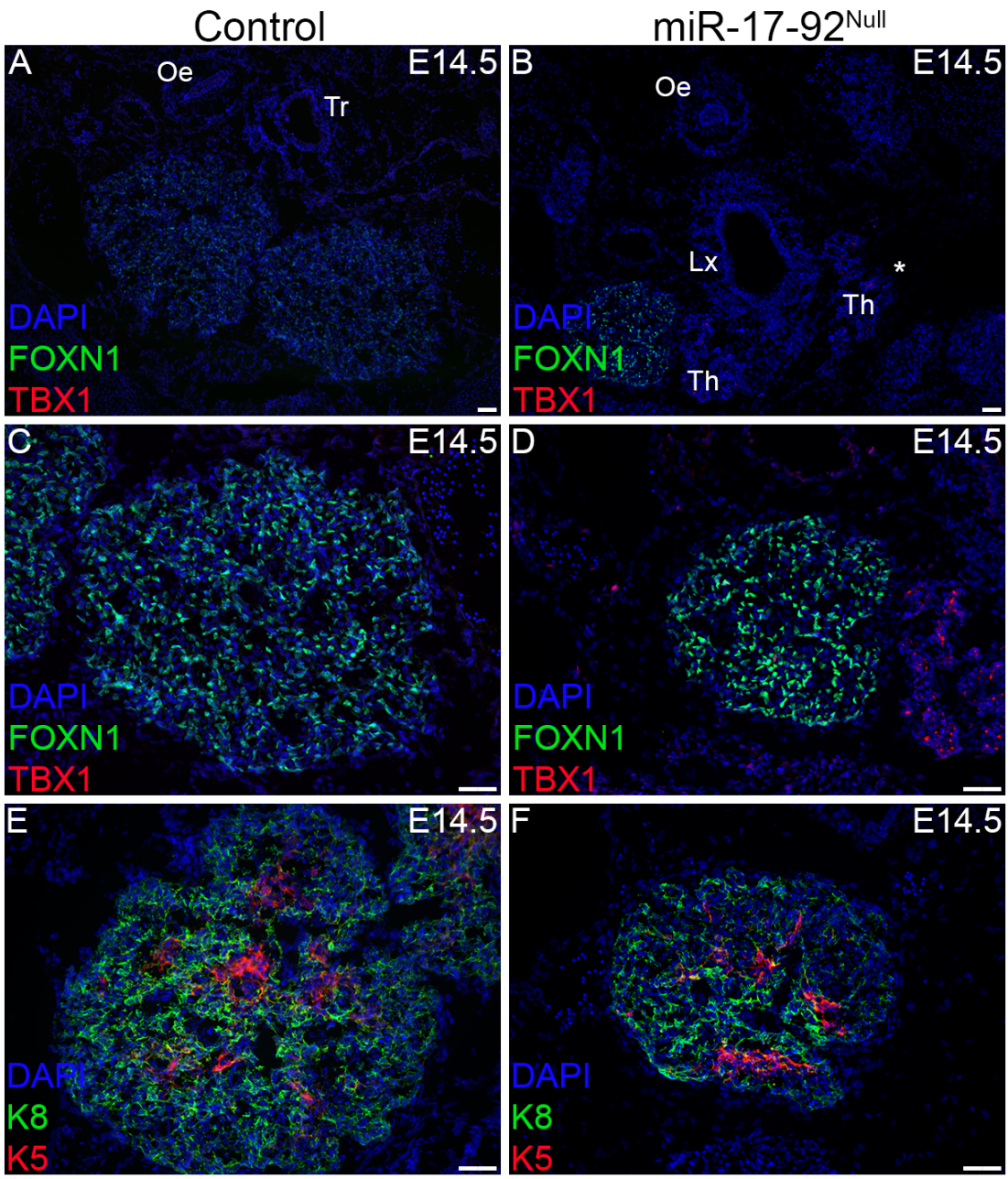

(80, 81, 162). This slight difference in developmental timing during normal organogenesis may be exacerbated in the absence of *miR-17-92*, thus contributing to the phenotype we are observing at E14.5 in *miR-17-92*$^{Null}$ embryos. However, it will be necessary to analyze additional null mutants to reach a conclusion on this point.

The reduced expression of FOXN1 at E11.5 may contribute to the hypoplastic thymic phenotype, given that it is required for TEC proliferation (57, 87, 88, 99, 142). However, FOXN1 was expressed throughout the right lobe at levels comparable to that of the control littermate (Fig.18A-B,C-D), suggesting that the few FOXN1 positive cells present in the 3$^{rd}$ pouch were capable of proliferation. Next, we wanted to determine if TBX1 was ectopically expressed in the E14.5 right lobe given that its expression persists in cardiomyocytes in the absence of *miR-17-92 (82)*. Despite the loss of *miR-17-92*, TBX1 expression was not detected in the mutant lobe, but was apparent in the thyroid (Fig.18B,D). This further supports the premise that additional mechanisms regulate *Tbx1* expression at E10.5 in the 3$^{rd}$ pp endoderm.

To determine whether or not TEC differentiation was altered in the ectopic, hypoplastic lobe, we analyzed the expression pattern of cytokeratins used to identify TEC sublineages. The *miR-17-92*$^{Null}$ right thymic lobe had distinct cortical and proto-medullary regions as reflected by the expression of K8 and K5, respectively (Fig.18E-F). These results are not surprising given that FOXN1 was expressed throughout the lobe and is required for TEC maturation. Taken together, these preliminary results indicate that *miR-17-92* is required for proper thymus organogenesis and migration.

**Targeted deletion of *miR-17-92* in TECs affects expression of TBX1 in the 3rd pp endoderm and surrounding mesenchyme**

Our data suggest that global deletion of *miR-17-92*; 1) expands *Tbx1* expression into the ventral, thymus-fated domain, 2) reduces the frequency of *Foxn1* expressing cells in the E11.5 3rd pp endoderm and 3) does not affect GCM2 expression (Fig.17). These results are consistent with our hypothesis proposing that *miR-17-92* suppresses *Tbx1* expression in the ventral domain of the 3rd pp (Fig.4). Furthermore, as our model predicts, the altered 3rd pp patterning with respect to FOXN1 and GCM2 in *miR-17-92* null embryos is similar to that obtained in the $Foxn1^{Cre/+};R26^{iTbx/+}$ 3rd pp. However, a caveat to these results is that global deletion of the *miR-17-92* cluster in non-endodermal tissues, such as mesenchyme, may be at least partly responsible for the altered 3rd pp phenotype. Therefore, to further define the role of *miR-17-92*-mediated regulation of *Tbx1* in the 3rd pp, we employed a LOF model to site-specifically delete *miR-17-92* in TECs. Specifically, $miR\text{-}17\text{-}92^{Fl/Fl}$ female mice were crossed with $Foxn1^{Cre}$ males to delete expression of the miR cluster at ~E11.25 in thymus-fated cells of the 3rd pp endoderm.

Embryos were harvested at E11.5 and sagittal sections were obtained to determine whether $Foxn1^{Cre}$-mediated deletion of *miR-17-92* alters 3rd pp development and expression of region-specific markers including *Tbx1, Foxn1*, and *Foxg1*. There was not a noticeable difference in 3rd pp size between control and $Foxn1^{Cre/+};miR\text{-}17\text{-}92^{Fl/Fl}$ embryos. Interestingly, while TBX1 expression was restricted to the dorsal, PT-fated domain of the mutant 3rd pouch, the staining intensity appeared greater than that in the control (Fig.19A-B). Additionally, not only did we notice this increase in staining intensity in the endoderm, but also in the mesenchyme surrounding the mutant pouch (Fig.19A-B). Taken together, these data suggest that TEC expression of *miR-17-92* regulates TBX1 in regions adjacent to the ventral domain of the 3rd pp.

**Figure 19. Targeted deletion of *miR-17-92* in TECs affects expression of TBX1 in the 3rd pp endoderm and surrounding mesenchyme.**

(**A-D**) Representative IHC stains of sagittal sections of 3rd pp from control and *Foxn1*$^{Cre/+}$*; miRNA-17-92*$^{Fl/Fl}$ embryos at E11.5. *Foxn1*$^{Cre}$-mediated excision of *miR-17-92* specifically deletes expression of the miRNA cluster from thymus-fated cells at E11.5. (**A-B**) TBX1 expression (red) is not expanded into the ventral region of *Foxn1*$^{Cre/+}$*; miRNA-17-92*$^{Fl/Fl}$ 3rd pp as compared to control. However, there are a significant number of cells that co-express FOXN1 and TBX1 at the thymus and PT boundary (yellow arrows). (**C-D**) FOXG1 expression (red) is restricted to the ventral domain of the 3rd pp pouch. Note the FOXG1 positive, FOXN1 negative cells at the thymus, PT boundary (yellow arrows). v, ventral. d, dorsal. Scale Bars: 50 μm.

**Figure 19. Targeted deletion of *miR-17-92* in TECs affects expression of TBX1 in the 3rd pp endoderm and surrounding mesenchyme.**

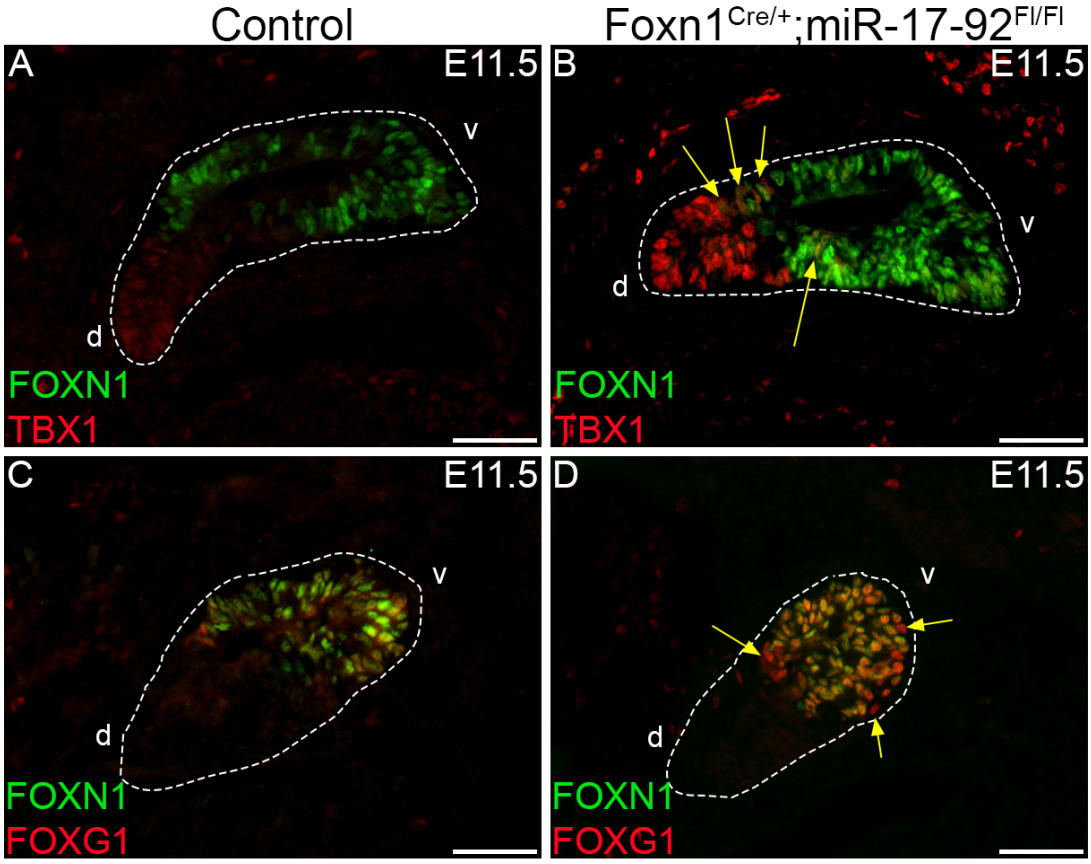

Since *Foxn1*$^{Cre}$ is not expressed until ~E11.25, it is not surprising that we did not observe a discernable difference in the frequency of FOXN1 positive cells among mutant offspring and somite-matched control littermates at E11.5 (Fig.19A-B). However, we did observe that the mutant pouch contained cells at the thymus-PT boundary that co-expressed FOXN1 and TBX1 (Fig.19B, yellow arrows). Such co-expressing cells are exceedingly rare in the E11.5 wildtype pouch (Fig.19A). This is interesting to note, as cells located at the thymus-PT boundary are the last to assume either organ-specific fate (51, 54, 111). These results suggest that deleting *miR-17-92* in cells at the thymus-PT boundary that have yet to fully commit to a thymus fate, prevents TBX1 downregulation, thus permitting co-expression of TBX1 and FOXN1. Also, given the fact that we are deleting expression of the miR cluster in *Foxn1*$^{Cre}$-specific endoderm, it is interesting to note that we are observing effects in TBX1 expression in the dorsal domain of the 3$^{rd}$ pp and surrounding mesenchyme.

We also analyzed expression of the transcription factor FOXG1 in the E11.5 3$^{rd}$ pp from mutant and control embryos. *Foxg1* is expressed in discrete regions of wildtype 3$^{rd}$ pp endoderm and is co-expressed with FOXN1 by TECs at late fetal and postnatal stages (108). Importantly, *Foxg1* is expressed in the 3$^{rd}$ pp prior to, and independent of *Foxn1* (Wei and Condie, unpublished data). Furthermore, we previously showed that FOXG1 is expressed in FOXN1 negative cells of the ventral 3$^{rd}$ pp in E11.5 *Foxn1*$^{Cre/+}$*; R26*$^{iTbx/+}$ embryos indicating that thymus cell fate is not altered in the presence of ectopic *Tbx1* (111). Similarly, we found abundant expression of FOXG1 in the 3$^{rd}$ pp of mutant embryos (Fig.19D). Furthermore, we identified a small population of cells within the ventral domain of the mutant 3$^{rd}$ pp that were FOXG1$^{+}$FOXN1$^{Neg\text{-}Low}$, with the majority of those cells being located at the thymus-PT boundary (Fig.19D, yellow arrows). This suggests that the cells co-expressing FOXN1 and TBX1 at that the thymus-PT boundary are likely to also express

the thymus-specific marker FOXG1, supporting the notion that they are committed to the thymus cell lineage.

**TBX1 positive cells persist in the anterior portion of *Foxn1*$^{Cre/+}$*; miR-17-92*$^{Fl/Fl}$ thymic lobes**

To determine if targeted deletion of *miR-17-92* in TEC progenitors alters TEC differentiation, *Foxn1*$^{Cre/+}$*;miR-17-92*$^{Fl/Fl}$ and control embryos were harvested at multiple stages throughout late fetal development. Serial transverse sections were obtained throughout the entirety of each lobe and analyzed for expression of various progenitor or lineage specific TEC markers. Unlike the thymic hypoplasia and ectopia observed in *miR-17-92*$^{Null}$ embryos, *Foxn1*$^{Cre/+}$*;miR-17-92*$^{Fl/Fl}$ thymi are comparable in size and location to that of control embryos at E12.5, E14.5 and E17.5 and express similar levels of FOXN1 (Fig.20). This result is not surprising given that FOXN1 was widely expressed throughout the ventral domain of the mutant 3$^{rd}$ pp and that *Foxn1* is required for TEC differentiation and proliferation.

However, because there were cells in the E11.5 3$^{rd}$ pp that co-expressed FOXN1 and TBX1, we asked whether TBX1 is expressed in the mutant TECs at later developmental stages. Considering that *Tbx1* is not expressed in fetal or adult wildtype TECs (111, 122, 163) and that *Tbx1* expression does not extend into the ventral domain of the mutant 3$^{rd}$ pp, we expected very few, if any, TECs to co-express FOXN1 and TBX1. Indeed, we did not observe FOXN1 positive TECs in control thymi that co-expressed TBX1 (Fig.20A). Interestingly however, we found a rare subset of TECs in the most anterior region of the mutant lobes that expressed TBX1, but no (or extremely low levels) of FOXN1 at E12.5 (Fig. 20B, yellow arrows). Notably, the ectopic expression of TBX1 in the anterior portion of the thymic lobes persisted at E14.5 and E17.5 in the mutant embryos (Fig.20D,F, yellow

**Figure 20. TBX1 positive cells persist in the anterior portion of *Foxn1$^{Cre/+}$; miR-17-92$^{Fl/Fl}$* thymic lobes**

(**A-F**) Representative IHC stains of transverse sections from (**A, B**) E12.5, (**C, D**) E14.5 and (**E, F**) E17.5 control and *Foxn1$^{Cre/+}$;miRNA-17-92$^{Fl/Fl}$* thymic lobes. (**B, D, E**) Note the TBX1 positive (red), FOXN1 negative to low cells in the anterior portion of the *Foxn1$^{Cre/+}$; miRNA-17-92$^{Fl/Fl}$* thymic lobe (yellow arrows). (**A, C, E**) FOXN1 and TBX1 co-expressing cells are not present in the control. Scale bars: 50 μm.

**Figure 20. TBX1 positive cells persist in the anterior portion of *Foxn1$^{Cre/+}$; miR-17-92$^{Fl/Fl}$* thymic lobes.**

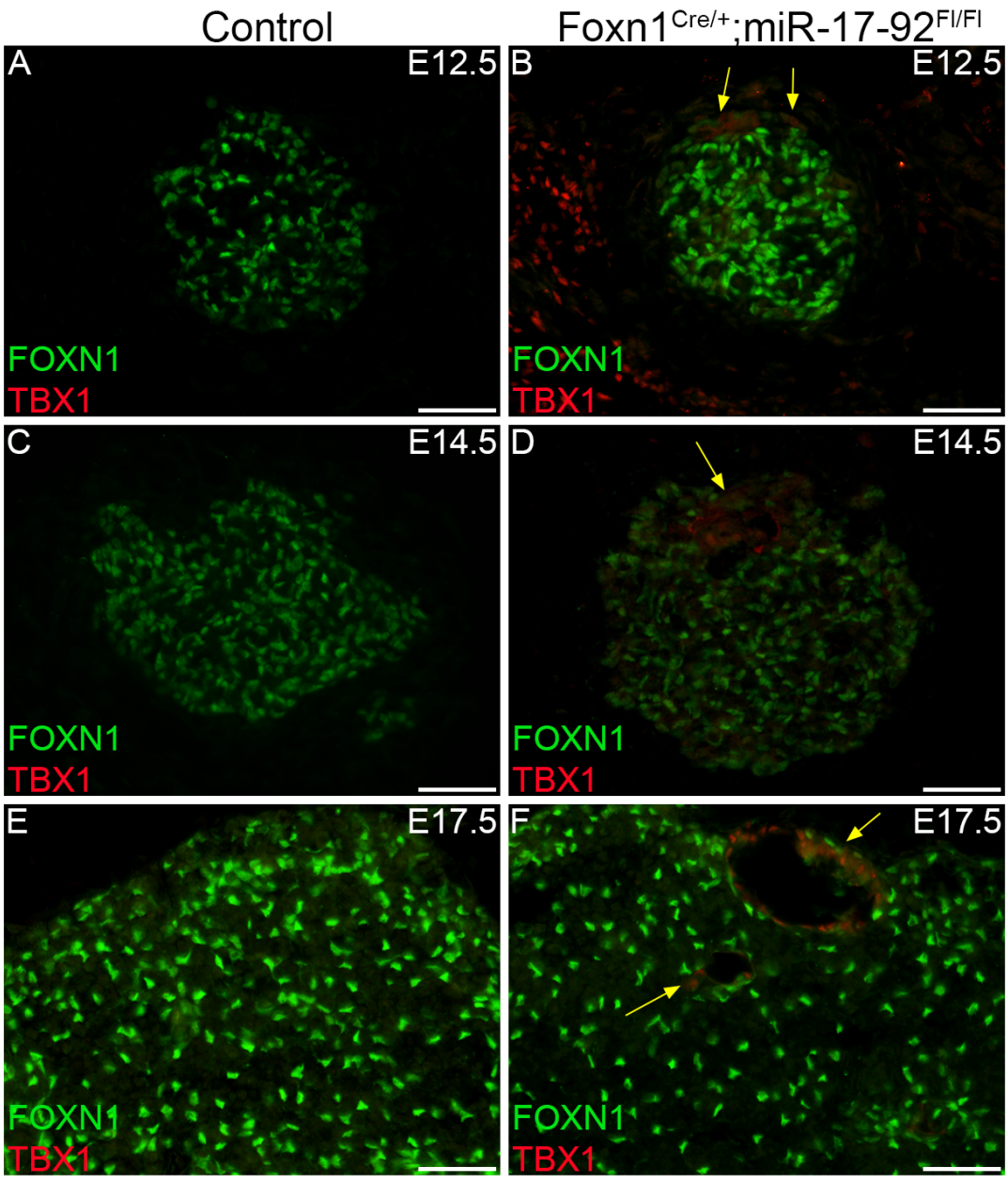

arrows). Furthermore, as was seen at E12.5, the TBX1 positive cells also expressed negative to low levels of FOXN1 (Fig.20D,F). Taken together, these data suggest that the *miR-17-92* cluster might not only be important in downregulating *Tbx1* at E10.5 in the ventral domain of the 3rd pp, but may play a role in maintaining continuous suppression of *Tbx1* in TECs at later stages during development.

The frequency and location of the FOXN1/TBX1 co-expressing cells within the mutant thymus at multiple stages of fetal development provides insight into what might be occurring in the *Foxn1*$^{Cre/+}$*;miR-17-92*$^{Fl/Fl}$ E11.5 pouch. The 3rd pp is oriented in such a way that the dorsal domain is anterior to that of the ventral domain. When the thymus and PT separate from one another and the thymus migrates to a more posterior location, those cells located at the boundary will presumably be located in the anterior region of the thymus lobe. Therefore, this suggests that the FOXN1$^{Neg\text{-}Low}$TBX1$^{+}$ cells located at the thymus-PT boundary in the E11.5 3rd pp persist in the mutant fetal thymus lobes. Taken together, these results support the hypothesis that *miR-17-92* plays an important, but not indispensable role in extinguishing *Tbx1* expression in *Foxn1* positive cells.

### *Foxn1*$^{Cre/+}$*; miR-17-92*$^{Fl/Fl}$ fetal thymi contain a rare population of TECs that co-express TBX1, PLET1 and low levels of FOXN1

The persistence of FOXN1$^{Neg\text{-}Low}$TBX1$^{+}$ cells from E11.5 in the *Foxn1*$^{Cre/+}$*;miR-17-92*$^{Fl/Fl}$ 3rd pp into the fetal thymic lobes at E17.5 may be attributable to one of the following; 1) cells at the thymus-PT boundary have committed to a thymus fate but are arrested at a progenitor-like state or 2) thymus cell fate has been reversed and TBX1 is downregulating FOXN1 to promote the establishment of PT fate. The first possibility is supported by our work using the *Foxn1*$^{Cre/+}$*;R26*$^{iTbx1/+}$ model in which ectopic expression of *Tbx1* in *Foxn1* positive cells results in an early arrest in TEC differentiation (111). Therefore, we predicted

that TEC maturation would be blocked when *miR-17-92* is deleted in *Foxn1* positive cells and TBX1 is ectopically expressed. To test this hypothesis, serial sections were taken at E14.5 and stained with either GCM2 (to determine if cell fate was reversed), PLET-1 (to determine if the cells were arrested in a bipotent TEC progenitor state) or with ΔNp63 (expressed by endodermal-derived cells).

Interestingly, the FOXN1$^{Neg\text{-}Low}$TBX1$^{+}$ cells are negative for GCM2 indicating that this rare population did not assume a PT cell fate. Furthermore, these cells tend to organize around regions devoid of thymic epithelium (TE). Studies are currently underway to identify what these cells are and if they provide a specialized niche that attracts this rare group of cells. Although the cells within the thymus did not express GCM2, the data show that there are a few GCM2 positive cells in close proximity to the mutant thymic lobe (Fig. 21B-C). This is not uncommon given that when the thymus and PT separate from one another during organogenesis, a few PT cells are often left behind and can be detected in proximity to the thymic lobes (164).

ΔNp63, an isoform of p63, is a target of FOXN1 and has been shown to regulate cell cycle progression and differentiation in TECs (100, 165). In the control, ΔNp63 is co-expressed with FOXN1 at relatively comparable levels throughout the thymus (Fig. 21D). Similar to that in the control, ΔNp63 was co-expressed with FOXN1 in the E14.5 mutant thymus, but at higher levels than that of FOXN1 (Fig. 21D-F). In addition, the FOXN1$^{Low\text{-}Neg}$TBX1$^{+}$ cells present in the mutant thymus were also ΔNp63 positive (Fig. 21E-F), providing evidence that this rare population of cells is of endodermal origin. However, these results do not determine if these cells are committed to the TEC lineage, but are blocked at an early progenitor stage. To resolve this question we analyzed Plet-1 expression. Plet-1 identifies bipotent TEC precursors that are capable of differentiating into both cortical and medullary lineages (90). Initially Plet-1 is widely detected in TEC progenitors, and as

**Figure 21. *Foxn1$^{Cre/+}$; miRNA-17-92$^{Fl/Fl}$* fetal thymi contain a rare population of TECs that co-express TBX1, PLET1 and low levels of FOXN1.**

(**A-I**) Representative IHC stains of transverse sections from E14.5 control and *Foxn1$^{Cre/+}$; miRNA-17-92$^{Fl/Fl}$* thymi. To determine the identity of the TBX1 positive cells in anterior portion of the *Foxn1$^{Cre/+}$; miRNA-17-92$^{Fl/Fl}$* fetal thymus, serial sections were stained with the (**A-C**) parathyroid marker GCM2 (red) and TEC progenitor markers (**D-F**) ΔNp63 (red) and (**G-I**) PLET1 (turquoise). (**B, C, E, F**) Note the few GCM2 positive cells in the anterior potion of the *Foxn1$^{Cre/+}$; miRNA-17-92$^{Fl/Fl}$* lobe. It is common for a few parathyroid cells to be attached to the thymus after the thymus and parathyroid separate earlier in development. The TBX1 positive cells in fetal *Foxn1$^{Cre/+}$; miRNA-17-92$^{Fl/Fl}$* thymi are GCM2 negative, but are positive for the TEC progenitor markers (**E,F,H,I**) ΔNp63 and PLET1. Scale bars: 50 μm.

**Figure 21. *Foxn1*$^{Cre/+}$*; miRNA-17-92*$^{Fl/Fl}$ fetal thymi contain a rare population of TECs that co-express TBX1, PLET1 and low levels of FOXN1.**

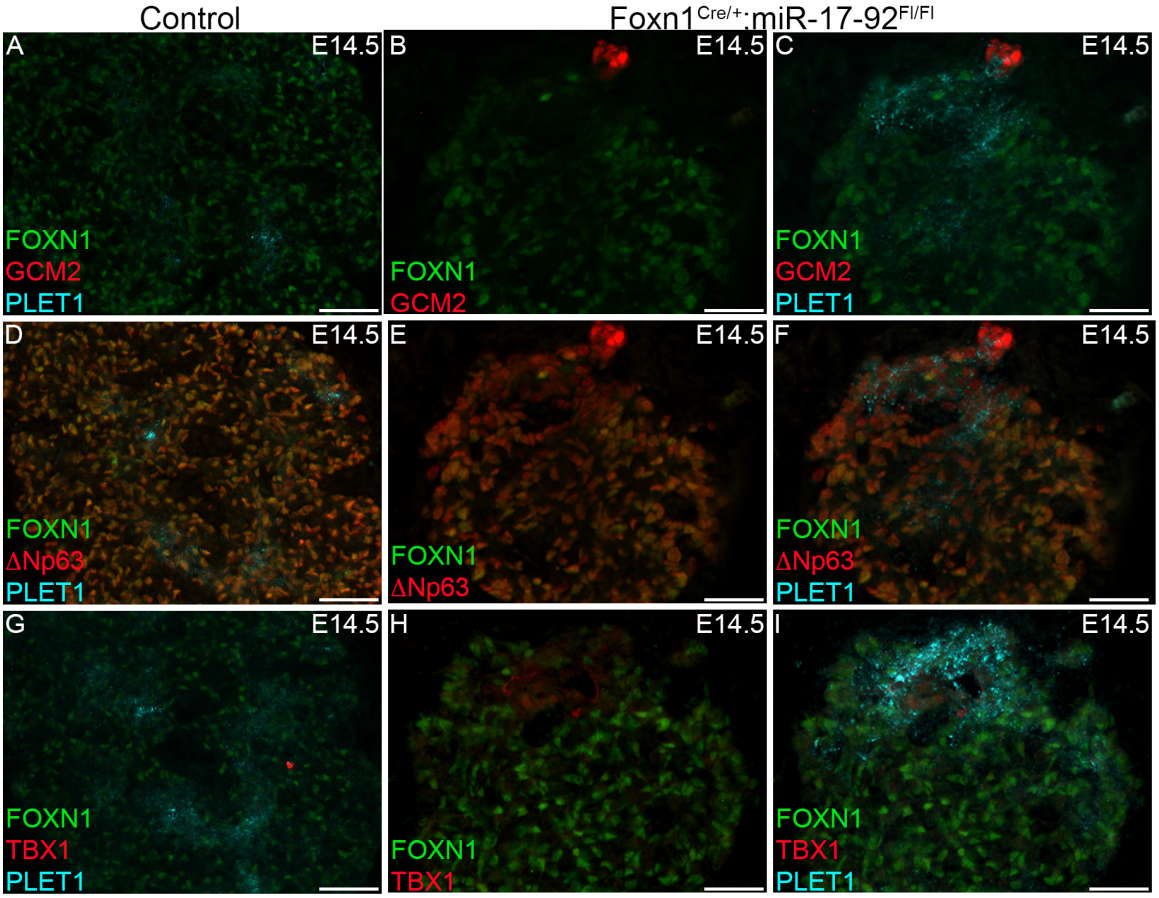

thymus development progresses the frequency of Plet-1$^{+}$ TECs is reduced and Plet-1$^{+}$ cells become restricted to the medullary region (90). At E14.5, PLET-1 expression is detected in a small population of mTECs in the control thymus (Fig. 21A,D,G). In contrast, Plet-1$^{+}$ cells are concentrated around the anterior region of the mutant lobe. Furthermore, the FOXN1$^{Neg-Low}$TBX1$^{+}$ cells in the mutant thymus co-stain for Plet-1 (Fig.21I). This striking phenotype suggests that deletion of *miR-17-92* in *Foxn1* positive cells causes an arrest in TEC differentiation at an early progenitor state. These data support our hypothesis that *miR-17-92* mediated downregulation of *Tbx1* is necessary to allow for proper TEC differentiation.

**Transgenic expression of *miR-17-92* downregulates TBX1, but not GCM2**

We started preliminary experiments using a GOF model to further analyze the role of *miR-17-92*-mediated regulation of *Tbx1* in the 3$^{rd}$ pp and the fetal thymus. We obtained mice in which an inducible *miR-17-92$^{OE}$* allele was inserted into the *Rosa26* locus and used *Foxn1$^{Cre}$* to express the *miR-17-92* cluster in TECs. Since *Foxn1* is expressed in the 3$^{rd}$ pp at ~E11.25 (54), we analyzed serial sections of E11.75 embryos for the expression of FOXN1, TBX1 and GCM2 to determine if expression of the *miR-17-92* transgene in *Foxn1* expressing cells results in an expansion of thymus cell fate into the dorsal domain of the pouch, at the expense of PT fate.

We hypothesized that overall pouch patterning would not be greatly affected in the 3$^{rd}$ pp of *Foxn1$^{Cre/+}$;miR-17-92$^{OE/+}$* embryos given that *miR-17*-92 was likely to be overexpressed in the ventral *Foxn1* expressing domain that presumably has already downregulated *Tbx1*. As expected, TBX1 was restricted to and expressed throughout the dorsal domain of the mutant pouch (Fig.22). However, the staining intensity of TBX1 was markedly reduced when compared to the control, where the staining intensity of TBX1 was readily detectable (Fig.22B). Assuming that *Foxn1$^{Cre}$* induces expression of the *miR-17-92* transgene in the ventral, and not the dorsal, domain of the 3$^{rd}$ pp, this result is quite

**Figure 22. Transgenic expression of *miR-17-92* downregulates TBX1, but not GCM2.**

(**A-D**) Representative IHC stains of sagittal sections from 3rd pp of *Foxn1*$^{Cre/+}$*; miR-17-92*$^{OE/+}$ and control E11.5 embryos. (**A-B**) TBX1 (red) is restricted to, and expressed throughout the dorsal, parathyroid-fated domain of the *Foxn1*$^{Cre/+}$*; miR-17-92*$^{OE/+}$, 3rd pp endoderm, but at significantly reduced levels when compared to the control. (**C-D**) Overexpression of *miR-17-92* does not affect the localization or frequency of GCM2 positive cells (red). v, ventral. d, dorsal. Scale Bars: 50 μm.

**Figure 22. Transgenic expression of *miR-17-92* downregulates TBX1, but not GCM2.**

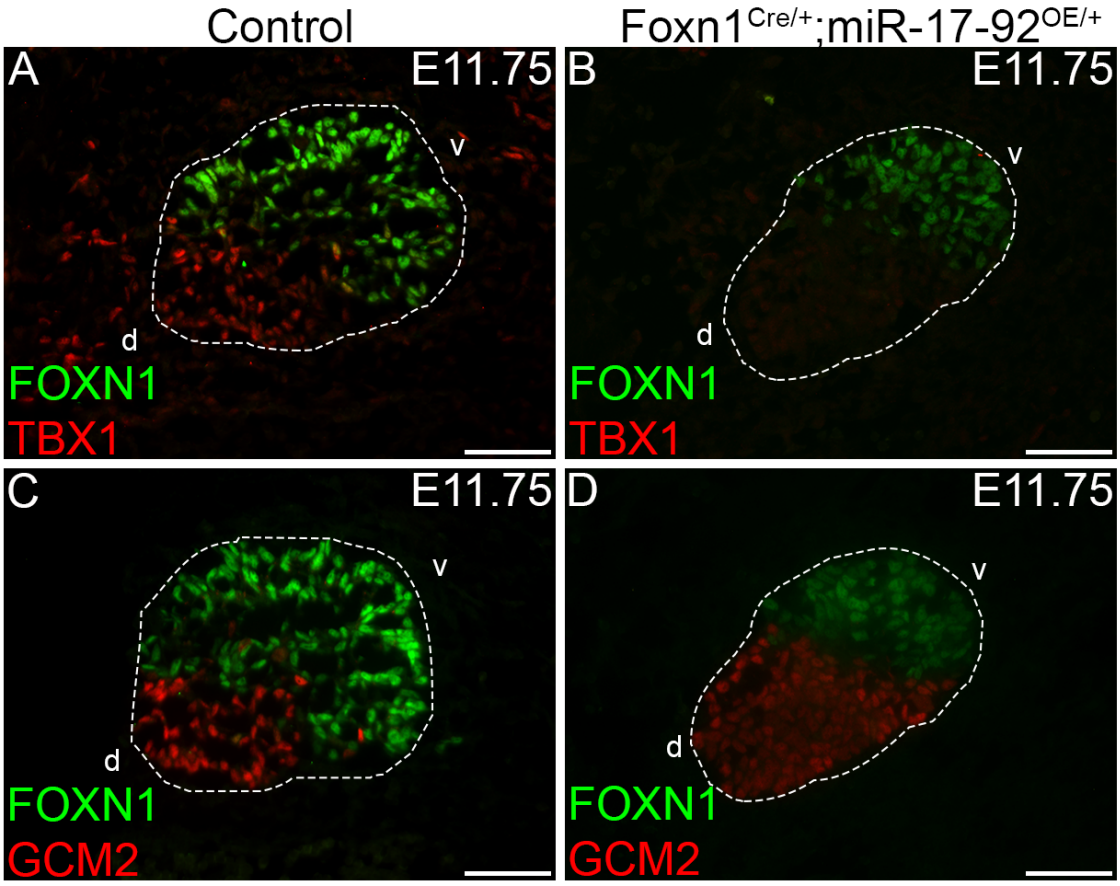

unexpected. Furthermore, we also observed a reduction in TBX1 positive cells in the mesenchyme surrounding the mutant 3rd pp when compared to the control (Fig.22A,B). Therefore, these data suggest that *miR-17-92* may function to regulate *Tbx1* expression in a non-cell autonomous manner given that TBX1 expression is reduced in tissues where the *miR-17-92* transgene should not be expressed. However, analysis of *miR-17-92* transgene expression is required to clarify these findings.

When expression of FOXN1 and GCM2 were analyzed, there was not a discernable difference in the overall patterning of the pouch. Expression of FOXN1 was restricted to the ventral domain of the mutant 3rd pp and did not expand into the dorsal domain (Fig.22B,D). In addition, GCM2 expression was not affected and remained restricted to the dorsal domain in both the control and mutant pouches (Fig.22C,D). Taken together, these data suggest that transgenic expression of *miR-17-92* does not change the frequency of cells fated to either a thymus or PT lineage. However, they do strongly support our model that *miR-17-92* directly targets *Tbx1* in the 3rd pp endoderm.

**Expression of a *miR-17-92 transgene in TECs* does not affect their differentiation**

Given that FOXN1 expression was not reduced and remained restricted to the ventral domain of the 3rd pp when *miR-17-92* was overexpressed, we did not expect to see a difference in thymus size or TEC differentiation at later fetal stages. As anticipated, E14.5 $Foxn1^{Cre/+}$;$miR\text{-}17\text{-}92^{OE/+}$ thymi were comparable in size to that of the controls and were located just anterior to the heart (Fig.23). Furthermore, FOXN1 positive cells were detected throughout the control and mutant thymus lobes at comparable frequencies and staining intensities (Fig.23).

To determine if overexpression of the *miR-17-92* cluster alters the frequency of TECs committed to either cTEC or mTEC lineages, we analyzed the FOXN1-dependent cTEC

**Figure 23. Transgenic expression of *miR-17-92* does not affect TEC differentiation.**

(**A-F**) Representative IHC stains of transverse sections from E14.5 control and *Foxn1*$^{Cre/+}$*; miR-17-92*$^{OE/+}$ thymi. To determine if transgenic expression of miR-17-92 in *Foxn1* positive cells affects TEC commitment to either a medullary or cortical lineage, serial sections were stained with (**A-B**) TEC marker FOXN1 (green) and mTEC marker UEA-1 (turquoise), (**C-D**) early mTEC marker Cldn3/4 (red) and early cTEC cell surface molecule CD205 (turquoise), (**E-F**) bipotent TEC progenitor marker Plet-1 (turquoise) and thymoproteosome subunit β5t (red). Note the mild increase in UEA-1 and Cldn3/4 along with expanded protomedullary regions expressing Plet-1. Scale bars: 50 μm.

**Figure 23. Transgenic expression of *miR-17-92* does not affect TEC differentiation.**

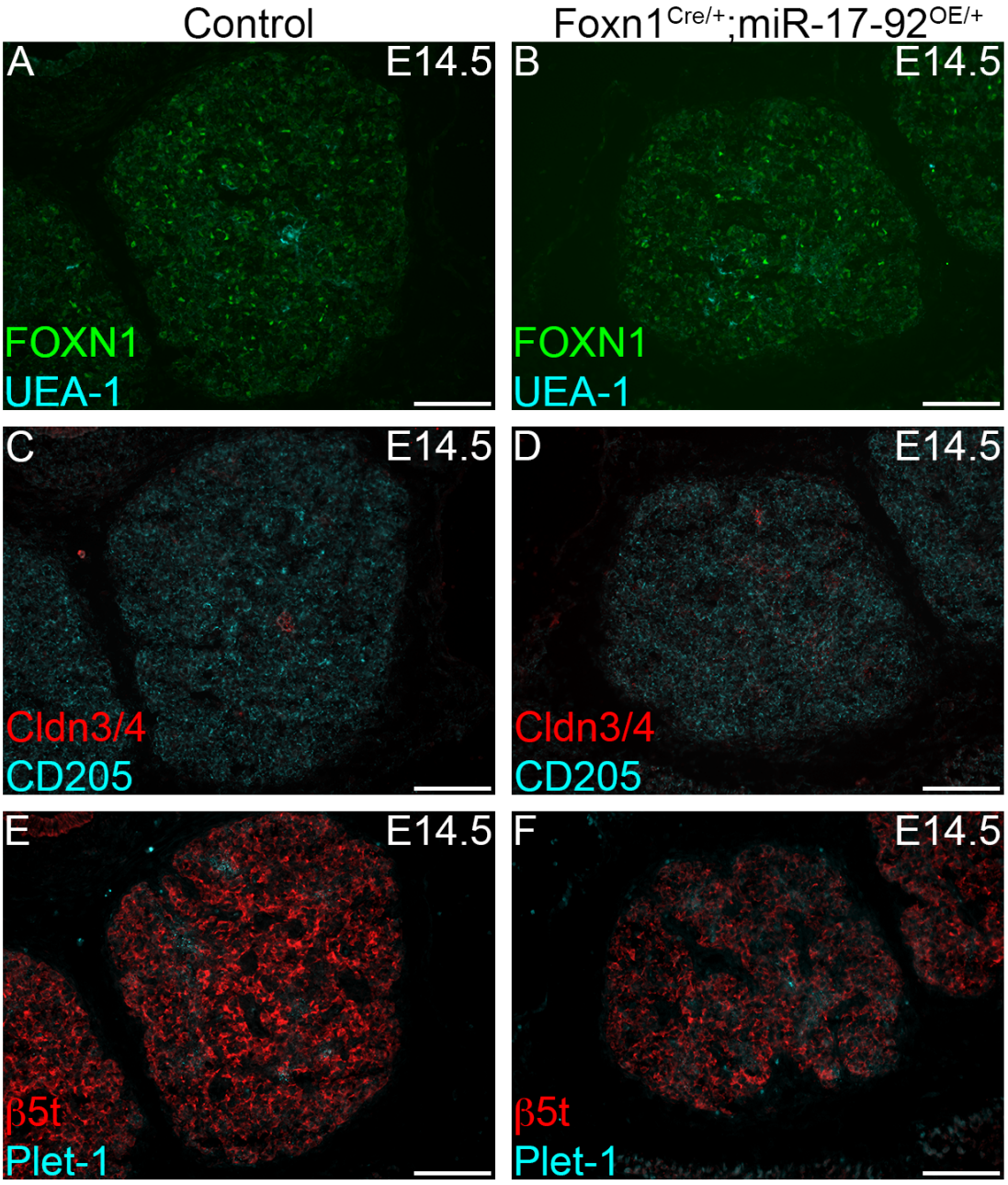

markers β5t and CD205 (92, 144, 146), mTEC markers UEA-1 and Cldn3/4 (147) and the bi-potent progenitor marker Plet-1(90). In wildtype mice, β5t and CD205 are expressed at early stages of cTEC differentiation, and are expressed by the vast the majority of mature cTECs (Fig.23C,E). Expression of β5t and CD205 were comparable in mutant and control thymi (Fig.23C-F), suggesting that early differentiation of the cTEC lineage is not altered when *miR-17-92* is overexpressed in *Foxn1* positive cells. Both UEA-1 and Cldn3/4 are expressed within the protomedullary regions of the E14.5 thymus (Fig.23A) as well as by mature mTECs (91). Interestingly, expression of Cldn3/4 and UEA-1 appeared to be increased in the proto-medullary regions of mutant thymi (Fig.23B,D).

Given the moderate increase in early mTEC-specific markers, we wanted to determine if there was a change in frequency of Plet-1 positive TEC progenitor cells. As expected, Plet-1 positive cells were detected in the proto-medullary regions of the control and mutant E14.5 thymus (Fig.23E,F). However, the medullary regions in the mutant thymus appear larger than those in the control and there is a concomitant increase in Plet-1 expression (Fig.23E,F). Taken together, these data suggest that transgenic expression of *miR-17-92* in TECs increases the frequency of Plet-1 positive cells and may skew TEC differentiation to the medullary lineage.

**CONCLUSIONS**

We have reported that *Tbx1* is a negative regulator of thymus development and must be downregulated in the ventral, thymus-fated domain of the 3$^{rd}$ pp to allow for TEC proliferation and differentiation (111). However, the molecular mechanisms that regulate *Tbx1* expression in the 3$^{rd}$ pp endoderm during thymus organogenesis remain to be defined. During cardiac development, *Tbx1* maintains cardiomyocytes in a progenitor-like state and is downregulated via a *Bmp2/4-miR-17-92*-mediated mechanism to promote cell differentiation (82). Given that *Bmp4* promotes the identification and differentiation of TECs,

and ectopic expression of *Tbx1* arrests TEC differentiation (81, 111), we hypothesized that a similar mechanism may regulate *Tbx1* in the 3rd pp, as shown in Figure 4. Through the use of *miR-17-92* LOF and GOF models, our results demonstrate that *miR-17-92* regulates *Tbx1* and influences patterning in the 3rd pp endoderm.

*The mir-17-92 cluster is expressed in the 3rd pp endoderm and surrounding mesenchyme*

Prior to our studies, the expression pattern of *miR-17-92* has never been defined in the 3rd pp endoderm. Using LNA probes to *miR-17*, *miR-19a* and *miR-92a*, we demonstrated that all three members of the *miR-17-92* cluster are expressed in the 3rd pp endoderm as well as in the adjacent mesenchyme. Although none of the miRNAs that were analyzed had the same expression pattern within the 3rd pouch, the difference among each individual miRNA might be attributable to the fact that each member of the *miR-17-92* cluster behaves differently within different tissues, at different times during development (reviewed in (130)). Furthermore, these data indicate that at E10.5, *miR-17*, *miR-19a* and *miR-92a* are acting not only in the ventral domain, but also the dorsal region of the pouch, suggesting that they may be functioning to temper expression of *Tbx1*. The continued expression of *miR-17*, *miR-19a* and *miR-92a* in the ventral domain of the 3rd pp at E11.5 also suggests that *miR-17-92* might serve as a mechanism to continuously suppress *Tbx1* within the thymus-fated domain of the pouch.

*Global deletion of miR-17-92 reduces FOXN1 expression in the 3rd pp and impairs thymus organogenesis and migration*

Global deletion of *miR-17-92* resulted in an expansion of TBX1 expression into the ventral domain of the 3rd pp. However, unlike the *Foxn1*$^{Cre/+}$*;R26*$^{iTbx1/+}$ mouse model, TBX1 was not detected in the ventral tip of the pouch. The fact that loss of *miR-17-92* did not alter

TBX1 expression to the same extent as ectopic expression in the *Foxn1*$^{Cre/+}$;*R26*$^{iTbx1/+}$ mouse model is not surprising. First, *Tbx1* was being driven from the strong *R26* promoter. Secondly, we know that miRNAs often have relatively minor effects on expression of their target genes. Therefore, the fact that TBX1 was not as robustly expressed suggests that additional mechanisms are in place to suppress *Tbx1* in this region of the pouch.

However, the observed increase in TBX1 did result in fewer FOXN1 positive cells located within the ventral domain of the 3$^{rd}$ pp. Furthermore, loss of *miR-17-92* did not have a detectable effect on GCM2 expression, which remained restricted to the dorsal domain. These data suggest that additional mechanisms regulate *Gcm2* expression in the pouch, further supporting the notion that *Tbx1* may not be directly upstream of *Gmc2*.

When analyzed at E14.5, one lobe of the null thymus was ectopic and hypoplastic and the second lobe was not detected within the thoracic cavity or neck region. Although the phenotype we observed at E14.5 was unexpected, the presence of the right lobe and absence of the left could be explained by developmental asymmetry. As previously discussed, the right side of the embryo tends to have a developmental advantage over the left, with the right thymus lobe being larger and separating from the pharynx prior to that of the left (80, 81, 162). Therefore, this difference in developmental timing could be amplified in the absence of *miR-17-92*. Given that we observed an ectopic thymus lobe, *miR-17-92* may also function to regulate thymus migration.

Interestingly, TEC differentiation was unaffected in the mutant lobe as FOXN1 was widely expressed by TECs, suggesting that the few FOXN1 positive cells present at E11.5 were capable of proliferation and differentiation. Taken together, these results support our hypothesis that *miR-17-92* regulates *Tbx1* in the developing 3$^{rd}$ pp and is therefore required for proper thymus organogenesis.

*Deletion of miR-17-92 in TECs results in higher levels and ectopic expression of TBX1*

Site-specific deletion of *miR-17-92* in TECs using *Foxn1*$^{Cre}$ does not affect overall patterning in the 3$^{rd}$ pp endoderm. FOXN1, GCM2 and TBX1 are restricted to, and expressed in their respective domains. Interestingly, although the TBX1 expression domain is not expanded in the absence of *miR-17-92* at E11.5, its staining intensity is higher in the dorsal domain as well as in the mesenchyme surrounding the mutant pouch than it is in the control. This suggests that TEC expression of *miR-17-92* may regulate expression of *Tbx1* not only in the ventral domain of the pouch, but also in PT-fated and mesenchymal cells.

Furthermore, we find a rare population of cells located at the thymus-PT boundary in the mutant 3$^{rd}$ pp endoderm that co-express FOXN1 and TBX1. This rare population of Foxn1$^{Neg\text{-}Low}$TBX1$^{+}$ cells persists in anterior region of E12.5, E14.5 and E17.5 fetal thymus lobes, and they express the bi-potent TEC progenitor marker Plet-1.

These data strongly support the notion that *miR-17-92*-mediated deletion of *Tbx1* in TECs that have not yet fully committed to the thymus lineage abrogates TEC differentiation and arrests endodermal cells at a progenitor stage.

*Transgenic expression of miR-17-92 in TECs non-cell autonomously regulates Tbx1*

Although we have yet to perform experiments confirming that *miR-17-92* is being overexpressed in the ventral domain of the 3$^{rd}$ pp, based on numerous studies showing that *Foxn1*$^{Cre}$ is expressed in ventral pouch and later in TECs, we anticipated that when *miR-17-92*$^{OE}$ mice were crossed with *Foxn1*$^{Cre}$ mice, the miR cluster would be expressed in these cell types. Therefore, based on the assumption that we were overexpressing *miR-17-92* in a region where *Tbx1* was already downregulated, we hypothesized that the thymus-fated domain would remain restricted to the ventral domain and not expand at the expense of the

PT-fated domain. Our results support this hypothesis as FOXN1 and GCM2 expression was not altered in the 3rd pp of *Foxn1*$^{Cre/+}$*;miR-17-92*$^{OE/+}$ embryos.

Interestingly, while TBX1 was expressed in the dorsal domain of the pouch, the staining intensity was greatly reduced when compared to the control. Moreover, a reduction in TBX1 staining intensity was also observed in the mesenchyme of the transgenic mutant mouse model. This result was quite surprising given the fact that we were observing non-cell autonomous effects when the *miR-17-92* cluster was being overexpressed in the ventral domain of the pouch. It has been reported that *miR-17-92* functions in both non-cell autonomous and cell autonomous manners, however its mode of action is highly dependent on the type of cell it is expressed in (166). Specifically, during tumorigenesis, *miR-17-92* functions in a non-call autonomous manner to promote angiogenesis (167). However, it functions in a cell autonomous manner to promote the proliferation and inhibit the differentiation of cancerous lung cells (168, 169). Although a role for *miR-17-92* in 3rd pp development and thymus organogenesis has never been reported, it is quite possible that in our model system, *miR-17-92* acts in a non-cell autonomous manner to regulate *Tbx1* expression. Given that miRNAs can be transferred between cells in exosomes (reviewed in (170)), non-cell autonomous *miR-17-92*-mediated regulation of *Tbx1* may occur as a result of this mechanism. Therefore, these data strongly suggest that *miR-17-92* may act in a non-cell autonomous manner within the 3rd pp endoderm to downregulate TBX1.

## CHAPTER 5: Additional mechanisms regulate TBX1 in the 3rd pp endoderm

### INTRODUCTION

Complex and dynamic signaling pathways are required to commit 3rd pp progenitors to a thymus fate and to regulate subsequent stages of TEC development. We previously showed that ectopic expression of *Tbx1* in thymus-fated cells inhibits TEC differentiation, resulting in extremely hypoplastic fetal thymus lobes that contain an accumulation of potentially bipotent TEC progenitors (111). These results led to the model in Figure 4 proposing that TBX1 is a key transcription factor regulating thymus development. We then focused on identifying factors that regulate *Tbx1* expression. This effort led to the discovery that *miR-17-92* regulates *Tbx1* in the 3rd pp endoderm and that deletion of *miR-17-92*, impairs thymus organogenesis as predicted by our model (Fig. 4). However, we noted that deletion of *miR-17-92* did not expand the TBX1 expression domain as dramatically as was seen in the $Foxn1^{Cre/+}$;$R26^{iTbx1/+}$ mouse model. Moreover, using a *miR-17-92* transgenic model, we noted that *miR-17-92* non-cell autonomously regulates TBX1 expression in the dorsal endoderm and mesenchyme. These data suggest that additional mechanisms must be in place to regulate *Tbx1* expression in the 3rd pp endoderm.

To further investigate the cellular and molecular mechanisms that regulate *Tbx1* expression, we have analyzed two additional mouse models that may provide clues to identifying factors that regulate 3rd pp patterning and thymus development. Using a model in which NCC migration is arrested ($Pax3^{Sp/Sp}$) as well as a model in which *Fgf8* is inserted into the *Tbx1* allele ($Tbx1^{FGF8}$), we observed an increase in the *Foxn1* expressing thymus-fated domain at the expense of the *Gcm2* expressing PT-fated domain. This phenotype is diametrically opposed to the phenotype we found in the $Foxn1^{Cre/+}$;$R26^{iTbx1/+}$ and *miR-17-92* deletion models. Therefore, the studies described in this Chapter were performed to test the

hypothesis that NCCs and/or Fgf8 play a role in regulating Tbx1 expression as proposed in Figure 4.

*Splotch mice*

Epithelial-mesenchymal interactions are essential for proper development of the thymic primordium. NCCs migrate ventrally from the dorsal neural tube and surround the 3rd pp. The migration, proliferation and survival of NCCs are dependent upon the transcription factor, *Pax3* (67-69). Specifically, a homozygous point mutation in the *Pax3* gene (*Splotch*), results in embryonic lethality by E13.5 due to numerous developmental defects (70). Although originally characterized as athymic, our lab showed that *Pax3*$^{Sp/Sp}$ mutants have ectopic, hyperplastic thymic lobes as compared to control littermates (18). Furthermore, when 3rd pp patterning was investigated at E11.5, there was an expansion of the *Foxn1* expressing domain and a significant reduction in the *Gcm2* expressing domain suggesting that NCCs play a role in patterning the 3rd pp. We used *Splotch* mice to test the hypothesis that NCCs mediate their effect on 3rd pp patterning by inhibiting TBX1 expression.

*Tbx1*$^{Fgf8}$ *mice*

As discussed in Chapter 1, BMP and FGF signaling between the pharyngeal endoderm and mesenchyme is critical for proper development of the 3rd pp. BMP4 promotes thymus organogenesis and is expressed in the 3rd pp endoderm and surrounding mesenchyme at E11.5, while *Fgf8* is expressed in the endoderm at E10.5, but minimally expressed, if at all, in the 3rd pp by E11.5. The expression pattern and timing of these factors in organogenesis suggests that BMP and FGF signaling may act in a linear or parallel pathway. During chick development, FGF8 signaling from the endoderm is hypothesized to induce the sequential BMP4-FGF10 signaling cascade that is necessary for thymus fate specification and *Foxn1* expression in the avian 3rd and 4th pps (85). A similar pathway may influence patterning as well as thymus fate acquisition in the mammalian 3rd pp. We used a knock-in model in which a *Tbx1* null allele drives *Fgf8* expression in the

*Tbx1* domain to test the hypothesis that enforced ectopic expression of *Fgf8* in the dorsal 3rd pp prevents or reverses PT fate and expands thymus fate.

## RESULTS

### TBX1 expression is reduced and FOXG1 expression is expanded in the 3rd pp of E10.5 *Pax3*$^{Sp/Sp}$ mutants

We previously reported that the NCC deficiency in Splotch (*Pax3*$^{Sp/Sp}$) mice alters 3rd pp patterning such that the *Foxn1* domain is expanded and the *Gcm2* domain is reduced (70). In a subsequent investigation, we found that *Tbx1* antagonizes FOXN1 expression in the 3rd pp (111). Therefore, we hypothesized that a deficiency in NCCs would reduce TBX1 expression and thus contribute to the expanded *Foxn1* expressing domain seen in the *Pax3*$^{Sp/Sp}$ 3rd pp. To test this premise, *Pax3*$^{Sp/Sp}$ embryos and littermate controls were harvested at E10.5 and sectioned throughout to analyze pouch patterning using thymus- and PT-region specific markers. The frequency of TBX1 positive cells appeared to be lower in the mutant endoderm (Fig.24A,B). However, TBX1 expression was not diminished in the mesodermal mesenchyme surrounding the mutant 3rd pp, therefore suggesting that NCCs play a role in initiating and/or maintaining Tbx1 expression in the ventral 3rd pp endoderm.

To determine if thymus fate was already expanded in the *Splotch* 3rd pp by E10.5, we stained for FOXG1, a transcription factor that is required for thymus development and is expressed independently of, and prior to, FOXN1 in the 3rd pp (108, 111). FOXG1 was detected in the ventral tip and proximal dorsal regions of the control 3rd pp at E10.5 (Fig.24C). However, in the *Pax3*$^{Sp/Sp}$ 3rd pp FOXG1 expression extended throughout the ventral region and into the dorsal domain (Fig.24D). Interestingly, the expression pattern of FOXG1 at

**Figure 24. Thymus fate is expanded in the *Pax3*$^{Sp/Sp}$ 3$^{rd}$ pp endoderm.**

(**A-D**) Representative IHC stains of sagittal sections from the 3$^{rd}$ pp of *Pax3*$^{Sp/Sp}$ and control E10.5 embryos. (**A, B**) A deficiency in NCC migration reduces the frequency of TBX1 positive cells in the 3$^{rd}$ pp of *Pax3*$^{Sp/Sp}$ mutant embryos when compared to control (red). (**C-D**) FOXG1 (red) is expressed in the ventral tip and proximal dorsal regions of the control 3$^{rd}$ pp, but is expanded throughout the ventral domain of the *Pax3*$^{Sp/Sp}$ 3$^{rd}$ pp. (**A-D**) EpCAM expression is reflected in green. v, ventral. d, dorsal. Scale Bars: 50 μm.

**Figure 24. Thymus fate is expanded in the *Pax3*$^{Sp/Sp}$ 3$^{rd}$ pp endoderm.**

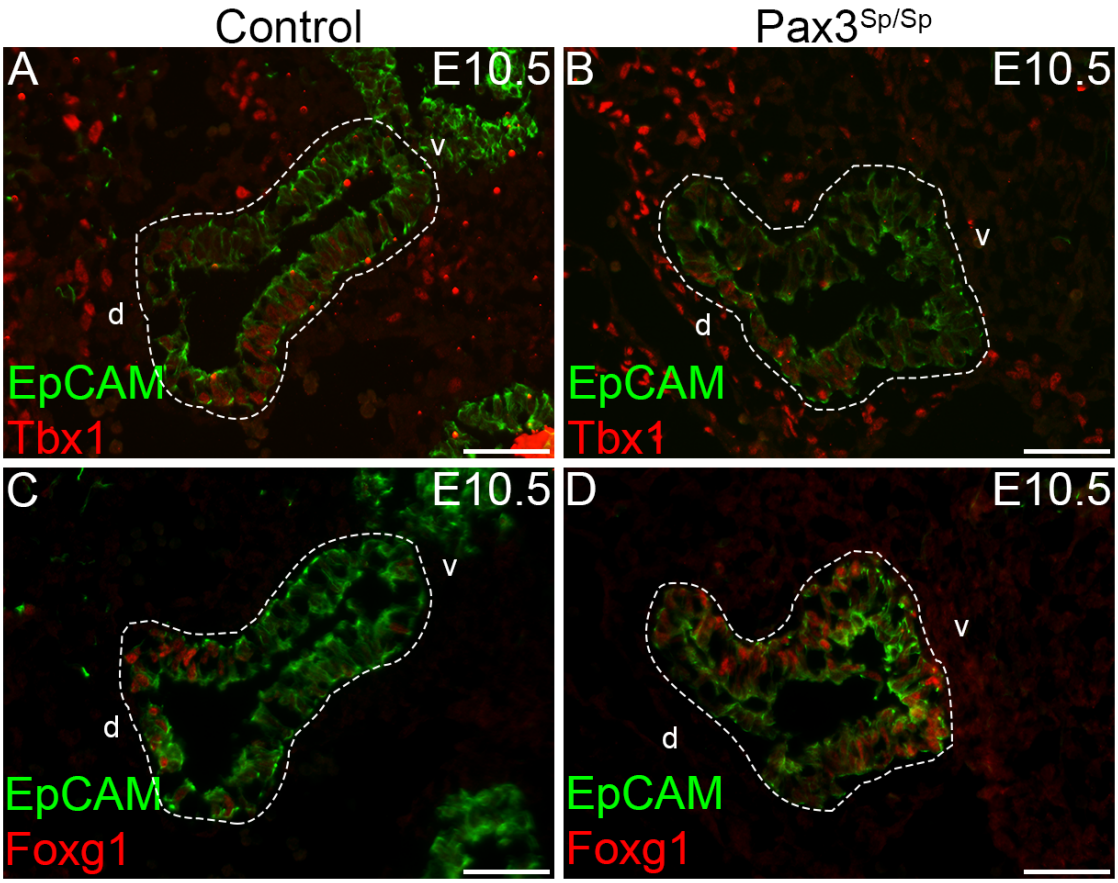

E10.5 is strikingly similar to that of FOXN1 at E11.5, as described by Griffith et al. (70) and suggests that the NCC deficiency in *Splotch* embryos expands the thymus fated domain as early as E10.5.

If thymus fate is expanded, then we would expect a reduction in PT-fated cells. Griffith et al. reported that at E10.5, *Gcm2* expression, detected by ISH, was similar in the mutant and wildtype 3$^{rd}$ pp. However, our preliminary IHC data suggest that there are fewer GCM2 positive cells in the mutant E11.5 3$^{rd}$ pp (Fig.25). If confirmed, the discrepancy between the current data and the previous ISH results may be due to differences in methodology (i.e. ISH versus IHC). It is possible that the ISH analysis was not sensitive enough to discern a subtle distinction in *Gcm2* expression or that the ISH analysis was performed on an insufficient number 3$^{rd}$ pp sections. Another possibility is that the NCC migration defect may be somewhat variable in different embryos requiring analysis of the extent of the NCC defect in addition to analysis of pouch phenotype to determine if there is a causal association of these parameters. In support of this notion, we observed that the size of the white belly spot in *Pax3*$^{Sp/+}$ adults is quite variable possibly due to differences in frequency and/or migration of NCCs in individual mutant mice. Finally, it should be noted that the ISH analysis of *Gcm2* was performed at E10.5, whereas the IHC staining for GCM2 was performed at E11.5. There could be a reduction in Gcm2 expression between E10.5 and E11.5.

Additional studies are needed to confirm the initial observations on FOXG1 and TBX1 expression and to resolve the apparent discrepancy in GCM2 expression. Nevertheless, the finding that TBX1 expressing cells are reduced at E10.5 in the *Pax3*$^{Sp/Sp}$ 3$^{rd}$ pp coupled with the expansion of FOXG1 expressing cells into the dorsal domain supports the hypothesis that cross-talk between pouch endoderm and NCCs plays a role in modulating Tbx1 expression.

**Figure 25. Reduced frequency of GCM2 positive cells within the *Pax3*$^{Sp/Sp}$ 3$^{rd}$ pp endoderm.**

(**A-B**) Representative IHC stains of sagittal sections from the 3$^{rd}$ pp of *Pax3*$^{Sp/Sp}$ and control E11.5 embryos. (**A, B**) A deficiency in NCC migration potentially reduces the frequency of PT-fated GCM2 positive cells in *Pax3*$^{Sp/S}$ mutant embryos when compared to control (red). EpCAM expression id reflected in green. v, ventral. d, dorsal. Scale Bars: 50 μm.

**Figure 25. Reduced frequency of GCM2 positive cells within the *Pax3*$^{Sp/Sp}$ 3$^{rd}$ pp endoderm.**

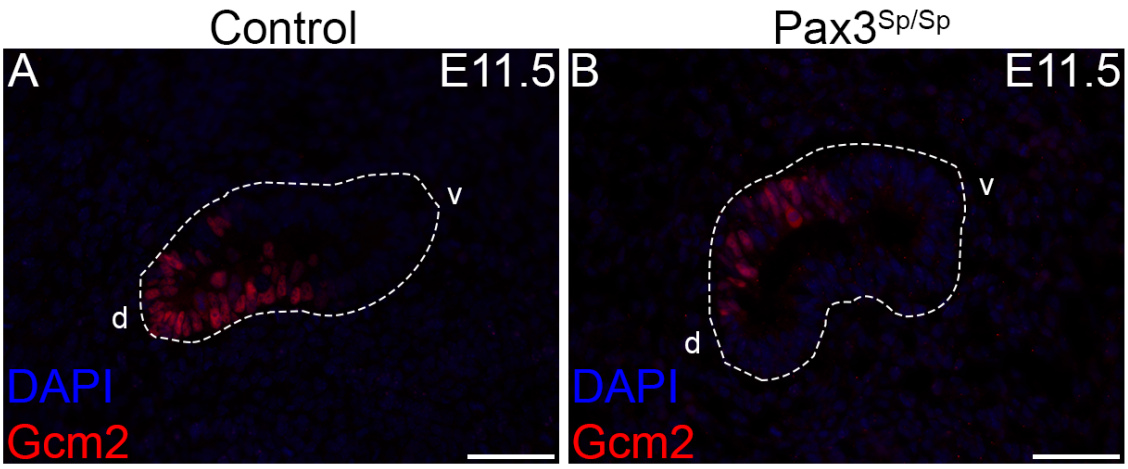

### *Fgf8* expression is enhanced and sustained in the 3rd pp endoderm of *Pax3*$^{Sp/Sp}$ mutants

Given that *Fgf8* is required for development of pharyngeal arch derivatives and NCC migration (78, 79), we analyzed its expression in the 3rd pp endoderm of NC-deficient *Pax3*$^{Sp/Sp}$ embryos. At E10.5, *Fgf8* is expressed in the ventral domain of the wildtype 3rd pp, whereas in the mutant, its expression is considerably upregulated and is also detected in the mesenchyme adjacent to the ventral domain (Fig.26A,B). By E11.5, *Fgf8* is minimally expressed, if at all, within the developing 3rd pp endoderm of the control (Fig.26C). However, not only was *Fgf8* expressed in the *Pax3*$^{Sp/Sp}$ 3rd pp, its expression was also detected in the dorsal domain (Fig.26D). The sustained expression of Fgf8 is particularly interesting in consideration of our previous report showing that the FOXN1-GCM2 expression boundary is shifted to expand the thymus fated domain in the *Pax3*$^{Sp/Sp}$ 3rd pp. Moreover, these data are consistent with the notion that *Fgf8* signaling promotes thymus cell fate (85).

### *Bmp4* expression is enhanced in the 3rd pp endoderm of Pax3$^{Sp/Sp}$ mutants

Our model predicts that *Fgf8* and *Bmp4* interact to pattern the 3rd pp endoderm and promote thymus cell fate. Therefore, we asked whether similar to *Foxn1* and FOXG1, *Bmp4* expression was expanded in the NC-deficient *Pax3*$^{Sp/Sp}$ 3rd pp. At E10.5, *Bmp4* is expressed in the ventral endoderm and mesenchyme of the control (Fig.27A). *Bmp4* staining intensity was dramatically increased in the ventral domain of the mutant 3rd pouch and its expression extended towards the dorsal domain in a gradient-like fashion (Fig.27B). Furthermore, the staining intensity of the *Bmp4* morphogen was also greatly increased in the mutant mesenchyme (Fig.27B).

**Figure 26. *Fgf8* is ectopically expressed at E11.5 in the 3rd pp endoderm of *Pax3*$^{Sp/Sp}$ mutants.**

(**A-D**) ISH analysis of *Fgf8* expression in the 3rd pp endoderm of *Pax3*$^{Sp/Sp}$ and control embryos at (**A,B**) E10.5 and (**C,D**) E11.5. Note the increased expression of *Fgf8* at E10.5 in the mutant 3rd pp and its continued expression at E11.5. v, ventral. d, dorsal. Scale Bars: 50 μm.

**Figure 26. *Fgf8* is ectopically expressed at E11.5 in the 3rd pp endoderm of *Pax3*$^{Sp/Sp}$ mutants.**

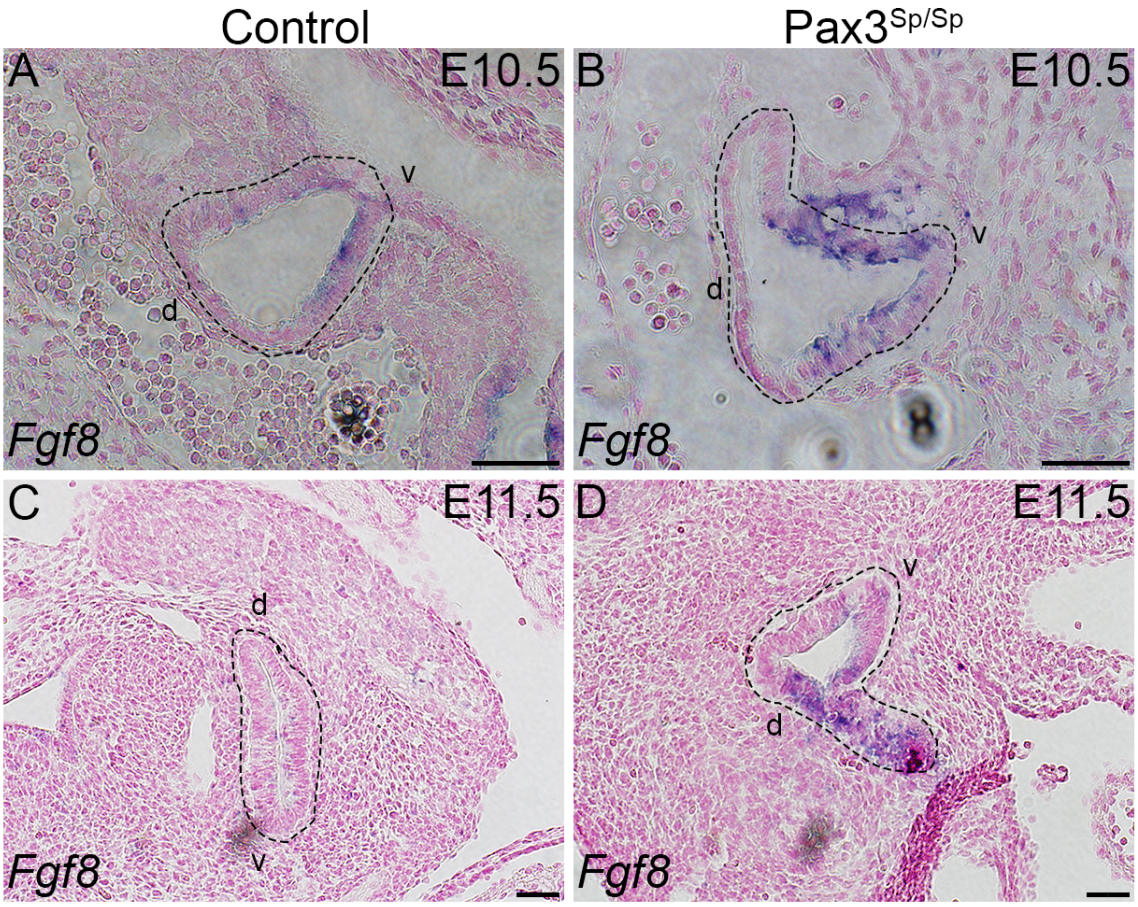

**Figure 27. *Bmp4* expression is enhanced in the 3rd pp endoderm of *Pax3*$^{Sp/Sp}$ mutants.**

(**A,B**) ISH analysis of *Bmp4* expression in the 3rd pp endoderm of *Pax3*$^{Sp/Sp}$ and control embryos at E10.5. Note the increased expression of *Bmp4* in the endoderm and mesenchyme of the mutant 3rd pp. v, ventral. d, dorsal. Scale Bars: 50 μm.

**Figure 27. *Bmp4* expression is enhanced in the 3rd pp endoderm of *Pax3*$^{Sp/Sp}$ mutants.**

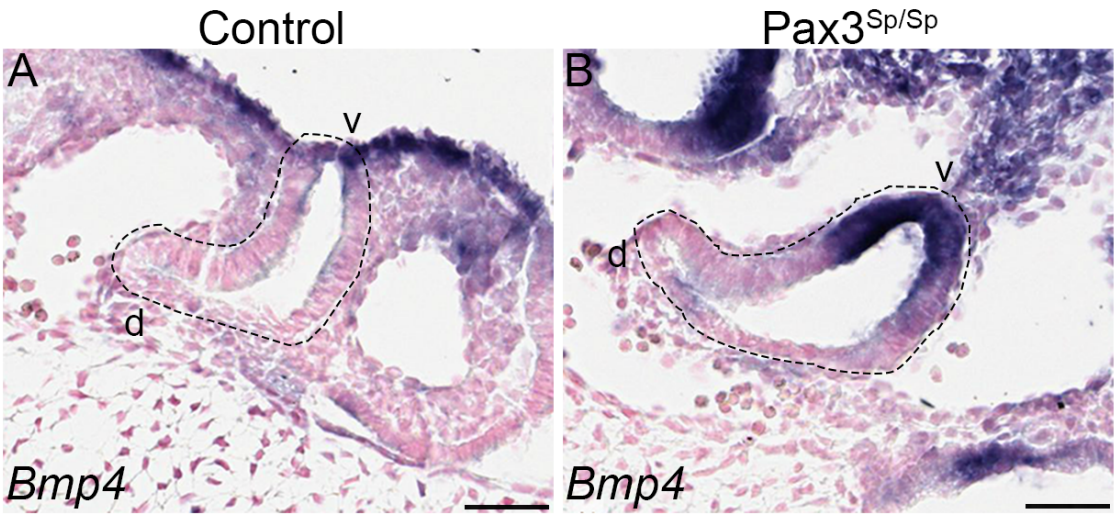

Taken together, these analyses support the premise that NCCs play a role in patterning the 3rd pp by promoting and/or sustaining TBX1 expression as well as by suppressing *Fgf8* and *Bmp4* expression. We have modified our working model to reflect this hypothesis.

**Enforced expression of *Fgf8* from the *Tbx1* allele promotes FOXN1 expression**

Given our data showing that expansion of the thymus fated domain in the $Pax3^{Sp/Sp}$ 3rd pp is associated with increased *Fgf8* and *Bmp4* expression as well as the recent report showing that *Fgf8* acts in a linear fashion with *Bmp4* to pattern 3rd pp endoderm in the chick (85), we asked whether enforced expression of *Fgf8* in the PT-fated domain would decrease specification of 3rd pp cells to a PT fate and conversely increase the frequency of thymus fated cells. To answer this question, we used mice in which *Fgf8* is inserted into a null *Tbx1* allele ($Tbx1^{Fgf8}$). Since *Tbx1* is expressed as early as E7.5, we would expect *Fgf8* to be ectopically expressed early in 3rd pp patterning, and therefore test the above hypothesis. *Fgf8* insertion into both *Tbx1* alleles ($Tbx1^{Fgf8/Fgf8}$) is embryonic lethal and in the absence of *Tbx1* expression, the 3rd pp does not form. Therefore, we analyzed mice in which there is only one copy of the $Tbx1^{Fgf8}$ allele.

$Tbx1^{Fgf8/+}$ and control littermates were harvested at E11.5 for ISH analysis of *Foxn1* and *Gcm2* in the 3rd pp. As expected, expression of both *Foxn1* and *Gcm2* mRNA was restricted to their respective domains in the control 3rd pp endoderm (Fig.28A,C). However, *Foxn1* was expressed throughout almost the entirety of the 3rd pp in the $Tbx1^{Fgf8/+}$ mutant (Fig.28B). Furthermore, *Gcm2* expression was reduced and restricted to the dorsal tip of the mutant pouch (Fig.28D). Additionally, we noted that in some sections of the mutant

**Figure 28. Enforced expression of *Fgf8* from the *Tbx1* allele promotes *Foxn1* expression.**

(**A**-**D**) ISH analysis of (**A,B**) *Foxn1* and (**C,**D) *Gcm2* expression in the 3rd pp endoderm of *Tbx1*$^{Fgf8/+}$ and control embryos at E11.5. Note the expansion of *Foxn1* at the expense of *Gcm2* within the mutant 3rd pp. Arrows indicate examples of detectable *Foxn1*/*Gcm2* mRNA. v, ventral. d, dorsal. Scale Bars: 50 μm.

**Figure 28. Enforced expression of *Fgf8* from the *Tbx1* allele promotes *Foxn1* expression.**

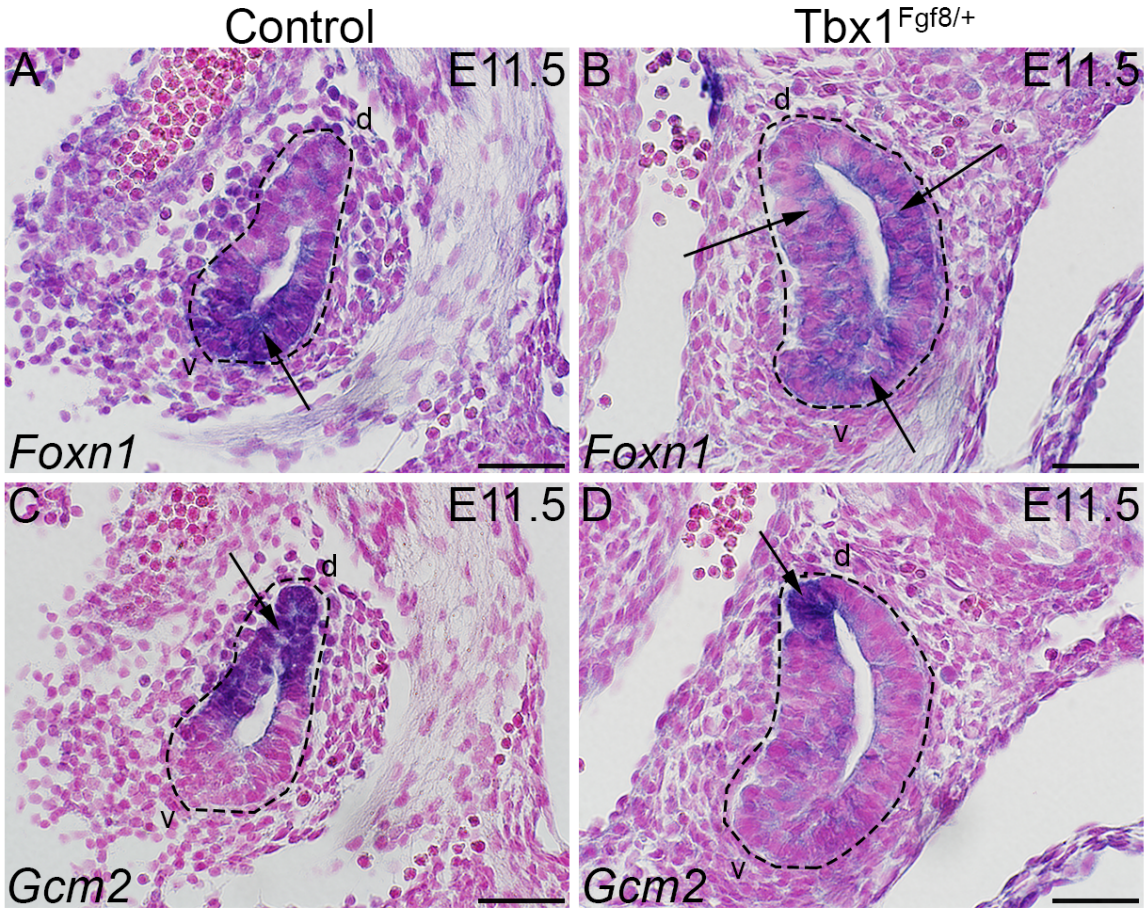

pouch, no *Gcm2* expression was detected as *Foxn1* was expressed throughout the pouch (data not shown). Taken together, these data strongly suggest that *Fgf8* expression is antagonistic to PT cell fate establishment and promotes thymus cell fate when ectopically expressed in the dorsal domain of the 3rd pp endoderm.

**Enforced expression of *Fgf8* from the *Tbx1* allele promotes thymus cell fate at the expense of PT fate**

To determine if ectopic expression of *Fgf8* in the PT-fated domain also reduced TBX1 expression, we performed IHC analyses on the E11.5 3rd pp. Compared to the control, TBX1 expression was greatly reduced in the $Tbx1^{Fgf8/+}$ 3rd pp (Fig.29A,B). The frequency and location of the TBX1 positive cells was similar to that of *Gcm2* expression analyzed by ISH. Furthermore, FOXN1 expression was detected throughout the ventral region of the mutant pouch and extended well into the dorsal domain (Fig.29B). However, FOXN1 was not co-expressed with the few TBX1 positive cells present in the mutant pouch. Interestingly, the expression pattern of GCM2 was congruent with the ISH data as well as TBX1 expression (Fig.29C,D). In the control, FOXG1 expression overlapped with that of FOXN1 and was restricted to the ventral domain of the pouch (Fig.29E). Similarly, FOXG1 expression was congruent with that of FOXN1 in the mutant and expanded into the dorsal domain of the mutant 3rd pp (Fig.29F). Taken together, these data support the notion that *Fgf8* promotes thymus fate in 3rd pp endoderm.

Additionally, it is important to note that the 3rd pp of the mutant embryo appeared larger than that of the control (Fig.29). Although cell counts will need to be obtained to confirm this finding, this result also suggests that ectopic, endodermal *Fgf8* expression may influence the size of the 3rd pp.

**Figure 29. Enforced expression of *Fgf8* from the *Tbx1* allele promotes thymus cell fate at the expense of PT fate.**

(**A-F**) Representative IHC stains of sagittal sections from 3rd pp of *Tbx1*$^{Fgf8/+}$ and control E11.5 embryos. (**A, B**) Ectopic expression of *Fgf8* reduces the frequency of TBX1 positive cells (red) in the 3rd pp of *Tbx1*$^{Fgf8/+}$ mutant embryos when compared to control. (**C, D**) Serial sections show a concomitant reduction in the frequency of GCM2 positive cells (red) in the 3rd pp of *Tbx1*$^{Fgf8/+}$ mutant embryos when compared to control. (**E,F**) FOXG1 (red) expression is expanded throughout the ventral and into the dorsal domain of *Tbx1*$^{Fgf8/+}$ 3rd pp and is co-expressed with FOXN1 (green). (**A-F**) Note the expansion in the FOXN1 expression domain of the mutant 3rd pp when compared to the control. v, ventral. d, dorsal. Scale Bars: 50 μm.

**Figure 29. Enforced expression of *Fgf8* from the *Tbx1* allele promotes thymus cell fate at the expense of PT fate.**

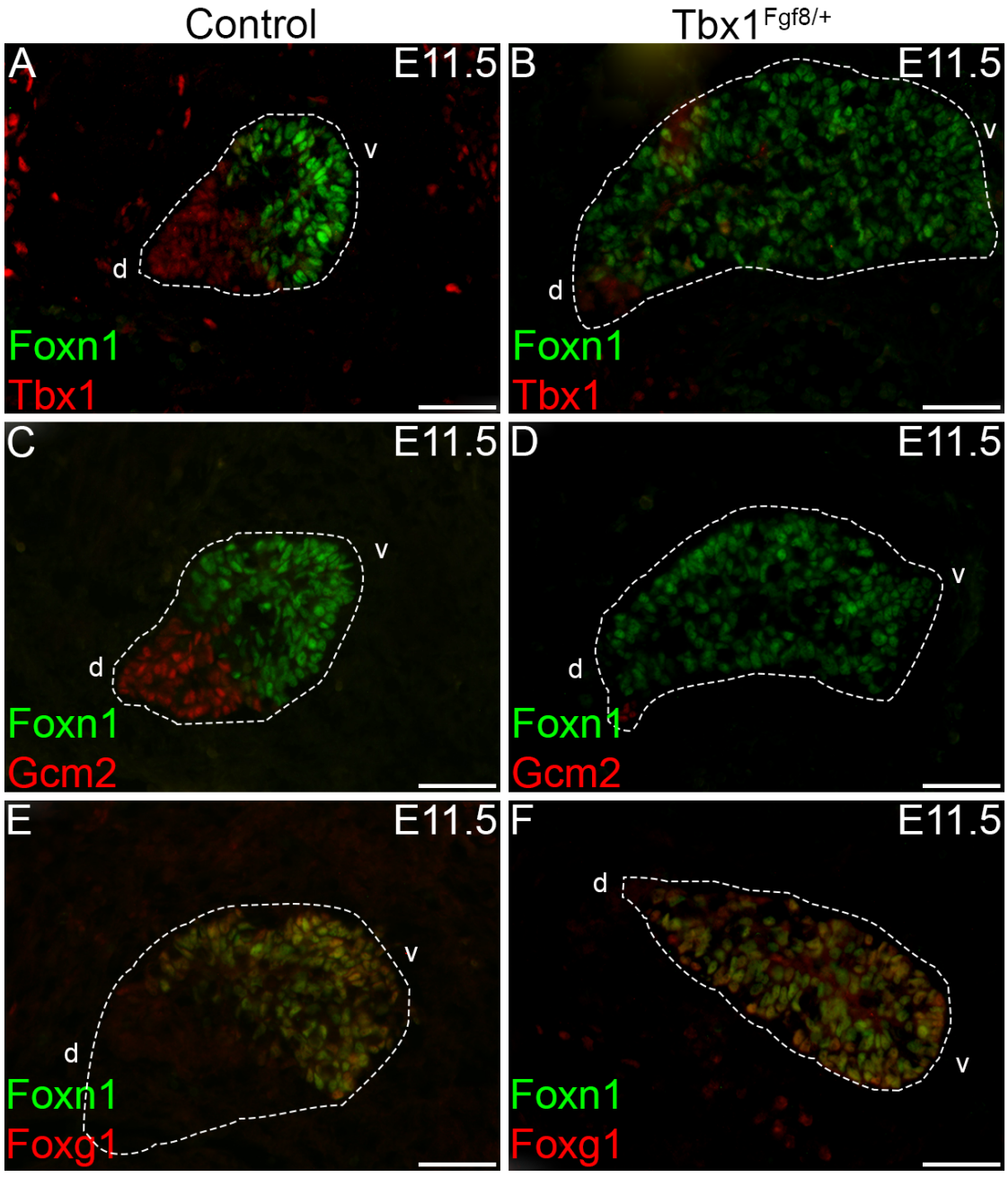

## CONCLUSIONS

The data presented in this Chapter confirm that a deficiency of NCCs expands the thymus-fated domain of the 3rd pp at the expense of the PT-fated domain. We also show for the first time that ectopic expression of *Fgf8* in the dorsal domain results in a similar phenotype. These results contribute additional insight into the molecular pathways that establish thymus fate and/or promote thymus organogenesis and are reflected in our working model. Interestingly, the phenotype in these two models is in stark contrast to the 3rd pp phenotypes reported in the *Foxn1*$^{Cre/+}$*;R26*$^{iTbx1/+}$ and *miR-17-92* deletion models (Chapters 3 and 4), in which there is a reduction in FOXN1 positive cells in the 3rd pp and aberrant thymus organogenesis.

### *Tbx1 expression is reduced and thymus cell fate expands in 3rd pp of NCC deficient Pax3*$^{Sp/Sp}$ *embryos*

Previous work from our lab has shown that the 3rd pp is aberrantly patterned and thymus cell fate is expanded in the absence of NCCs at E11.5 (70). However, the expression of *Tbx1* was not analyzed in the developing endoderm of the *Pax3*$^{Sp/Sp}$ embryo. The current investigation shows that TBX1 positive cells are reduced and FOXG1 positive cells are expanded in the *Splotch* 3rd pp at E10.5. This result suggests that NCC-derived signals may affect the establishment of organ fate boundaries by positively regulating *Tbx1* expression, which in turn suppresses thymus fate and promotes PT fate in 3rd pp progenitors. This scenario is consistent with our working model (Fig.4).

The reduction in TBX1 and expansion of FOXG1 expressing cells in the E10.5 *Pax3*$^{Sp/Sp}$ 3rd pp could be due either to altered fate commitment of endodermal progenitors or to reversal of PT-specified cell fate. Although there may be a reduction in GCM2 positive

cells in the E11.5 mutant pouch, the analysis of GCM2 does not resolve this issue since a number of these cells are readily detectable. Therefore, it will be necessary to repeat these experiments and quantify the number and frequency of GCM2 positive cells. Moreover, it will be interesting to determine whether the GCM2 positive cells in the mutant pouch co-express FOXG1 or FOXN1.

*Fgf8* is a morphogen that contributes to cell fate in several tissues (171, 172). Our data suggests that NC-derived signals play an essential role in limiting *Fgf8* expression in the 3rd pp. The fact that *Fgf8* expression is increased in the *Pax3*$^{Sp/Sp}$ 3rd pp at E10.5 and sustained at E11.5 has interesting implications for thymus fate specification and the potential relationship between *Fgf8* and *Tbx1* expression. A recent study of 3rd pp patterning in the chick suggested that *Fgf8* might be a key factor in establishing thymus fate given its temporal and spatial expression pattern in the developing 3rd and 4th pharyngeal pouches. In this regard, it is interesting that *Fgf8* is highly expressed in the ventral tip of the wildtype 3rd pp. This is the region where *Foxn1* is first expressed. Moreover, the ventral most region of the 3rd pp is relatively refractory to down-regulation of FOXN1 expression mediated by ectopic *Tbx1* expression in our *Foxn1*$^{Cre/+}$;*R26*$^{iTbx1/+}$ mutants. Therefore, high levels of *Fgf8* in 3rd pp progenitors may be sufficient to establish or even reverse organ fate. Furthermore, *Fgf8* may mediate its effect on 3rd pp patterning, at least in part, by suppressing TBX1 expression. Indeed, the analysis of TBX1 expression in the *Tbx1*$^{Fgf8/+}$ 3rd pp supports this notion. Alternatively or in addition, TBX1 may regulate FGF8 expression. Interestingly, *Fgf8* has been reported as a downstream mediator of *Tbx1* function to pattern the aortic arch (163).

*Bmp4* is another morphogen that contributes to the patterning of the 3rd pp endoderm. We have shown that its expression is significantly increased in the absence of

NCCs at E10.5. This suggests that *Bmp4* is independent of NC-derived signals and that similar to *Fgf8*, NCCs may be required to dampen its expression to allow for PT fate establishment. As seen in the *Fgf8* model, *Bmp4* was highly upregulated in the ventral tip of the mutant pouch. This suggests that *Bmp4* signaling may serve as a protective mechanism against *Foxn1* downregulation, thus establishing or maintaining thymus cell fate in the 3$^{rd}$ pouch. Furthermore, *Fgf8* has been proposed to act upstream of a *Bmp4* signaling cascade that is required for *Foxn1* expression in the chick 3$^{rd}$ and 4$^{th}$ pps. While our results cannot confirm that *Fgf8* is acting upstream of *Bmp4*, their similar expression patterns do suggest that *Fgf8* and *Bmp4* interact to promote thymus cell fate.

*Enforced expression of Fgf8 in the PT domain promotes thymus cell fate at the expense of PT fate*

*Fgf8* is hypothesized to initiate the BMP4-FGF10 signlaing cascade necessary for the establishment of thymus cell fate in the chick (85). It stands to reason that in our model system, *Fgf8* may function in a similar way given its expression pattern during development. *Fgf8* is first expressed in the wildtype embryos at E6.5 during gastrulation (79) and appears in the 3$^{rd}$ pp at E9.0, is downregulated by E10.5 and is almost absent form the pouch by E11.5 (79, 86, 173). This suggests that the role of *Fgf8* in patterning the 3$^{rd}$ pp occurs early in development and prior to the establishment of cell fate boundaries. Our data support this hypothesis as ectopic and sustained expression of *Fgf8* promotes thymus cell fate at the expense of PT fate. Specifically, TBX1 expression is attenuated and both FOXN1 and FOXG1 expression domains are substantially expanded throughout almost the entirety of the *Tbx1*$^{Fgf8/+}$ 3$^{rd}$ pp.

Similar to what was seen in the *Pax3*$^{Sp/Sp}$ mutants, the reduction in PT-fated cells (as reflected by reduced TBX1 and GCM2) and expansion in thymus fate (as reflected by increased FOXN1 and FOXG1) may be due to a reversion in PT fate to thymus fate, or to alterations in initial fate commitment. Given that *Fgf8* is expressed throughout the pharyngeal endoderm, it is possible that commitment to the PT lineage never occurred. However, given that GCM2 was expressed in the dorsal tip of the 3$^{rd}$ pp suggests that there are mechanisms in place to impart irreversible PT cell fate commitment and prevent *Fgf8* from downregulating TBX1 and otherwise interfering with PT fate.

Finally, it is important to emphasize that the data from analysis of 3$^{rd}$ pp patternng in *Tbx1*$^{Fgf8/+}$ mutants coincide with the results generated using the *Pax3*$^{Sp/Sp}$ mutants. We demonstrated that a paucity of NCCs results in sustained *Fgf8* expression, reduced TBX1 and expanded FOXN1 expression domains prior to E11.5. This suggests that NCCs not only positively regulate TBX1 expression and negatively regulate *Fgf8*, but are also necessary to preserve 3$^{rd}$ pp patterning and more importantly, PT cell fate possibly through the regulation of *Fgf8*. Given that endodermal-mesenchymal crosstalk is required for patterning the 3$^{rd}$ pp, this hypothesis is quite plausible.

## CHAPTER 6: Discussion

Thymus involution occurs due to the loss of TECs in aging individuals, and this process is accelerated in patients undergoing cytoablative therapies. As a result, the involuted thymus is no longer able to support T cell development, thus restricting the diversity of the TCR repertoire. Consequently, cancer patients as well as aging non-patients are not capable of mounting robust immune responses towards vaccines, cancers or newly encountered infections. Therefore, preventing thymus involution and maintaining naive T cell output would greatly improve overall health and wellbeing. In order to facilitate the development of therapeutic strategies that will prevent or reverse thymus involution, the aim of this dissertation is to identify the genetic pathways necessary to specify endodermal progenitors to a thymus fate and maintain TEC differentiation.

By using LOF and GOF mouse models to study the potential role of transcriptional regulators of thymus organogenesis, we have defined three significant pathways that contribute to thymus fate specification within the 3$^{rd}$ pp endoderm. First, we have demonstrated *Tbx1* is antagonistic to FOXN1 expression and must be downregulated for proper thymus organogenesis to occur. Secondly, we have shown that *miR-17-92* may function to regulate *Tbx1* in both cell-autonomous and non-cell autonomous manners during 3$^{rd}$ pp patterning. Finally, we found that *Tbx1* expression, and thus 3$^{rd}$ pp patterning, are dependent upon NCC and *Fgf8* regulation. Together, these data suggest that *Tbx1* is a master regulator of 3$^{rd}$ pp patterning and multiple mechanisms must be in place to regulate its expression in order for thymus development to occur. Furthermore, we have incorporated these findings into a current working model that describes the temporal and spatial regulation of *Tbx1* and the molecular mechanisms necessary for the establishment of thymus fate (Fig.30).

**Figure 30. Model of molecular pathways that establish thymus cell fate in the 3rd pp endoderm.**

Model system of molecular signaling networks necessary for 3rd pp patterning and thymus cell fate, adjusted to incorporate the role of NCCs. Bold lines indicate those pathways that are discussed and tested in this dissertation.

**Figure 30. Model of molecular pathways that establish thymus cell fate in the 3rd pp endoderm.**

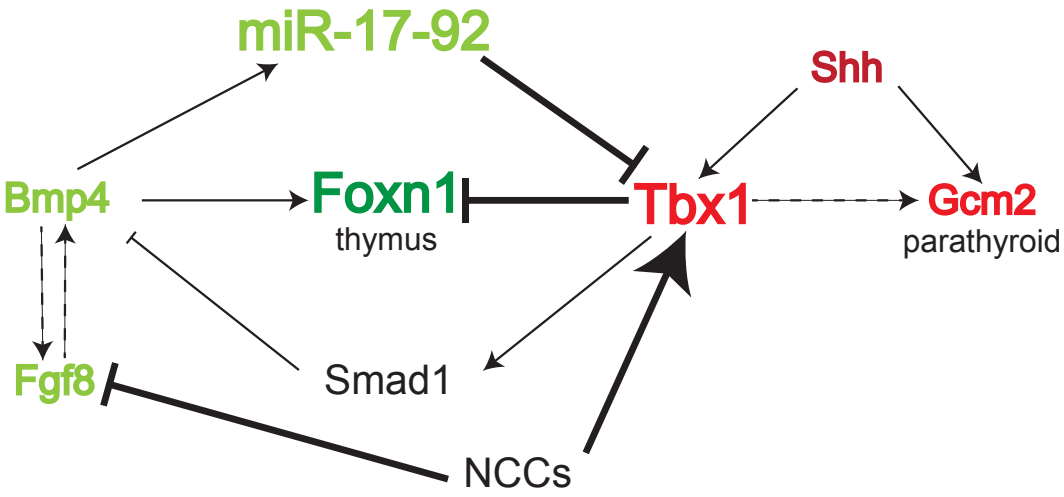

### *Tbx1* indirectly regulates *Foxn1* expression in the 3rd pp endoderm

Since loss or haploinsufficency of *Tbx1* has been reported to cause thymus aplasia or hypoplasia (114-116), it has been generally accepted that *Tbx1* plays an indispensible role in thymus organogenesis. However, the underlying reason for this thymus phenotype is that *Tbx1* is required for segmentation of the pharyngeal endoderm and in its absence 3rd pp formation does not occur. Therefore, aberrant thymus development is secondary to defects in 3rd pp development.

Our published data demonstrated that contrary to previous suggestions, *Tbx1* expression is antagonistic to thymus development. Enforced, ectopic expression of *Tbx1* in *Foxn1* positive cells resulted in an immediate downregulation of FOXN1 at E11.5. This phenotype was unexpected as *Tbx1* was not expressed in TECs until ~E11.25. Nevertheless, by E11.5, we found a significant reduction in FOXN1 expression in the ventral domain of the 3rd pouch. Interestingly, FOXN1 and TBX1 co-expressing cells were present in the $Foxn1^{Cre/+}$;$R26^{iTbx1/+}$ 3rd pp endoderm suggesting that as soon as ectopic TBX1 is expressed from the $R26^{iTbx1}$ allele, there is a rapid downregulation of endogenous FOXN1 expression. It is likely that TBX1 regulates *Foxn1* expression through an indirect mechanism, as there is not a putative *Tbx1* binding site in the *Foxn1* promoter (BLAT; UCSC Genome Bioinformatics).

Despite the ectopic expression of *Tbx1*, thymus cell fate was not reversed as the *Foxn1*-independent markers of thymus cell fate, *IL-7* and FOXG1, were expressed throughout the ventral domain of the mutant 3rd pp. Given that thymus cell fate is established prior to the expression of *Foxn1*, it is not surprising that thymus cell fate was preserved in the mutant. The fact that thymus cell fate was not abrogated in this model is further supported by the notion the 3rd pp cell fate is established by E9.5, as isolation and

transplantation of the 3rd pp under the kidney capsule differentiates into a thymus (50). Given that thymus cell fate was unaffected, these data further support the notion that cell fate is specified prior to E10.5 and *Tbx1* expression after this point is unable to alter fate decisions within the pouch. Therefore, it would be interesting to sustain *Tbx1* expression throughout the 3rd pp endoderm beginning at E9.0.

We have performed preliminary experiments using $Foxa2^{Cre}$ to sustain and ectopically express the $R26^{iTbx1}$ allele throughout the pharyngeal endoderm to determine if early, sustained expression of *Tbx1* abrogates thymus cell fate. As expected, $Foxa2^{Cre}$ induces TBX1 expression throughout the 3rd pp. We find a number of cells in the $Foxa2^{Cre};R26^{iTbx1}$ 3rd pp that co-express TBX1 and FOXN1. In addition, pouch patterning is aberrant as FOXN1 is expressed in both the ventral and dorsal domains of the 3rd pp. The continued expression of FOXN1 despite sustained *Tbx1* expression may be due to a mosaic phenotype as using this Cre line, which has been previously reported (104). Alternatively, mechanisms may exist to ensure endodermal commitment to the thymus lineage, despite the presence of *Tbx1*. Regardless, because these FOXN1 positive cells co-express TBX1, we hypothesize that TEC differentiation will be arrested at a progenitor stage, similar to what was seen in our $Foxn1^{Cre/+};R26^{iTbx1/+}$ mouse model. However, additional experiments need to be performed to verify this initial data at E11.5 as well as to analyze fetal thymus development.

### *Tbx1* is antagonistic to thymus development

Despite the significant reduction in FOXN1, the few FOXN1 positive cells in the ventral region of $Foxn1^{Cre/+};R26^{iTbx1/+}$ 3rd pp were able to proliferate and generate thymic lobes. This resulted is hypoplastic fetal thymi beginning at E12.5 that persisted throughout

ontogeny and into postnatal stages. Given that *Foxn1* is required for TEC proliferation and differentiation (57, 87, 88, 99, 143), the thymus hypoplasia may be attributable to the significant reduction in FOXN1 expression at E11.5. Interestingly, there was a significant accumulation of Plet-1 expressing TEC progenitors in the fetal *Foxn1*$^{Cre/+}$;*R26*$^{iTbx1/+}$ thymus lobes. These cells co-expressed TBX1 and tended to localize in the subcapsular region of the thymus, suggesting that enforced expression of ectopic TBX1 arrests TECs in a primitive stage and prevents their differentiation. Additionally, we observed that the mutant lobes have a larger than normal NC-derived mesenchymal capsule that persists throughout ontogeny. Given that endodermal-mesenchymal interactions are required for pattering and development of the 3$^{rd}$ pp, the persistent capsule coupled with the location of the progenitor cells suggests that cellular crosstalk may be occurring between these two populations that promotes a microenvironment conducive to the maintenance of TEC progenitors.

### *MiR-17-92* regulates *Tbx1* expression in the 3$^{rd}$ pp endoderm

While the role of *miR-17-92* has been well studied in various model systems, its function during 3$^{rd}$ pp patterning and thymus development has never been defined. During cardiac development, BMP2/4 promotes the expression of *miR-17-92*, which in turn binds the 3' UTR of *Tbx1* (82, 132). This miR-mediated silencing of *Tbx1* is required for cardiomyocyte differentiation, and in its absence, the persistence of *Tbx1* maintains cardiac cells in a progenitor state (82). Interestingly, *Bmp4* is a known regulator of thymus development and our data have clearly demonstrated that *Tbx1* is antagonistic to thymus organogenesis through indirect regulation of FOXN1 (51, 81, 111). Given the striking similarities among the transcriptional regulators during cardiac and thymus development, we

hypothesized that a similar *Bmp-miR*-mediated mechanism regulated *Tbx1* expression in the developing 3rd pp to promote thymus fate or organogenesis.

*MiR-17-92 is expressed in the developing 3rd pp endoderm*

Using LNA probes to *miR-17*, *miR-19a* and *miR-92a*, we demonstrated that these members of the *miR-17-92* cluster are indeed expressed in the wildtype 3rd pp endoderm at E10.5 and E11.5. Furthermore, we also detected their expression in the mesenchyme surrounding the third pouch. As previously reported, *Tbx1* is expressed in the 3rd pp endoderm as well as by non-NC-derived mesenchyme (174). Since *Tbx1* contains seed sequences for *miR-17-92* binding, it is not surprising that *miR17-92* family members are expressed in the mesenchyme. Notably, we found distinct expression patterns in the endoderm and mesenchyme for each of the miRNAs that we analyzed. This may be attributable to the fact that although co-transcribed, each member of the cluster is differentially processed and regulated within specific tissues and at different times (175, 176). This adds an interesting complexity to miRNA regulation of mRNA given that members of polycystronic miRNAs, such as *miR-17-92*, are found sequentially on the same transcript (177). However, this suggests that each member of the *miR-17-92* cluster may serve different functions during pouch formation and its subsequent patterning. Interestingly, we detected *miR-17*, *miR-19a* and *miR-92a* expression in either the ventral or dorsal endoderm at E10.5. However, by E11.5, although expressed at different levels, each member was detected in the ventral domain, and only moderately extended into the dorsal domain of the 3rd pp. These results suggest that members of the *miR-17-92* cluster are functioning to downregulate *Tbx1* in the ventral domain of the 3rd pp endoderm, thus supporting our model.

Additionally, the images of *pri-miR-17-92* in the E11.5 3rd pp endoderm sent from Dr. James Martin confirmed that the primary *miR-17-92* transcript is restricted to the ventral domain of wildtype 3rd pp at E11.5. Furthermore, these images also showed that the polycystronic cluster is expressed in the mesenchyme. These results coincide with our data analyzing mature members of the primary transcript. Overall, expression of *miR-17-92* family members in the ventral domain of the 3rd pp is consistent with the notion that *miR-17-92* regulates *Tbx1* expression in this region of the pouch. Taken together, these data strongly support our hypothesis that *miR-17-92* plays an important role in suppressing *Tbx1* expression in the ventral domain of the 3rd pp to enable *Foxn1* expression, and thus TEC differentiation.

*MiR-17-92 regulates Tbx1 expression in a non-cell autonomous manner*

Global or site-specific deletion of *miR-17-92* results in aberrant TBX1 expression within the 3rd pp endoderm at E11.5. Upon global deletion of *miR-17-92*, TBX1 no longer remained restricted to the dorsal domain, but rather expanded towards the ventral region of the 3rd pouch. We also observed an increase in the mesenchymal staining intensity of TBX1 in *miR-17-92*$^{Null}$ embryos at E11.5. This observed increase in TBX1 expression in both the endoderm and mesenchyme of mutant embryos is not surprising given that *miR-17-92* has directly binds the 3'UTR of *Tbx1* (82) and our studies have shown that *miR-17-92* is expressed in both tissue types. Additionally, these data suggest that *miR-17-92* may function to regulate the abundance of *Tbx1* transcript in a cell autonomous manner, as we observed changes in the staining intensity of TBX1 in endodermal and mesenchymal cells.

Although cells expressing TBX1 were detected in the ventral domain of the *miR-17-92*$^{Null}$ 3rd pp endoderm, we did not observe TBX1 positive cells in the most ventral region of

the pouch as was seen in the *Foxn1*$^{Cre/+}$;*R26*$^{iTbx1/+}$ mouse model. Given that in the latter case we were enforcing expression of *Tbx1* from the strong *R26* promoter in *Foxn1* positive cells, whereas in the later case we deleted only one potential regulator of *Tbx1* mRNA translation, it is not surprising that we did not see a more dramatic phenotype in the *miR-17-92* null 3rd pp. Furthermore, *Bmp4* is expressed in the mesenchyme surrounding the ventral tip of the 3rd pp at E10.5 and E11.5 (81), which may serve as a protective mechanism to prevent *Tbx1* from being expressed in these cells, thus ensuring that TEC differentiation will occur in some, but not all cells within the pouch.

In contrast, site-specific deletion of *miR-17-92* in TECs did not result in an expansion of the TBX1 domain, but resulted in increased staining intensity of TBX1 in the dorsal endoderm and throughout the mesenchyme. This phenotype is surprising given that we are deleting *miR-17-92* in the ventral domain of the 3rd pp endoderm and observing effects on TBX1 expression within regions where no genetic manipulation is occurring. Interestingly, *miR-17-92* has been shown to act in both cell autonomous and non-cell autonomous manners (166). In the global deletion model, *miR-17-92* appears to be acting in a cell autonomous manner to regulate *Tbx1* expression in endodermal and mesenchymal tissues, whereas in our site-specific deletion models it is acting in a non-cell autonomous manner.

We again observed *miR-17-92* acting in a non-cell autonomous manner when the cluster was overexpressed in TECs. TBX1 remained restricted to the dorsal, PT-fated domain, but the staining intensity was greatly reduced in the *Foxn1*$^{Cre/+}$;*miR-17-92*$^{OE/+}$ E11.5 3rd pp. Furthermore, TBX1 expression was reduced in the mesenchyme surrounding the mutant pouch. Interestingly, the effect on TBX1 in the mesenchyme was only detected in mesenchymal cells adjacent to the pouch. Specifically, TBX1 expression in cells located further away from the 3rd pp domain were unaffected by expression of the *miR-17-92*

transgene in TECs and the staining intensity remained comparable to what is seen in the control littermate. There is precedence of non-cell autonomous effects of *miR-17-92*. For example, overexpression of the *miR-17-92* cluster in epithelail and endothelial cells has been shown to act in a non-cell autonomous manner to promote angiogenesis through Myc activation (167, 178). These reports lend credence to the possibility that reduced TBX1 staining intensity in mesenchymal cells of embryos expressing a *miR-17-92* transgene in ventral 3$^{rd}$ pp endoderm is due to a non-cell autonomous effect.

Together the data obtained using LOF and GOF models supports our working model in which *miR-17-92* regulates *Tbx1* expression in the 3$^{rd}$ pp endoderm. In addition, we unexpectedly found evidence that *miR-17-92* also regulates *Tbx1* expression non-cell autonomously in mesenchyme surrounding the 3$^{rd}$ pp.

*MiR-17-92 regulation of Tbx1 promotes Foxn1 expression*

Thymus and PT cell fate is first established in the most ventral and dorsal regions of the pouch, respectively. Then as the pouch endoderm continues to proliferate particularly in the ventral domain, thymus fate acquisition moves dorsally towards the eventual thymus-PT boundary by E11.5 (54). At this developmental stage, there are very few, if any, cells in the 3$^{rd}$ pp that have not yet committed to either organ fate (50, 51, 54). However, if there are cells present in the E11.5 3$^{rd}$ pp that have yet to commit to either lineage, those cells tend to be located at the thymus and PT boundary as this is the region of the pouch that is last to assume an organ specific fate. Interestingly, we observed cells in the E11.5 *miR-17-92*$^{Null}$ 3$^{rd}$ pp that did not express any of the organ-specific markers that we analyzed. Therefore, these results suggest that in the absence of *miR-17-92*; 1) thymus cell fate is reversed 2) thymus cell fate was never established or 3) these triple negative cells have assumed a

thymus identity, but are arrested in an early progenitor state and have yet to express *Foxn1*. To prove that there is a reversion in cell fate, we would need to analyze patterning before E11.5 to determine the frequency and location of cells that express TBX1, GCM2 or FOXG1. If cells in the ventral region express FOXG1 at E10.5 and fail to express both thymus- and PT-specific markers at E11.5, then this would suggest a reversion in cell fate to an endodermal progenitor. This would be a very interesting outcome given that it would suggest that in the absence of *miR-17-92*, cells of the 3rd pp are extremely plastic endodermal progenitors. However, if thymus cell fate were never established in the absence of the miRNA cluster, we would see a persistent population of cells within the 3rd pp endoderm from E10.5 to E11.5 that never express any marker associated with thymus cell fate (e.g. *Foxg1*, *Foxn1*, *Bmp4*). The most likely outcome is that these FOXN1, TBX1 and GCM2 negative cells within the ventral domain of the 3rd pp have assumed a thymus identity, but are arrested and cannot differentiate. To prove this hypothesis, we will need to analyze the *miR-17-92*$^{Null}$ 3rd pp at E10.5 and E11.5 for FOXG1 expression. Given that FOXG1 is a *Foxn1*-independent predictor of thymus fate, its expression would suggest that these cells are committed to the thymus lineage, but unable to express *Foxn1* and differentiate into TECs.

In contrast to the global deletion of *miR-17-92* in the null embryos, *Foxn1*$^{Cre}$-mediated deletion of the miR cluster in TECs does not occur until *Foxn1* is turned on in the ventral domain of the 3rd pp. We do not observe any triple negative cells nor do we observe a discernable change in FOXN1 expression in the *Foxn1*$^{Cre/+}$*;miR-17-92*$^{Fl/Fl}$ 3rd pp. This is not surprising given that the mechanisms which regulate 3rd pp patterning remain intact until cell fate boundaries are established. Interestingly however, we do observe cells at the thymus and PT boundary that co-express FOXN1 and TBX1. Given that we have shown

that *Tbx1* must be downregulated to enable FOXN1 expression, co-expression of these two transcription factors within one cell is extremely rare, thus making this finding notable. As previously discussed, the cells located at the organ boundary are the last to assume either a thymus or PT cell fate (50, 51, 54). This understanding coupled with the notion that *miR-17-92* may function in a non-cell autonomous manner suggests that *miR-17-92* expression in the ventral tip of the 3rd pp may be necessary to downregulate *Tbx1* in cells at the thymus-PT boundary, thus enabling these cells to express *Foxn1* and differentiate into TECs.

We do not expect to see deletion of *miR-17-92* in *Foxn1*$^{Cre/+}$*;miR-17-92*$^{Fl/Fl}$ embryos until ~E11.25 when *Foxn1* is turned on in the 3rd pp endoderm. However, the frequency of cells that co-express FOXN1 and TBX1 may be significantly increased when *miR-17-92* is deleted in 3rd pp endoderm at an earlier developmental stage, prior to cell fate-acquisition. Using an early endoderm-specific Cre, such as *Foxa2* or *Sox17*, will enable us to resolve this issue. If *miR-17-92* is deleted in the 3rd pp prior to cell fate commitment, it is possible that TBX1 would be expressed throughout much of the 3rd pp endoderm and would prevent the establishment of thymus cell fate. However, given that 1) multiple mechanisms regulate *Tbx1* expression in the 3rd pp, 2) FOXN1 is expressed in *miR-17-92* global deletion mutants and 3) our preliminary results using the *Foxa2*$^{CreERt2/+}$;*R26*$^{iTbx1/+}$ model showing that FOXN1 is expressed despite sustained expression of *Tbx1* throughout the 3rd pp endoderm, it seems likely that thymus fate commitment would still occur in the 3rd pp even when *miR-17-92* is deleted at an early stage in 3rd pp development. This outcome would further support the notion that there are multiple mechanisms to ensure thymus cell fate.

*MiR-17-92 regulation of Tbx1 promotes thymus organogenesis*

To date, we have examined thymus organogenesis in only one *miR-17-92*$^{Null}$ embryo at E14.5. However, we observed a strikingly aberrant thymus phenotype. Despite the paucity of FOXN1 positive cells at E11.5 in *miR-17-92*$^{Null}$ embryos, the right thymic lobe was present in the E14.5 embryo and contained both cTECs and mTECs. However, this lobe was hypoplastic and extremely ectopic and the left lobe was absent from the thoracic cavity. The absence of the left lobe was an unexpected result given that both left and right 3$^{rd}$ pps developed and expressed FOXN1 in E11.5 *miR-17-92*$^{Null}$ embryos. However, left-right asymmetry has been described during thymus organogenesis (81). Specifically, the right pouch tends to be larger and begins organ-specific migration prior to the left 3$^{rd}$ pp (80, 81, 162). The ectopic location of the right thymic lobe suggests that *miR-17-92* may play a role in separation from the pharyngeal endoderm and/or in the timing or execution of thymus migration. While *miR-17-92* has not been implicated in organ migration, a member of the cluster, *miR-17*, has been shown to regulate lung morphogenesis through FGF10 and STAT3 signaling (179). FGF10-mediated signaling from the NC-derived mesenchyme is required for proper thymus development (72, 73) and NCCs promote separation and migration of the thymus and parathyroid (62-65). Therefore, these findings may suggest a novel role for *miR-17-92* in organ migration. Interestingly, we observed a similar phenotype in the *Foxn1*$^{Cre/+}$;*R26R*$^{iTbx1/+}$ mouse model. Enforced ectopic expression of *Tbx1* in TECs resulted in extremely hypoplastic fetal thymic lobes, although both lobes were present and not ectopic. These data suggest that although reduced in frequency, the few cells that express *Foxn1* in both models are capable of proliferating and differentiating into a thymus. They also suggest that dysregulation of *Tbx1* does not completely abrogate *Foxn1* expression, but is sufficient to disrupt proper thymus organogenesis.

*MiR-17-92* regulates gene expression in multiple tissues throughout development and its importance throughout ontogeny is underscored by the fact that *miR-17-92* null mice die at birth (161). Therefore, the E11.5 3rd pp and E14.5 thymus phenotypes we observe in *miR-17-92*$^{Null}$ embryos may be attributable to indirect effects of deleting this cluster in other tissues, such as the mesenchyme. To address this, we site-specifically deleted *miR-17-92* in TECs using *Foxn1*$^{Cre}$. At E12.5, both thymic lobes in *Foxn1*$^{Cre/+}$*;miR-17-92*$^{Fl/Fl}$ embryos were comparable in size and location to those in the control. This result further supports the notion that mesenchymal expression of *miR-17-92* does plays a role in thymus migration.

Although thymus size and location in *Foxn1*$^{Cre/+}$*;miR-17-92*$^{Fl/Fl}$ embryos was preserved, we observed ectopic expression of TBX1 within a rare population of cells located at the anterior-most region of the mutant thymic lobe. These cells expressed very low to negative levels of FOXN1 and persisted until E17.5. Interestingly, these cells also expressed the TEC progenitor marker, Plet-1. Rare TECs with the same phenotype were also found in *Foxn1*$^{Cre/+}$;*R26*$^{iTbx1/+}$ thymic lobes. Clearly, enforced expression of TBX1 reduces FOXN1 expression and arrests TECs in a primitive state. Furthermore, these data illustrate that despite the presence of TBX1, these cells are committed to the thymus, and not PT, lineage. Similarly, in the absence of *miR-17-92*, cardiac progenitors are unable to differentiate due to the persistence of *Tbx1* expression (82). However, they are still committed to the cardiomyocyte lineage. These observations suggest that *Tbx1* expression in the 3rd pp may not indicate a “default” to PT cell fate, but rather identify true endodermal progenitors that are capable of differentiating into thymus-fated cells depending on what signals they receive. This notion is further supported by the fact that PT cell fate, as reflected by GCM2 expression, is unaffected when *miR-17-92* is overexpressed in TECs, despite the greatly reduced staining intensity of TBX1.

Taken together, these results suggest a multifaceted and temporally regulated role for *Tbx1* during 3rd pp development and patterning. Specifically, *Tbx1* is required early in ontogeny for segmentation of the pharyngeal endoderm and initiation of 3rd pp patterning; however by E10.5, its expression is required to promote PT organogenesis by interfering with thymus organogenesis.

### *Fgf8*, NCCs and thymus fate

We have shown that despite ectopic expression of *Tbx1* or the absence of its regulators, thymus cell fate is still established in the 3rd pp endoderm, and even though few in numbers, the FOXN1 positive cells are able to give rise to a thymus. These models have also demonstrated that additional mechanisms regulate *Tbx1* expression in the 3rd pp and that despite genetic manipulation, thymus cell fate may be attenuated, but it is not abrogated.

NCCs play multiple roles in thymus organogenesis. At E10.5-E11.5, NCCs provide signals required for appropriate patterning of 3rd pp endoderm. By E12.5, NCCs condense to form a mesenchymal capsule around the developing thymic lobes and secrete numerous growth factors to promote the proliferation and differentiation of TECs (64). By E14.5 NCCs migrate into the thymic lobes to form pericytes surrounding the vascular network (66). This dynamic role for NCC function during development is not surprising given that NCC are an extremely plastic population of cells that give rise to numerous cell types (58).

Our previous study reported that the deficiency of NCCs in *Pax3*$^{Sp/Sp}$ embryos resulted in a shift in the thymus-PT cell fate boundary in the E11.5 3rd pp (70). Our current work shows that NCCs influence 3rd pp patterning even earlier. Specifically, we demonstrate that at E10.5 the TBX1 expression domain is reduced and there is a compensatory

expansion of FOXG1 in the 3rd pp of *Pax3*$^{Sp/Sp}$ mutants. These data could be interpreted to suggest that NCCs are necessary to establish PT rather than thymus fate in the developing pouch. The deficiency in NCCs in *Pax3*$^{Sp/Sp}$ mutants may prevent initial establishment or cause reversal of PT fate. This issue may be resolved by analyzing Gcm2 expression, which is expressed as early as E9.5. Therefore, it will be important to determine whether or not Gcm2 expression is altered in the 3rd pp of *Pax3*$^{Sp/Sp}$ mutants.

Additionally, our work with the *Pax3*$^{Sp/Sp}$ embryos has shown that in the absence of NCCs, *Fgf8* expression is sustained and expanded in the ventral domain of the mutant 3rd pp endoderm and surrounding mesenchyme. Furthermore, *Fgf8* is thought to induce the *Bmp4* signaling cascade to necessary to establish thymus fate in the chick endoderm (85). Interestingly, we observed a substantial increase in *Bmp4* expression, similar to that of *Fgf8*, in the NC-deficient model. These results strongly support a similar hypothesis in our model system that *Fgf8* is an important regulator of thymus cell fate and may function upstream of *Bmp4* to pattern the murine 3rd pp.

The analysis of 3rd pp patterning in *Pax3*$^{Sp/Sp}$ mutants suggests that NCCs are required to sustain *Tbx1* expression in the dorsal domain and extinguish *Fgf8* expression in the ventral region. Previous studies have demonstrated a genetic interaction between *Tbx1* and *Fgf8* (163). Indeed, we have shown that *Tbx1* expression is reduced in the 3rd pp of *Tbx1*$^{Fgf8/+}$ embryos. The ectopic expression of *Fgf8* in the dorsal domain results in a phenotype that is strikingly similar to that of the *Pax3*$^{Sp/Sp}$ mutants. ISH analysis revealed an expansion of *Foxn1* and a reduction in *Gcm2* expression.

In summary, we have shown that *Tbx1* negatively regulates FOXN1 expression in the 3rd pp endoderm and must be downregulated for TEC differentiation to occur. Through the use of LOF and GOF mouse models, we demonstrated that *miR-17-92* regulates *Tbx1*

expression in the 3rd pp endoderm, potentially via both cell autonomous and non-cell autonomous mechanisms. Interestingly, this regulation may occur as a result of *Bmp2/4* promoting the endodermal expression of *miR-17-92* at E10.5, which in turn binds the 3'UTR of *Tbx1* and silences its expression in the ventral domain of the 3rd pp endoderm. Furthermore, our data suggest that NCCs play an indispensible role in patterning the 3rd pp and are necessary to maintain PT-cell fate and *Tbx1* expression. In their absence, *Fgf8* and *Bmp4* expression are dramatically upregulated, resulting in the expansion of thymus fate within the 3rd pp endoderm. Moreover, ectopic expression of *Fgf8* from the *Tbx1* allele abrogates PT fate and downregulates TBX1, further supporting the notion that *Fgf8* is required for the establishment of thymus fate. Based on these data, we have modified our initial working model to reflect the multiple mechanisms necessary to regulate *Tbx1* in the 3rd pp endoderm, and thus promote the establishment of thymus fate (Fig.30).

**Future Directions**

Our preliminary data strongly suggest that FOXN1 expression is maintained despite sustained and ectopic expression of *Tbx1* prior to the establishment of cell fate within the 3rd pp. However, it is important to determine if thymus organogenesis occurs in this model, and if so, how TEC differentiation is affected. Furthermore, the *Foxa2$^{Cre}$;R26$^{iTbx1}$* and *Foxn1$^{Cre}$;R26$^{iTbx1}$* models will allow us to address how *Fgf8* and *Tbx1* interact to pattern the 3rd pp. Our data imply that *Fgf8* negatively regulates *Tbx1* in the 3rd pp. However, a key experiment will be to determine if *Fgf8* is still expressed either model. Furthermore, if *Fgf8* were expressed in proximity to the few FOXN1 positive cells, this result would strongly implicate the growth factor as an important regulator of thymus fate.

It would also be interesting to temporally and spatially delete *Fgf8* in the 3rd pp to determine if thymus cell fate is abrogated in the absence of *Fgf8*. If true, this would establish *Fgf8* as a key component in 3rd pp patterning and cell fate commitment. However, another outcome would be that FOXN1 is expressed in the absence of *Fgf8*. Based on our models, this outcome is also plausible given that FOXN1 positive cells are present in the ventral tip of the 3rd pp despite ectopic TBX1 expression. This result would bolster the conclusion that there are mechanisms in place to ensure that thymus development does occur. Given that *Bmp4* positively regulates thymus development and it is upregulated in the absence of NCCs, similar to *Fgf8*, exploring the expression pattern of *Bmp4* in all of these models will further define how these factors are interacting to pattern the 3rd pp.

We hypothesize that both *Bmp4* and *Fgf8* act upstream of *miR-17-92*. Therefore, analyzing the expression pattern and staining intensity of the miRNA cluster in models that express significant amounts of *Bmp4* would clarify if *miR-17-92* is functioning downstream of *Bmp* in our model system. Another approach to address this point would be to analyze pouch patterning, thymus development and *miR-17-92* expression in *Bmp2/4* compound mutants.

Although *miR-17-92* functions in both cell autonomous and non-cell autonomous manners, its mode of action is highly dependent upon cell type (168, 169). It has been shown that miRNAs are present in exosomes and are able to fuse with the membrane of distant or neighboring cells through multiple mechanisms. Exosomes can interact with receptors on the cell surface, fuse with the plasma membrane or become internalized and either released or degraded by the cell (180-182). Therefore, it will be very interesting to determine if a similar mechanism is occurring in our model systems.

Taken together, the aims of this thesis have identified novel genetic pathways that are critical in defining TEC fate, maintaining TEC differentiation and demonstrated how they can potentially be incorporated into a regulatory network, which up until now have been elusive. These mechanisms, as well as molecular targets of these mechanisms, can be used to develop therapeutic strategies to generate TECs from endodermal progenitors in order to produce a functional thymus, or regenerate an involuted thymus, which can support and promote T cell development *in vivo* or *in vitro*. Ultimately, this will restore robust immune responses in immunocompromised and aging, non-patients.

**BIBLIOGRAPHY**


1. Manley, N. R., E. R. Richie, C. C. Blackburn, B. G. Condie, and J. Sage. 2011. Structure and function of the thymic microenvironment. *Frontiers in bioscience* 16: 2461-2477.

2. Berzins, S. P., R. L. Boyd, and J. F. Miller. 1998. The role of the thymus and recent thymic migrants in the maintenance of the adult peripheral lymphocyte pool. *The Journal of experimental medicine* 187: 1839-1848.

3. Sempowski, G. D., M. E. Gooding, H. X. Liao, P. T. Le, and B. F. Haynes. 2002. T cell receptor excision circle assessment of thymopoiesis in aging mice. *Molecular immunology* 38: 841-848.

4. Hale, J. S., T. E. Boursalian, G. L. Turk, and P. J. Fink. 2006. Thymic output in aged mice. *Proceedings of the National Academy of Sciences of the United States of America* 103: 8447-8452.

5. Wils, E.-J., B. van der Holt, A. E. C. Broers, S. J. Posthumus-van Sluijs, J.-W. Gratama, E. Braakman, and J. J. Cornelissen. 2011. Insufficient recovery of thymopoiesis predicts for opportunistic infections in allogeneic hematopoietic stem cell transplant recipients. *Haematologica* 96: 1846-1854.

6. Griffith, A. V., M. Fallahi, T. Venables, and H. T. Petrie. 2012. Persistent degenerative changes in thymic organ function revealed by an inducible model of organ regrowth. *Aging cell* 11: 169-177.

7. Lynch, H. E., G. L. Goldberg, A. Chidgey, M. R. Van den Brink, R. Boyd, and G. D. Sempowski. 2009. Thymic involution and immune reconstitution. *Trends in immunology* 30: 366-373.

8. Ventevogel, M. S., and G. D. Sempowski. 2013. Thymic rejuvenation and aging. *Current opinion in immunology* 25: 516-522.

9. Wilkinson, B., J. J. Owen, and E. J. Jenkinson. 1999. Factors regulating stem cell recruitment to the fetal thymus. *Journal of immunology* 162: 3873-3881.

10. Love, P. E., and A. Bhandoola. 2011. Signal integration and crosstalk during thymocyte migration and emigration. *Nature reviews. Immunology* 11: 469-477.

11. Liu, C., F. Saito, Z. Liu, Y. Lei, S. Uehara, P. Love, M. Lipp, S. Kondo, N. Manley, and Y. Takahama. 2006. Coordination between CCR7- and CCR9-mediated chemokine signals in prevascular fetal thymus colonization. *Blood* 108: 2531-2539.

12. Zamisch, M., B. Moore-Scott, D. M. Su, P. J. Lucas, N. Manley, and E. R. Richie. 2005. Ontogeny and regulation of IL-7-expressing thymic epithelial cells. *Journal of immunology* 174: 60-67.

13. Koch, U., and F. Radtke. 2011. Mechanisms of T cell development and transformation. *Annual review of cell and developmental biology* 27: 539-562.

14. Shah, D. K., and J. C. Zuniga-Pflucker. 2014. An overview of the intrathymic intricacies of T cell development. *Journal of immunology* 192: 4017-4023.

15. Radtke, F., A. Wilson, G. Stark, M. Bauer, J. van Meerwijk, H. R. MacDonald, and M. Aguet. 1999. Deficient T cell fate specification in mice with an induced inactivation of Notch1. *Immunity* 10: 547-558.

16. Capone, M., R. D. Hockett, Jr., and A. Zlotnik. 1998. Kinetics of T cell receptor beta, gamma, and delta rearrangements during adult thymic development: T cell receptor rearrangements are present in CD44(+)CD25(+) Pro-T thymocytes. *Proceedings of the National Academy of Sciences of the United States of America* 95: 12522-12527.

17. Livak, F., M. Tourigny, D. G. Schatz, and H. T. Petrie. 1999. Characterization of TCR gene rearrangements during adult murine T cell development. *Journal of immunology* 162: 2575-2580.

18. Balciunaite, G., R. Ceredig, H. J. Fehling, J. C. Zuniga-Pflucker, and A. G. Rolink. 2005. The role of Notch and IL-7 signaling in early thymocyte proliferation and differentiation. *European journal of immunology* 35: 1292-1300.

19. Ciofani, M., and J. C. Zuniga-Pflucker. 2005. Notch promotes survival of pre-T cells at the beta-selection checkpoint by regulating cellular metabolism. *Nature immunology* 6: 881-888.

20. Maillard, I., L. Tu, A. Sambandam, Y. Yashiro-Ohtani, J. Millholland, K. Keeshan, O. Shestova, L. Xu, A. Bhandoola, and W. S. Pear. 2006. The requirement for Notch signaling at the beta-selection checkpoint in vivo is absolute and independent of the pre-T cell receptor. *The Journal of experimental medicine* 203: 2239-2245.

21. Porritt, H. E., K. Gordon, and H. T. Petrie. 2003. Kinetics of steady-state differentiation and mapping of intrathymic-signaling environments by stem cell transplantation in nonirradiated mice. *The Journal of experimental medicine* 198: 957-962.

22. Penit, C., B. Lucas, and F. Vasseur. 1995. Cell expansion and growth arrest phases during the transition from precursor (CD4-8-) to immature (CD4+8+) thymocytes in normal and genetically modified mice. *Journal of immunology* 154: 5103-5113.

23. Klein, L., B. Kyewski, P. M. Allen, and K. A. Hogquist. 2014. Positive and negative selection of the T cell repertoire: what thymocytes see (and don't see). *Nature reviews. Immunology* 14: 377-391.

24. Klein, L., M. Hinterberger, G. Wirnsberger, and B. Kyewski. 2009. Antigen presentation in the thymus for positive selection and central tolerance induction. *Nature reviews. Immunology* 9: 833-844.

25. Murata, S., K. Sasaki, T. Kishimoto, S. Niwa, H. Hayashi, Y. Takahama, and K. Tanaka. 2007. Regulation of CD8+ T cell development by thymus-specific proteasomes. *Science* 316: 1349-1353.

26. Kwan, J., and N. Killeen. 2004. CCR7 directs the migration of thymocytes into the thymic medulla. *Journal of immunology* 172: 3999-4007.

27. Gotter, J., B. Brors, M. Hergenhahn, and B. Kyewski. 2004. Medullary epithelial cells of the human thymus express a highly diverse selection of tissue-specific genes

colocalized in chromosomal clusters. *The Journal of experimental medicine* 199: 155-166.

28. Kyewski, B., J. Derbinski, J. Gotter, and L. Klein. 2002. Promiscuous gene expression and central T-cell tolerance: more than meets the eye. *Trends in immunology* 23: 364-371.

29. Le Borgne, M., E. Ladi, I. Dzhagalov, P. Herzmark, Y. F. Liao, A. K. Chakraborty, and E. A. Robey. 2009. The impact of negative selection on thymocyte migration in the medulla. *Nature immunology* 10: 823-830.

30. Anderson, M. S., E. S. Venanzi, L. Klein, Z. Chen, S. P. Berzins, S. J. Turley, H. von Boehmer, R. Bronson, A. Dierich, C. Benoist, and D. Mathis. 2002. Projection of an immunological self shadow within the thymus by the aire protein. *Science* 298: 1395-1401.

31. Koh, A. S., A. J. Kuo, S. Y. Park, P. Cheung, J. Abramson, D. Bua, D. Carney, S. E. Shoelson, O. Gozani, R. E. Kingston, C. Benoist, and D. Mathis. 2008. Aire employs a histone-binding module to mediate immunological tolerance, linking chromatin regulation with organ-specific autoimmunity. *Proceedings of the National Academy of Sciences of the United States of America* 105: 15878-15883.

32. Org, T., F. Chignola, C. Hetenyi, M. Gaetani, A. Rebane, I. Liiv, U. Maran, L. Mollica, M. J. Bottomley, G. Musco, and P. Peterson. 2008. The autoimmune regulator PHD

finger binds to non-methylated histone H3K4 to activate gene expression. *EMBO reports* 9: 370-376.

33. Liston, A., S. Lesage, J. Wilson, L. Peltonen, and C. C. Goodnow. 2003. Aire regulates negative selection of organ-specific T cells. *Nature immunology* 4: 350-354.

34. Koble, C., and B. Kyewski. 2009. The thymic medulla: a unique microenvironment for intercellular self-antigen transfer. *The Journal of experimental medicine* 206: 1505-1513.

35. Millet, V., P. Naquet, and R. R. Guinamard. 2008. Intercellular MHC transfer between thymic epithelial and dendritic cells. *European journal of immunology* 38: 1257-1263.

36. Josefowicz, S. Z., L. F. Lu, and A. Y. Rudensky. 2012. Regulatory T cells: mechanisms of differentiation and function. *Annual review of immunology* 30: 531-564.

37. Ritter, M. A., and R. L. Boyd. 1993. Development in the thymus: it takes two to tango. *Immunology today* 14: 462-469.

38. Anderson, G., and E. J. Jenkinson. 2001. Lymphostromal interactions in thymic development and function. *Nature reviews. Immunology* 1: 31-40.

39. van Ewijk, W., E. W. Shores, and A. Singer. 1994. Crosstalk in the mouse thymus. *Immunology today* 15: 214-217.

40. Hollander, G., J. Gill, S. Zuklys, N. Iwanami, C. Liu, and Y. Takahama. 2006. Cellular and molecular events during early thymus development. *Immunol Rev* 209: 28-46.

41. Klug, D. B., C. Carter, E. Crouch, D. Roop, C. J. Conti, and E. R. Richie. 1998. Interdependence of cortical thymic epithelial cell differentiation and T-lineage commitment. *Proceedings of the National Academy of Sciences of the United States of America* 95: 11822-11827.

42. Wang, J. H., A. Nichogiannopoulou, L. Wu, L. Sun, A. H. Sharpe, M. Bigby, and K. Georgopoulos. 1996. Selective defects in the development of the fetal and adult lymphoid system in mice with an Ikaros null mutation. *Immunity* 5: 537-549.

43. Klug, D. B., C. Carter, I. B. Gimenez-Conti, and E. R. Richie. 2002. Cutting edge: thymocyte-independent and thymocyte-dependent phases of epithelial patterning in the fetal thymus. *Journal of immunology* 169: 2842-2845.

44. Jenkinson, W. E., S. W. Rossi, E. J. Jenkinson, and G. Anderson. 2005. Development of functional thymic epithelial cells occurs independently of lymphostromal interactions. *Mechanisms of development* 122: 1294-1299.

45. Hale, L. P. 2004. Histologic and molecular assessment of human thymus. *Annals of diagnostic pathology* 8: 50-60.

46. Peschon, J. J., P. J. Morrissey, K. H. Grabstein, F. J. Ramsdell, E. Maraskovsky, B. C. Gliniak, L. S. Park, S. F. Ziegler, D. E. Williams, C. B. Ware, J. D. Meyer, and B.

L. Davison. 1994. Early lymphocyte expansion is severely impaired in interleukin 7 receptor-deficient mice. *The Journal of experimental medicine* 180: 1955-1960.

47. von Freeden-Jeffry, U., P. Vieira, L. A. Lucian, T. McNeil, S. E. Burdach, and R. Murray. 1995. Lymphopenia in interleukin (IL)-7 gene-deleted mice identifies IL-7 as a nonredundant cytokine. *The Journal of experimental medicine* 181: 1519-1526.

48. Erickson, M., S. Morkowski, S. Lehar, G. Gillard, C. Beers, J. Dooley, J. S. Rubin, A. Rudensky, and A. G. Farr. 2002. Regulation of thymic epithelium by keratinocyte growth factor. *Blood* 100: 3269-3278.

49. Gordon, J., and N. R. Manley. 2011. Mechanisms of thymus organogenesis and morphogenesis. *Development* 138: 3865-3878.

50. Gordon, J., V. A. Wilson, N. F. Blair, J. Sheridan, A. Farley, L. Wilson, N. R. Manley, and C. C. Blackburn. 2004. Functional evidence for a single endodermal origin for the thymic epithelium. *Nature immunology* 5: 546-553.

51. Gordon, J., and N. R. Manley. 2011. Mechanisms of thymus organogenesis and morphogenesis. *Development* 138: 3865-3878.

52. Manley, N. R. 2000. Thymus organogenesis and molecular mechanisms of thymic epithelial cell differentiation. *Seminars in Immunology* 12: 421-428.

53. Gordon, J., A. R. Bennett, C. C. Blackburn, and N. R. Manley. 2001. Gcm2 and Foxn1 mark early parathyroid- and thymus-specific domains in the developing third pharyngeal pouch. *Mechanisms of Development* 103: 141-143.

54. Gordon, J., A. R. Bennett, C. C. Blackburn, and N. R. Manley. 2001. Gcm2 and Foxn1 mark early parathyroid- and thymus-specific domains in the developing third pharyngeal pouch. *Mechanisms of development* 103: 141-143.

55. Bennett, A. R., A. Farley, N. F. Blair, J. Gordon, L. Sharp, and C. C. Blackburn. 2002. Identification and characterization of thymic epithelial progenitor cells. *Immunity* 16: 803-814.

56. Jenkinson, E. J., W. Van Ewijk, and J. J. Owen. 1981. Major histocompatibility complex antigen expression on the epithelium of the developing thymus in normal and nude mice. *The Journal of experimental medicine* 153: 280-292.

57. Nowell, C. S., N. Bredenkamp, S. Tetelin, X. Jin, C. Tischner, H. Vaidya, J. M. Sheridan, F. H. Stenhouse, R. Heussen, A. J. Smith, and C. C. Blackburn. 2011. Foxn1 regulates lineage progression in cortical and medullary thymic epithelial cells but is dispensable for medullary sublineage divergence. *PLoS genetics* 7: e1002348.

58. Garcia-Castro, M., and M. Bronner-Fraser. 1999. Induction and differentiation of the neural crest. *Current opinion in cell biology* 11: 695-698.

59. Jiang, X., D. H. Rowitch, P. Soriano, A. P. McMahon, and H. M. Sucov. 2000. Fate of the mammalian cardiac neural crest. *Development* 127: 1607-1616.

60. Le Lievre, C. S., and N. M. Le Douarin. 1975. Mesenchymal derivatives of the neural crest: analysis of chimaeric quail and chick embryos. *Journal of embryology and experimental morphology* 34: 125-154.

61. Bockman, D. E., and M. L. Kirby. 1984. Dependence of thymus development on derivatives of the neural crest. *Science* 223: 498-500.

62. Auerbach, R. 1960. Morphogenetic interactions in the development of the mouse thymus gland. *Developmental biology* 2: 271-284.

63. Foster, K., J. Sheridan, H. Veiga-Fernandes, K. Roderick, V. Pachnis, R. Adams, C. Blackburn, D. Kioussis, and M. Coles. 2008. Contribution of neural crest-derived cells in the embryonic and adult thymus. *Journal of immunology* 180: 3183-3189.

64. Jenkinson, W. E., E. J. Jenkinson, and G. Anderson. 2003. Differential requirement for mesenchyme in the proliferation and maturation of thymic epithelial progenitors. *The Journal of experimental medicine* 198: 325-332.

65. Muller, S. M., C. C. Stolt, G. Terszowski, C. Blum, T. Amagai, N. Kessaris, P. Iannarelli, W. D. Richardson, M. Wegner, and H. R. Rodewald. 2008. Neural crest origin of perivascular mesenchyme in the adult thymus. *Journal of immunology* 180: 5344-5351.

66. Bryson, J. L., A. V. Griffith, B. Hughes, 3rd, F. Saito, Y. Takahama, E. R. Richie, and N. R. Manley. 2013. Cell-autonomous defects in thymic epithelial cells disrupt endothelial-perivascular cell interactions in the mouse thymus. *PloS one* 8: e65196.

67. Conway, S. J., J. Bundy, J. Chen, E. Dickman, R. Rogers, and B. M. Will. 2000. Decreased neural crest stem cell expansion is responsible for the conotruncal heart defects within the splotch (Sp(2H))/Pax3 mouse mutant. *Cardiovascular research* 47: 314-328.

68. Epstein, J. A., J. Li, D. Lang, F. Chen, C. B. Brown, F. Jin, M. M. Lu, M. Thomas, E. Liu, A. Wessels, and C. W. Lo. 2000. Migration of cardiac neural crest cells in Splotch embryos. *Development* 127: 1869-1878.

69. Pani, L., M. Horal, and M. R. Loeken. 2002. Rescue of neural tube defects in Pax-3-deficient embryos by p53 loss of function: implications for Pax-3- dependent development and tumorigenesis. *Genes & development* 16: 676-680.

70. Griffith, A. V., K. Cardenas, C. Carter, J. Gordon, A. Iberg, K. Engleka, J. A. Epstein, N. R. Manley, and E. R. Richie. 2009. Increased thymus- and decreased parathyroid-fated organ domains in Splotch mutant embryos. *Developmental biology* 327: 216-227.

71. Zhang, Z., T. Huynh, and A. Baldini. 2006. Mesodermal expression of Tbx1 is necessary and sufficient for pharyngeal arch and cardiac outflow tract development. *Development* 133: 3587-3595.

72. Revest, J. M., R. K. Suniara, K. Kerr, J. J. Owen, and C. Dickson. 2001. Development of the thymus requires signaling through the fibroblast growth factor receptor R2-IIIb. *Journal of immunology* 167: 1954-1961.

73. Suniara, R. K., E. J. Jenkinson, and J. J. Owen. 2000. An essential role for thymic mesenchyme in early T cell development. *The Journal of experimental medicine* 191: 1051-1056.

74. Rossi, S. W., L. T. Jeker, T. Ueno, S. Kuse, M. P. Keller, S. Zuklys, A. V. Gudkov, Y. Takahama, W. Krenger, B. R. Blazar, and G. A. Hollander. 2007. Keratinocyte growth factor (KGF) enhances postnatal T-cell development via enhancements in proliferation and function of thymic epithelial cells. *Blood* 109: 3803-3811.

75. Gray, D. H., D. Tull, T. Ueno, N. Seach, B. J. Classon, A. Chidgey, M. J. McConville, and R. L. Boyd. 2007. A unique thymic fibroblast population revealed by the monoclonal antibody MTS-15. *Journal of immunology* 178: 4956-4965.

76. Guo, L., L. Degenstein, and E. Fuchs. 1996. Keratinocyte growth factor is required for hair development but not for wound healing. *Genes & development* 10: 165-175.

77. Zou, D., D. Silvius, J. Davenport, R. Grifone, P. Maire, and P. X. Xu. 2006. Patterning of the third pharyngeal pouch into thymus/parathyroid by Six and Eya1. *Developmental biology* 293: 499-512.

78. Frank, D. U., L. K. Fotheringham, J. A. Brewer, L. J. Muglia, M. Tristani-Firouzi, M. R. Capecchi, and A. M. Moon. 2002. An Fgf8 mouse mutant phenocopies human 22q11 deletion syndrome. *Development* 129: 4591-4603.

79. Abu-Issa, R., G. Smyth, I. Smoak, K. Yamamura, and E. N. Meyers. 2002. Fgf8 is required for pharyngeal arch and cardiovascular development in the mouse. *Development* 129: 4613-4625.

80. Patel, S. R., J. Gordon, F. Mahbub, C. C. Blackburn, and N. R. Manley. 2006. Bmp4 and Noggin expression during early thymus and parathyroid organogenesis. *Gene expression patterns : GEP* 6: 794-799.

81. Gordon, J., S. R. Patel, Y. Mishina, and N. R. Manley. 2010. Evidence for an early role for BMP4 signaling in thymus and parathyroid morphogenesis. *Developmental biology* 339: 141-154.

82. Wang, J., S. B. Greene, M. Bonilla-Claudio, Y. Tao, J. Zhang, Y. Bai, Z. Huang, B. L. Black, F. Wang, and J. F. Martin. 2010. Bmp signaling regulates myocardial differentiation from cardiac progenitors through a MicroRNA-mediated mechanism. *Developmental cell* 19: 903-912.

83. Bleul, C. C., and T. Boehm. 2005. BMP signaling is required for normal thymus development. *Journal of immunology* 175: 5213-5221.

84. Soza-Ried, C., C. C. Bleul, M. Schorpp, and T. Boehm. 2008. Maintenance of thymic epithelial phenotype requires extrinsic signals in mouse and zebrafish. *Journal of immunology* 181: 5272-5277.

85. Neves, H., E. Dupin, L. Parreira, and N. M. Le Douarin. 2012. Modulation of Bmp4 signalling in the epithelial-mesenchymal interactions that take place in early thymus

and parathyroid development in avian embryos. *Developmental biology* 361: 208-219.

86. Moore-Scott, B. A., and N. R. Manley. 2005. Differential expression of Sonic hedgehog along the anterior-posterior axis regulates patterning of pharyngeal pouch endoderm and pharyngeal endoderm-derived organs. *Developmental biology* 278: 323-335.

87. Bleul, C. C., T. Corbeaux, A. Reuter, P. Fisch, J. S. Monting, and T. Boehm. 2006. Formation of a functional thymus initiated by a postnatal epithelial progenitor cell. *Nature* 441: 992-996.

88. Blackburn, C. C., C. L. Augustine, R. Li, R. P. Harvey, M. A. Malin, R. L. Boyd, J. F. Miller, and G. Morahan. 1996. The nu gene acts cell-autonomously and is required for differentiation of thymic epithelial progenitors. *Proceedings of the National Academy of Sciences of the United States of America* 93: 5742-5746.

89. Gill, J., M. Malin, G. A. Hollander, and R. Boyd. 2002. Generation of a complete thymic microenvironment by MTS24(+) thymic epithelial cells. *Nature immunology* 3: 635-642.

90. Depreter, M. G., N. F. Blair, T. L. Gaskell, C. S. Nowell, K. Davern, A. Pagliocca, F. H. Stenhouse, A. M. Farley, A. Fraser, J. Vrana, K. Robertson, G. Morahan, S. R. Tomlinson, and C. C. Blackburn. 2008. Identification of Plet-1 as a specific marker of

early thymic epithelial progenitor cells. *Proceedings of the National Academy of Sciences of the United States of America* 105: 961-966.

91. Hamazaki, Y., H. Fujita, T. Kobayashi, Y. Choi, H. S. Scott, M. Matsumoto, and N. Minato. 2007. Medullary thymic epithelial cells expressing Aire represent a unique lineage derived from cells expressing claudin. *Nature immunology* 8: 304-311.

92. Ripen, A. M., T. Nitta, S. Murata, K. Tanaka, and Y. Takahama. 2011. Ontogeny of thymic cortical epithelial cells expressing the thymoproteasome subunit beta5t. *European journal of immunology* 41: 1278-1287.

93. Baik, S., E. J. Jenkinson, P. J. Lane, G. Anderson, and W. E. Jenkinson. 2013. Generation of both cortical and Aire(+) medullary thymic epithelial compartments from CD205(+) progenitors. *European journal of immunology* 43: 589-594.

94. Chidgey, A. P., N. Seach, J. Dudakov, M. V. Hammett, and R. L. Boyd. 2008. Strategies for reconstituting and boosting T cell-based immunity following haematopoietic stem cell transplantation: pre-clinical and clinical approaches. *Seminars in immunopathology* 30: 457-477.

95. Rode, I., and T. Boehm. 2012. Regenerative capacity of adult cortical thymic epithelial cells. *Proceedings of the National Academy of Sciences of the United States of America* 109: 3463-3468.

96. Ucar, A., O. Ucar, P. Klug, S. Matt, F. Brunk, T. G. Hofmann, and B. Kyewski. 2014. Adult thymus contains FoxN1(-) epithelial stem cells that are bipotent for medullary and cortical thymic epithelial lineages. *Immunity* 41: 257-269.

97. Wong, K., N. L. Lister, M. Barsanti, J. M. Lim, M. V. Hammett, D. M. Khong, C. Siatskas, D. H. Gray, R. L. Boyd, and A. P. Chidgey. 2014. Multilineage potential and self-renewal define an epithelial progenitor cell population in the adult thymus. *Cell reports* 8: 1198-1209.

98. Jin, X., C. S. Nowell, S. Ulyanchenko, F. H. Stenhouse, and C. C. Blackburn. 2014. Long-term persistence of functional thymic epithelial progenitor cells in vivo under conditions of low FOXN1 expression. *PloS one* 9: e114842.

99. Chen, L., S. Xiao, and N. R. Manley. 2009. Foxn1 is required to maintain the postnatal thymic microenvironment in a dosage-sensitive manner. *Blood* 113: 567-574.

100. Bredenkamp, N., C. S. Nowell, and C. C. Blackburn. 2014. Regeneration of the aged thymus by a single transcription factor. *Development* 141: 1627-1637.

101. Manley, N. R., and M. R. Capecchi. 1998. Hox group 3 paralogs regulate the development and migration of the thymus, thyroid, and parathyroid glands. *Developmental biology* 195: 1-15.

102. Manley, N. R., and M. R. Capecchi. 1997. Hox group 3 paralogous genes act synergistically in the formation of somitic and neural crest-derived structures. *Developmental biology* 192: 274-288.

103. Manley, N. R., and M. R. Capecchi. 1995. The role of Hoxa-3 in mouse thymus and thyroid development. *Development* 121: 1989-2003.

104. Chojnowski, J. L., K. Masuda, H. A. Trau, K. Thomas, M. Capecchi, and N. R. Manley. 2014. Multiple roles for HOXA3 in regulating thymus and parathyroid differentiation and morphogenesis in mouse. *Development* 141: 3697-3708.

105. Xu, P. X., W. Zheng, C. Laclef, P. Maire, R. L. Maas, H. Peters, and X. Xu. 2002. Eya1 is required for the morphogenesis of mammalian thymus, parathyroid and thyroid. *Development* 129: 3033-3044.

106. Manley, N. R., and B. G. Condie. 2010. Transcriptional regulation of thymus organogenesis and thymic epithelial cell differentiation. *Progress in molecular biology and translational science* 92: 103-120.

107. Laclef, C., E. Souil, J. Demignon, and P. Maire. 2003. Thymus, kidney and craniofacial abnormalities in Six 1 deficient mice. *Mechanisms of development* 120: 669-679.

108. Wei, Q., and B. G. Condie. 2011. A focused in situ hybridization screen identifies candidate transcriptional regulators of thymic epithelial cell development and function. *PloS one* 6: e26795.

109. Cai, C. L., X. Liang, Y. Shi, P. H. Chu, S. L. Pfaff, J. Chen, and S. Evans. 2003. Isl1 identifies a cardiac progenitor population that proliferates prior to differentiation and contributes a majority of cells to the heart. *Developmental cell* 5: 877-889.

110. Hidaka, K., T. Nitta, R. Sugawa, M. Shirai, R. J. Schwartz, T. Amagai, S. Nitta, Y. Takahama, and T. Morisaki. 2010. Differentiation of pharyngeal endoderm from mouse embryonic stem cell. *Stem cells and development* 19: 1735-1743.

111. Reeh, K. A., K. T. Cardenas, V. E. Bain, Z. Liu, M. Laurent, N. R. Manley, and E. R. Richie. 2014. Ectopic TBX1 suppresses thymic epithelial cell differentiation and proliferation during thymus organogenesis. *Development* 141: 2950-2958.

112. Vitelli, F., M. Morishima, I. Taddei, E. A. Lindsay, and A. Baldini. 2002. Tbx1 mutation causes multiple cardiovascular defects and disrupts neural crest and cranial nerve migratory pathways. *Human molecular genetics* 11: 915-922.

113. Lindsay, E. A., A. Botta, V. Jurecic, S. Carattini-Rivera, Y. C. Cheah, H. M. Rosenblatt, A. Bradley, and A. Baldini. 1999. Congenital heart disease in mice deficient for the DiGeorge syndrome region. *Nature* 401: 379-383.

114. Jerome, L. A., and V. E. Papaioannou. 2001. DiGeorge syndrome phenotype in mice mutant for the T-box gene, Tbx1. *Nature genetics* 27: 286-291.

115. Lindsay, E. A., F. Vitelli, H. Su, M. Morishima, T. Huynh, T. Pramparo, V. Jurecic, G. Ogunrinu, H. F. Sutherland, P. J. Scambler, A. Bradley, and A. Baldini. 2001. Tbx1

haploinsufficieny in the DiGeorge syndrome region causes aortic arch defects in mice. *Nature* 410: 97-101.

116. Merscher, S., B. Funke, J. A. Epstein, J. Heyer, A. Puech, M. M. Lu, R. J. Xavier, M. B. Demay, R. G. Russell, S. Factor, K. Tokooya, B. S. Jore, M. Lopez, R. K. Pandita, M. Lia, D. Carrion, H. Xu, H. Schorle, J. B. Kobler, P. Scambler, A. Wynshaw-Boris, A. I. Skoultchi, B. E. Morrow, and R. Kucherlapati. 2001. TBX1 is responsible for cardiovascular defects in velo-cardio-facial/DiGeorge syndrome. *Cell* 104: 619-629.

117. Vitelli, F., T. Huynh, and A. Baldini. 2009. Gain of function of Tbx1 affects pharyngeal and heart development in the mouse. *Genesis* 47: 188-195.

118. Chapman, D. L., N. Garvey, S. Hancock, M. Alexiou, S. I. Agulnik, J. J. Gibson-Brown, J. Cebra-Thomas, R. J. Bollag, L. M. Silver, and V. E. Papaioannou. 1996. Expression of the T-box family genes, Tbx1-Tbx5, during early mouse development. *Dev Dyn* 206: 379-390.

119. Arnold, J. S., U. Werling, E. M. Braunstein, J. Liao, S. Nowotschin, W. Edelmann, J. M. Hebert, and B. E. Morrow. 2006. Inactivation of Tbx1 in the pharyngeal endoderm results in 22q11DS malformations. *Development* 133: 977-987.

120. Xu, H., F. Cerrato, and A. Baldini. 2005. Timed mutation and cell-fate mapping reveal reiterated roles of Tbx1 during embryogenesis, and a crucial function during segmentation of the pharyngeal system via regulation of endoderm expansion. *Development* 132: 4387-4395.

121. Liu, Z., S. Yu, and N. R. Manley. 2007. Gcm2 is required for the differentiation and survival of parathyroid precursor cells in the parathyroid/thymus primordia. *Developmental biology* 305: 333-346.

122. Manley, N. R., L. Selleri, A. Brendolan, J. Gordon, and M. L. Cleary. 2004. Abnormalities of caudal pharyngeal pouch development in Pbx1 knockout mice mimic loss of Hox3 paralogs. *Developmental biology* 276: 301-312.

123. Garg, V., C. Yamagishi, T. Hu, I. S. Kathiriya, H. Yamagishi, and D. Srivastava. 2001. Tbx1, a DiGeorge syndrome candidate gene, is regulated by sonic hedgehog during pharyngeal arch development. *Dev Biol* 235: 62-73.

124. Yamagishi, H., J. Maeda, T. Hu, J. McAnally, S. J. Conway, T. Kume, E. N. Meyers, C. Yamagishi, and D. Srivastava. 2003. Tbx1 is regulated by tissue-specific forkhead proteins through a common Sonic hedgehog-responsive enhancer. *Genes Dev* 17: 269-281.

125. Bartel, D. P. 2004. MicroRNAs: genomics, biogenesis, mechanism, and function. *Cell* 116: 281-297.

126. Ambros, V. 1989. A hierarchy of regulatory genes controls a larva-to-adult developmental switch in C. elegans. *Cell* 57: 49-57.

127. Ruvkun, G., and J. Giusto. 1989. The Caenorhabditis elegans heterochronic gene lin-14 encodes a nuclear protein that forms a temporal developmental switch. *Nature* 338: 313-319.

128. Ha, M., and V. N. Kim. 2014. Regulation of microRNA biogenesis. *Nature reviews. Molecular cell biology* 15: 509-524.

129. Tanzer, A., and P. F. Stadler. 2004. Molecular evolution of a microRNA cluster. *Journal of molecular biology* 339: 327-335.

130. Mogilyansky, E., and I. Rigoutsos. 2013. The miR-17/92 cluster: a comprehensive update on its genomics, genetics, functions and increasingly important and numerous roles in health and disease. *Cell death and differentiation* 20: 1603-1614.

131. Marcelis, C. L., F. A. Hol, G. E. Graham, P. N. Rieu, R. Kellermayer, R. P. Meijer, D. Lugtenberg, H. Scheffer, H. van Bokhoven, H. G. Brunner, and A. P. de Brouwer. 2008. Genotype-phenotype correlations in MYCN-related Feingold syndrome. *Human mutation* 29: 1125-1132.

132. Wang, J., Y. Bai, H. Li, S. B. Greene, E. Klysik, W. Yu, R. J. Schwartz, T. J. Williams, and J. F. Martin. 2013. MicroRNA-17-92, a direct Ap-2alpha transcriptional target, modulates T-box factor activity in orofacial clefting. *PLoS genetics* 9: e1003785.

133. Fulcoli, F. G., T. Huynh, P. J. Scambler, and A. Baldini. 2009. Tbx1 Regulates the BMP-Smad1 Pathway in a Transcription Independent Manner. *PLoS ONE* 4: e6049.

134. Gordon, J., S. Xiao, B. Hughes, 3rd, D. M. Su, S. P. Navarre, B. G. Condie, and N. R. Manley. 2007. Specific expression of lacZ and cre recombinase in fetal thymic epithelial cells by multiplex gene targeting at the Foxn1 locus. *BMC Dev Biol* 7: 69.

135. Gray, D. H., A. P. Chidgey, and R. L. Boyd. 2002. Analysis of thymic stromal cell populations using flow cytometry. *Journal of immunological methods* 260: 15-28.

136. Baldini, A. 2005. Dissecting contiguous gene defects: TBX1. *Curr Opin Genet Dev* 15: 279-284.

137. Dooley, J., M. Erickson, W. J. Larochelle, G. O. Gillard, and A. G. Farr. 2007. FGFR2IIIb signaling regulates thymic epithelial differentiation. *Dev Dyn* 236: 3459-3471.

138. Zhang, Z., F. Cerrato, H. Xu, F. Vitelli, M. Morishima, J. Vincentz, Y. Furuta, L. Ma, J. F. Martin, A. Baldini, and E. Lindsay. 2005. Tbx1 expression in pharyngeal epithelia is necessary for pharyngeal arch artery development. *Development* 132: 5307-5315.

139. Ivins, S., K. Lammerts van Beuren, C. Roberts, C. James, E. Lindsay, A. Baldini, P. Ataliotis, and P. J. Scambler. 2005. Microarray analysis detects differentially expressed genes in the pharyngeal region of mice lacking Tbx1. *Developmental biology* 285: 554-569.

140. Repass, J. F., M. N. Laurent, C. Carter, B. Reizis, M. T. Bedford, K. Cardenas, P. Narang, M. Coles, and E. R. Richie. 2009. IL7-hCD25 and IL7-Cre BAC transgenic mouse lines: New tools for analysis of IL-7 expressing cells. *Genesis*.

141. Itoi, M., H. Kawamoto, Y. Katsura, and T. Amagai. 2001. Two distinct steps of immigration of hematopoietic progenitors into the early thymus anlage. *Int Immunol* 13: 1203-1211.

142. Su, D. M., S. Navarre, W. J. Oh, B. G. Condie, and N. R. Manley. 2003. A domain of Foxn1 required for crosstalk-dependent thymic epithelial cell differentiation. *Nature immunology* 4: 1128-1135.

143. Corbeaux, T., I. Hess, J. B. Swann, B. Kanzler, A. Haas-Assenbaum, and T. Boehm. 2010. Thymopoiesis in mice depends on a Foxn1-positive thymic epithelial cell lineage. *Proc Natl Acad Sci U S A* 107: 16613-16618.

144. Shakib, S., G. E. Desanti, W. E. Jenkinson, S. M. Parnell, E. J. Jenkinson, and G. Anderson. 2009. Checkpoints in the development of thymic cortical epithelial cells. *J Immunol* 182: 130-137.

145. Xiao, S., and N. R. Manley. 2010. Impaired thymic selection and abnormal antigen-specific T cell responses in Foxn1(Delta/Delta) mutant mice. *PLoS One* 5: e15396.

146. Nowell, C. S., E. Richie, N. R. Manley, and C. C. Blackburn. 2008. Thymus and Parathyroid Organogenesis. In *Principles of Tissue Engineering*, 3rd ed. R. Lanza, R. Langer, and J. Vacanti, eds. Elsevier.

147. Klug, D. B., C. Carter, E. Crouch, D. Roop, C. J. Conti, and E. R. Richie. 1998. Interdependence of cortical thymic epithelial cell differentiation and T-lineage commitment. *Proc Natl Acad Sci U S A* 95: 11822-11827.

148. Gardner, J. M., A. L. Fletcher, M. S. Anderson, and S. J. Turley. 2009. AIRE in the thymus and beyond. *Curr Opin Immunol* 21: 582-589.

149. Gillard, G. O., J. Dooley, M. Erickson, L. Peltonen, and A. G. Farr. 2007. Aire-dependent alterations in medullary thymic epithelium indicate a role for Aire in thymic epithelial differentiation. *J Immunol* 178: 3007-3015.

150. Bennett, A. R., A. Farley, N. F. Blair, J. Gordon, L. Sharp, and C. C. Blackburn. 2002. Identification and characterization of thymic epithelial progenitor cells. *Immunity* 16: 803-814.

151. Rossi, S. W., W. E. Jenkinson, G. Anderson, and E. J. Jenkinson. 2006. Clonal analysis reveals a common progenitor for thymic cortical and medullary epithelium. *Nature* 441: 988-991.

152. Anderson, G., and Y. Takahama. 2012. Thymic epithelial cells: working class heroes for T cell development and repertoire selection. *Trends Immunol* 33: 256-263.

153. Nitta, T., I. Ohigashi, Y. Nakagawa, and Y. Takahama. 2011. Cytokine crosstalk for thymic medulla formation. *Curr Opin Immunol* 23: 190-197.

154. Ritter, M. A., and R. L. Boyd. 1993. Development in the thymus: it takes two to tango. *Immunol Today* 14: 462-469.

155. van Ewijk, W., E. W. Shores, and A. Singer. 1994. Crosstalk in the mouse thymus. *Immunol Today* 15: 214-217.

156. Georgopoulos, K., D. D. Moore, and B. Derfier. 1992. Ikaros, an early T cell restricted transcripton factor: a putative mediator for T cell commitment. *Science* 258: 808-812.

157. Tennant, R. W., J. A. Otten, F. E. Myer, and R. J. Rascati. 1982. *Cancer Res.* 42: 3050-3055.

158. Gunther, T., Z. F. Chen, J. Kim, M. Priemel, J. M. Rueger, M. Amling, J. M. Moseley, T. J. Martin, D. J. Anderson, and G. Karsenty. 2000. Genetic ablation of parathyroid glands reveals another source of parathyroid hormone. *Nature* 406: 199-203.

159. Jeker, L. T., and J. A. Bluestone. 2013. MicroRNA regulation of T-cell differentiation and function. *Immunological reviews* 253: 65-81.

160. Hackl, M., S. Brunner, K. Fortschegger, C. Schreiner, L. Micutkova, C. Muck, G. T. Laschober, G. Lepperdinger, N. Sampson, P. Berger, D. Herndler-Brandstetter, M. Wieser, H. Kuhnel, A. Strasser, M. Rinnerthaler, M. Breitenbach, M. Mildner, L. Eckhart, E. Tschachler, A. Trost, J. W. Bauer, C. Papak, Z. Trajanoski, M. Scheideler, R. Grillari-Voglauer, B. Grubeck-Loebenstein, P. Jansen-Durr, and J. Grillari. 2010. miR-17, miR-19b, miR-20a, and miR-106a are down-regulated in human aging. *Aging cell* 9: 291-296.

161. Ventura, A., A. G. Young, M. M. Winslow, L. Lintault, A. Meissner, S. J. Erkeland, J. Newman, R. T. Bronson, D. Crowley, J. R. Stone, R. Jaenisch, P. A. Sharp, and T.

Jacks. 2008. Targeted deletion reveals essential and overlapping functions of the miR-17 through 92 family of miRNA clusters. *Cell* 132: 875-886.

162. Su, D., S. Ellis, A. Napier, K. Lee, and N. R. Manley. 2001. Hoxa3 and pax1 regulate epithelial cell death and proliferation during thymus and parathyroid organogenesis. *Developmental biology* 236: 316-329.

163. Vitelli, F., I. Taddei, M. Morishima, E. N. Meyers, E. A. Lindsay, and A. Baldini. 2002. A genetic link between Tbx1 and fibroblast growth factor signaling. *Development* 129: 4605-4611.

164. Liu, Z., A. Farley, L. Chen, B. J. Kirby, C. S. Kovacs, C. C. Blackburn, and N. R. Manley. 2010. Thymus-associated parathyroid hormone has two cellular origins with distinct endocrine and immunological functions. *PLoS genetics* 6: e1001251.

165. Candi, E., A. Rufini, A. Terrinoni, A. Giamboi-Miraglia, A. M. Lena, R. Mantovani, R. Knight, and G. Melino. 2007. DeltaNp63 regulates thymic development through enhanced expression of FgfR2 and Jag2. *Proceedings of the National Academy of Sciences of the United States of America* 104: 11999-12004.

166. Olive, V., Q. Li, and L. He. 2013. mir-17-92: a polycistronic oncomir with pleiotropic functions. *Immunological reviews* 253: 158-166.

167. Dews, M., A. Homayouni, D. Yu, D. Murphy, C. Sevignani, E. Wentzel, E. E. Furth, W. M. Lee, G. H. Enders, J. T. Mendell, and A. Thomas-Tikhonenko. 2006.

Augmentation of tumor angiogenesis by a Myc-activated microRNA cluster. *Nature genetics* 38: 1060-1065.

168. Hayashita, Y., H. Osada, Y. Tatematsu, H. Yamada, K. Yanagisawa, S. Tomida, Y. Yatabe, K. Kawahara, Y. Sekido, and T. Takahashi. 2005. A polycistronic microRNA cluster, miR-17-92, is overexpressed in human lung cancers and enhances cell proliferation. *Cancer research* 65: 9628-9632.

169. Lu, J., G. Getz, E. A. Miska, E. Alvarez-Saavedra, J. Lamb, D. Peck, A. Sweet-Cordero, B. L. Ebert, R. H. Mak, A. A. Ferrando, J. R. Downing, T. Jacks, H. R. Horvitz, and T. R. Golub. 2005. MicroRNA expression profiles classify human cancers. *Nature* 435: 834-838.

170. Zhang, J., S. Li, L. Li, M. Li, C. Guo, J. Yao, and S. Mi. 2015. Exosome and exosomal microRNA: trafficking, sorting, and function. *Genomics, proteomics & bioinformatics* 13: 17-24.

171. Jacques, B. E., M. E. Montcouquiol, E. M. Layman, M. Lewandoski, and M. W. Kelley. 2007. Fgf8 induces pillar cell fate and regulates cellular patterning in the mammalian cochlea. *Development* 134: 3021-3029.

172. Ciruna, B., and J. Rossant. 2001. FGF signaling regulates mesoderm cell fate specification and morphogenetic movement at the primitive streak. *Developmental cell* 1: 37-49.

173. Macatee, T. L., B. P. Hammond, B. R. Arenkiel, L. Francis, D. U. Frank, and A. M. Moon. 2003. Ablation of specific expression domains reveals discrete functions of ectoderm- and endoderm-derived FGF8 during cardiovascular and pharyngeal development. *Development* 130: 6361-6374.

174. Moraes, F., A. Novoa, L. A. Jerome-Majewska, V. E. Papaioannou, and M. Mallo. 2005. Tbx1 is required for proper neural crest migration and to stabilize spatial patterns during middle and inner ear development. *Mechanisms of development* 122: 199-212.

175. Tang, G. Q., and E. S. Maxwell. 2008. Xenopus microRNA genes are predominantly located within introns and are differentially expressed in adult frog tissues via post-transcriptional regulation. *Genome research* 18: 104-112.

176. Thomson, J. M., M. Newman, J. S. Parker, E. M. Morin-Kensicki, T. Wright, and S. M. Hammond. 2006. Extensive post-transcriptional regulation of microRNAs and its implications for cancer. *Genes & development* 20: 2202-2207.

177. Megraw, M., P. Sethupathy, B. Corda, and A. G. Hatzigeorgiou. 2007. miRGen: a database for the study of animal microRNA genomic organization and function. *Nucleic acids research* 35: D149-155.

178. Suarez, Y., C. Fernandez-Hernando, J. Yu, S. A. Gerber, K. D. Harrison, J. S. Pober, M. L. Iruela-Arispe, M. Merkenschlager, and W. C. Sessa. 2008. Dicer-dependent

endothelial microRNAs are necessary for postnatal angiogenesis. *Proceedings of the National Academy of Sciences of the United States of America* 105: 14082-14087.

179. Carraro, G., A. El-Hashash, D. Guidolin, C. Tiozzo, G. Turcatel, B. M. Young, S. P. De Langhe, S. Bellusci, W. Shi, P. P. Parnigotto, and D. Warburton. 2009. miR-17 family of microRNAs controls FGF10-mediated embryonic lung epithelial branching morphogenesis through MAPK14 and STAT3 regulation of E-Cadherin distribution. *Developmental biology* 333: 238-250.

180. Mulcahy, L. A., R. C. Pink, and D. R. Carter. 2014. Routes and mechanisms of extracellular vesicle uptake. *Journal of extracellular vesicles* 3.

181. Munich, S., A. Sobo-Vujanovic, W. J. Buchser, D. Beer-Stolz, and N. L. Vujanovic. 2012. Dendritic cell exosomes directly kill tumor cells and activate natural killer cells via TNF superfamily ligands. *Oncoimmunology* 1: 1074-1083.

182. Tian, T., Y. L. Zhu, F. H. Hu, Y. Y. Wang, N. P. Huang, and Z. D. Xiao. 2013. Dynamics of exosome internalization and trafficking. *Journal of cellular physiology* 228: 1487-1495.

## VITA

Kaitlin Alyssa Gutierrez Reeh was born in San Antonio, Texas on February 19, 1987. She is the daughter of Kathryn A. Gutierrez and Michael A. Gutierrez, and sister to Cameron A. Gutierrez. After graduating from Ronald Reagan High School, San Antonio, Texas, in 2005, she attended Texas A&M University in College Station, Texas. She received a Bachelor of Science with a major in Animal Science in May 2009. In August of 2009, she entered The University of Texas Graduate School of Biomedical Sciences at Houston.

Permanent Address:

481 Cherry Mountain Loop

Fredericksburg, Texas 78624